DOCUMENTATION OF R-UNSAT, A COMPUTER MODEL FOR THE SIMULATION OF REACTIVE, MULTISPECIES TRANSPORT IN THE UNSATURATED ZONE

By Matthew A. Lahvis and Arthur L. Baehr

U.S. GEOLOGICAL SURVEY
Open-File Report 97-630

West Trenton, New Jersey
1997

U.S. DEPARTMENT OF THE INTERIOR

BRUCE BABBITT, *Secretary*

U.S. GEOLOGICAL SURVEY

Mark Schaefer, *Acting Director*

For additional information
write to:

District Chief
U.S Geological Survey
Mountain View Office Park
810 Bear Tavern Road, Suite 206
West Trenton, NJ 08628

Copies of this report can be
purchased from:

U.S. Geological Survey
Branch of Information Services
Box 25286
Denver, CO 80225-0286

CONTENTS

Page

ILLUSTRATIONS

ILLUSTRATIONS--Continued

TABLES

TABLES--Continued

CONVERSION FACTORS

Multiply	By	To obtain
	Length	
inch (in)	2.54	centimeter (cm)
	Area	
square foot (ft^2)	929.0	square centimeter (cm^2)
	Mass	
pound (lb)	2204.6	gram (g)
	Time	
second (s)	1.1574×10^{-5}	day (d)
	Temperature	
degree Celsius (^oC)	degree Kelvin (K)	degree Fahrenheit (^oF)
	$^oC=K-273.15$	
	$^oF=1.8^oC + 32$	
	$^oC=(^oF-32)/1.8$	

DOCUMENTATION OF R-UNSAT, A COMPUTER MODEL FOR THE SIMULATION OF REACTIVE, MULTISPECIES TRANSPORT IN THE UNSATURATED ZONE

By Matthew A. Lahvis and Arthur L. Baehr

ABSTRACT

This report documents R-UNSAT, a computer code to simulate reactive, multispecies transport in the unsaturated zone. R-UNSAT can be used in a calibration mode to quantify constituent fluxes or in a predictive mode to calculate constituent concentrations as a function of time and space. One of two solution options can be chosen depending on the complexity of the model problem. A numerical solution implements a two-dimensional (r,z) axisymmetric finite-difference algorithm that accounts for source-sink reactions, sediment layering, and depth-dependent sediment properties. R-UNSAT also employs one-dimensional analytical solutions for simulating nonreactive, vertical transport in relatively homogeneous unsaturated-zone sediments. Both solutions incorporate Fick's law definitions of gas flux and assume equilibrium partitioning of mass among the air, water, solid, and immiscible phases.

Alternative boundary conditions are available to selectively characterize the source. Depending on the solver selected, the source can be modeled as a time-dependent-concentration, specified-flux, or specified-concentration boundary condition. Conditions for the remaining model boundaries can also be varied to span a full range of flow types. These boundary-condition options provide the user with flexibility to apply R-UNSAT to a vast range of transport problems. Model application examples presented in this report demonstrate the types of transport problems that can be solved and the model features available to facilitate these solutions.

R-UNSAT is written in FORTRAN 77 and will run, with minor modification, on most computer platforms with a FORTRAN compiler. On-screen programming is used to construct input files that can be modified for subsequent model applications. Examples of the input and output files associated with each model application are presented.

SECTION 1--INTRODUCTION AND USER'S GUIDE

Biogeochemical reactions in the unsaturated zone can occur naturally, as in pedogenic or plant-related processes, or by a disruption in the natural subsurface equilibrium as a result of human activities. The latter can result from the introduction of thermodynamically unstable compounds, such as fertilizers, pesticides, and petroleum products, to the subsurface or by alteration of the chemical oxidation state of the subsurface through mining and soil-excavation operations. If not confined, the parent compounds, intermediates, or end products of these reactions, many of which are known human carcinogens, can migrate through the unsaturated zone and pose a long-term threat to ground-water resources. For these cases, a quantitative understanding of reactive transport in the unsaturated zone is important in order to evaluate the environmental risk, to predict potential exposure pathways, and to design effective remediation solutions. The transport model R-UNSAT documented in this report is intended to provide this quantitative information. For example, R-UNSAT can be used to predict multiconstituent fate and transport of hydrocarbons from an immiscible plume, to assess mass losses or loading rates to ground water from fertilizer and pesticide applications, to design covers on organic-waste disposal sites and mine-tailing dumps, to calculate radon-gas emissions, or to estimate radionuclide transport from radioactive-waste repositories.

Although R-UNSAT can be applied to any of the aforementioned transport problems, this report focuses on applications to simulate the fate and transport of hazardous organic substances in the unsaturated zone, arguably the most common cause of ground-water contamination in the industrialized world. These hydrocarbon compounds can infiltrate aquifers from a variety of sources including surface spills and leaky underground storage tanks and pipelines. Although remediation technology is developing rapidly, engineered efforts to treat or remove the source are often incomplete and cost-prohibitive because of the physiochemical properties of the hydrocarbons and the transport properties of the sediments. Restoration of a contaminated aquifer can occur naturally, however, by volatilization to the atmosphere and by molecular (biotic or abiotic) transformation of the hydrocarbons. In some well-documented cases, these natural cleansing processes have reduced contaminant concentrations well below regulatory limits before the contaminant plume reaches a point of contact, even with little or no source removal (Wiedemeier and others, 1994). By quantifying hydrocarbon-fate pathways, regulators can deduce the natural assimilative capacity of an aquifer system and implement the most cost-effective remediation strategy.

Section 2 of this documentation presents a theoretical overview of R-UNSAT that includes the derivation of numerical and analytical solutions to the governing transport equations. The numerical solutions are designed for two-dimensional model applications involving multispecies transport in heterogeneous unsaturated-zone sediments (fig. 1). The numerical solver is based on a two-dimensional (r,z), axisymmetric, finite-difference algorithm developed by Baehr (1987) and modified by Lahvis (1993). The analytical solutions are designed for simulating one-dimensional, vertical transport of nonreactive species in a relatively uniform unsaturated zone (fig. 1). Both mathematical solutions incorporate Fick's Law definitions of gas diffusion, which may be inappropriate for certain transport applications where gaseous-phase advection is significant. The user is referred to Section 2.4.1 to assess these limitations.

Four alternative boundary conditions are available to selectively characterize the source:

Option 1: A specified-flux boundary
Option 2: A specified-concentration boundary
[1] Option 3: A time-dependent-concentration boundary
[1] Option 4: A constant-radial-flux boundary

[1] Available only with numerical solver.

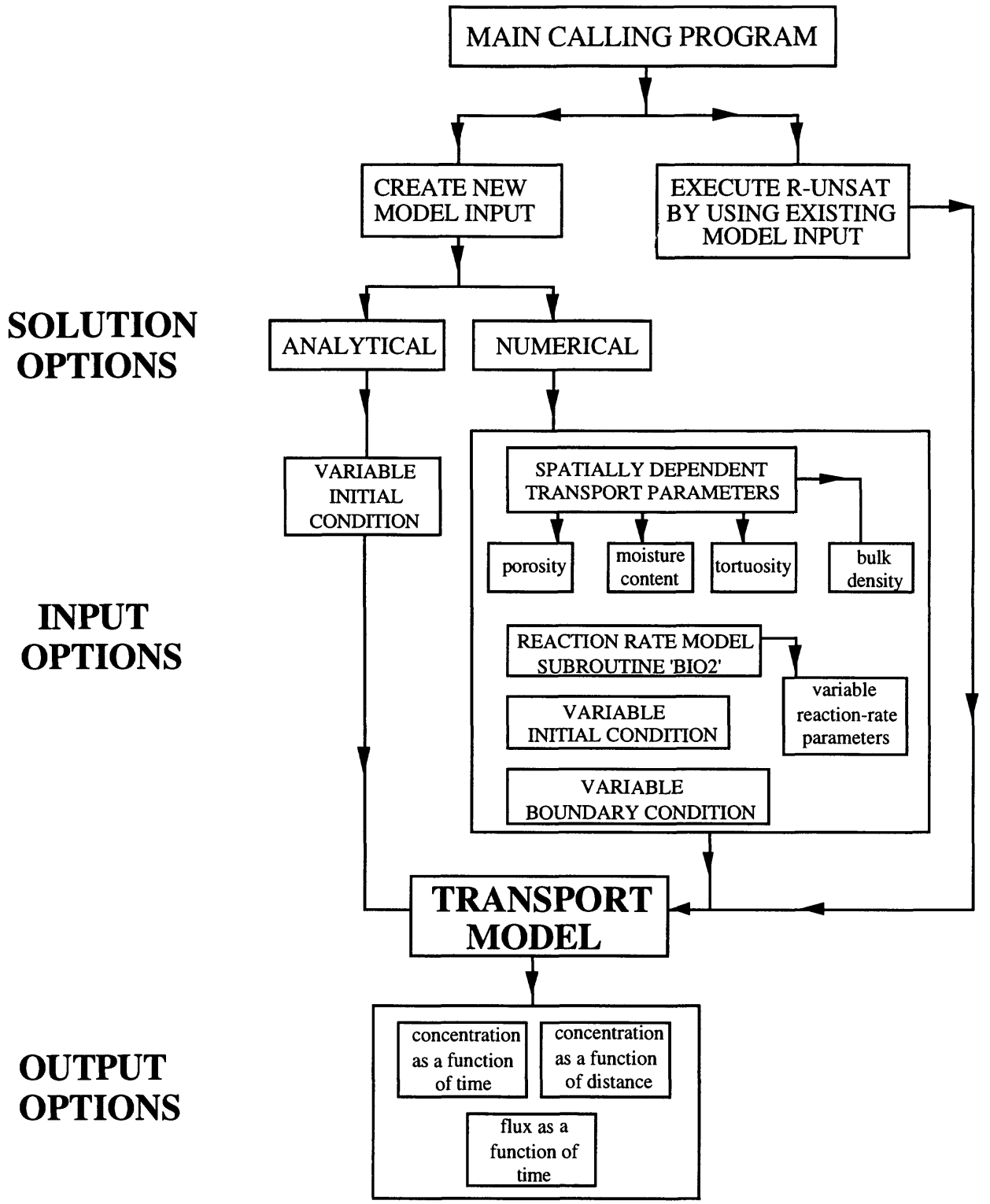

Figure 1. Flow chart of R-UNSAT transport model.

Options 1 and 2 are designed for modeling hydrocarbon or reactive-gas transport from a source at land surface or the water table. The source strength remains constant over the duration of the simulated event. The magnitude of the source boundary can be computed by model calibration to experimental gas-concentration data. Option 3 is appropriate for predicting the fate and transport of a multispecies contaminant located at or above the water table. The source composition is readjusted at each time step in accordance with constituent-mass fluxes across source boundaries. Option 4 is designed to simulate gas transport from a constant-radial-flux source (for example, an injection probe) located in the unsaturated zone. By applying this boundary condition, the model can be used in a calibration mode to quantify the gas-transport properties of unsaturated-zone sediments provided the flux of the injected gas is known.

Section 3 describes the basic operations and applications of R-UNSAT as well as the format and contents of input and output files. The components and overall flow of information in R-UNSAT are illustrated in figure 2. From a main calling program, the user can either create new model input or execute the model provided formatted input files exist. The framework for creating new input files is menu-driven. In general, numerical solutions require more data input than the analytical solutions because of their potential to simulate multispecies transport and unsaturated-zone heterogeneity. For example, the numerical solutions can accommodate spatially dependent transport data, a user-specified reaction-rate model, and variable boundary- and initial-condition data (fig. 2). The analytical solutions, in contrast, can accommodate only a variable initial condition. Model output from either solution is written as concentration as a function of time (breakthrough) or concentration as a function of distance (snapshot) data. Flux as a function of time data also can be obtained for source boundary condition Option 2.

With minor modifications, R-UNSAT will run on a variety of computing platforms, including mainframe and personal computers. The website address contains the following source codes, which must be compiled with a FORTRAN F77 compiler for execution:

R-UNSAT.FOR	-	the FORTRAN source code for personal computers
R-UNSAT.F77	-	the FORTRAN source code for main frame computers
EXAMPLE.FIL	-	examples of R-UNSAT applications presented in Section 3.4

The compiling procedure for mainframe and personal computers is presented in Section 3. The source codes must be recompiled to incorporate the changes in the executable version of the program code. Input files are also included for test problems that are presented in Section 3.4. Before executing R-UNSAT, the user is encouraged to test his or her understanding of the software package by performing one of the test simulations.

The numerical algorithm is verified in Section 4 by comparing numerical solutions to known steady-state analytical solutions for simplified test cases. The algorithm is verified for various boundary-condition applications as well as for the ability to simulate aquifer heterogeneity and reactions.

This report was prepared as part of the U.S. Geological Survey Toxics Substances Hydrology Program (website address--http://www.toxics.usgs.gov/toxics) with assistance from the Office of Ground Water. The documentation, source code, and executable versions of R-UNSAT can be accessed at the following website address: http://wwwnj.er.usgs.gov/.

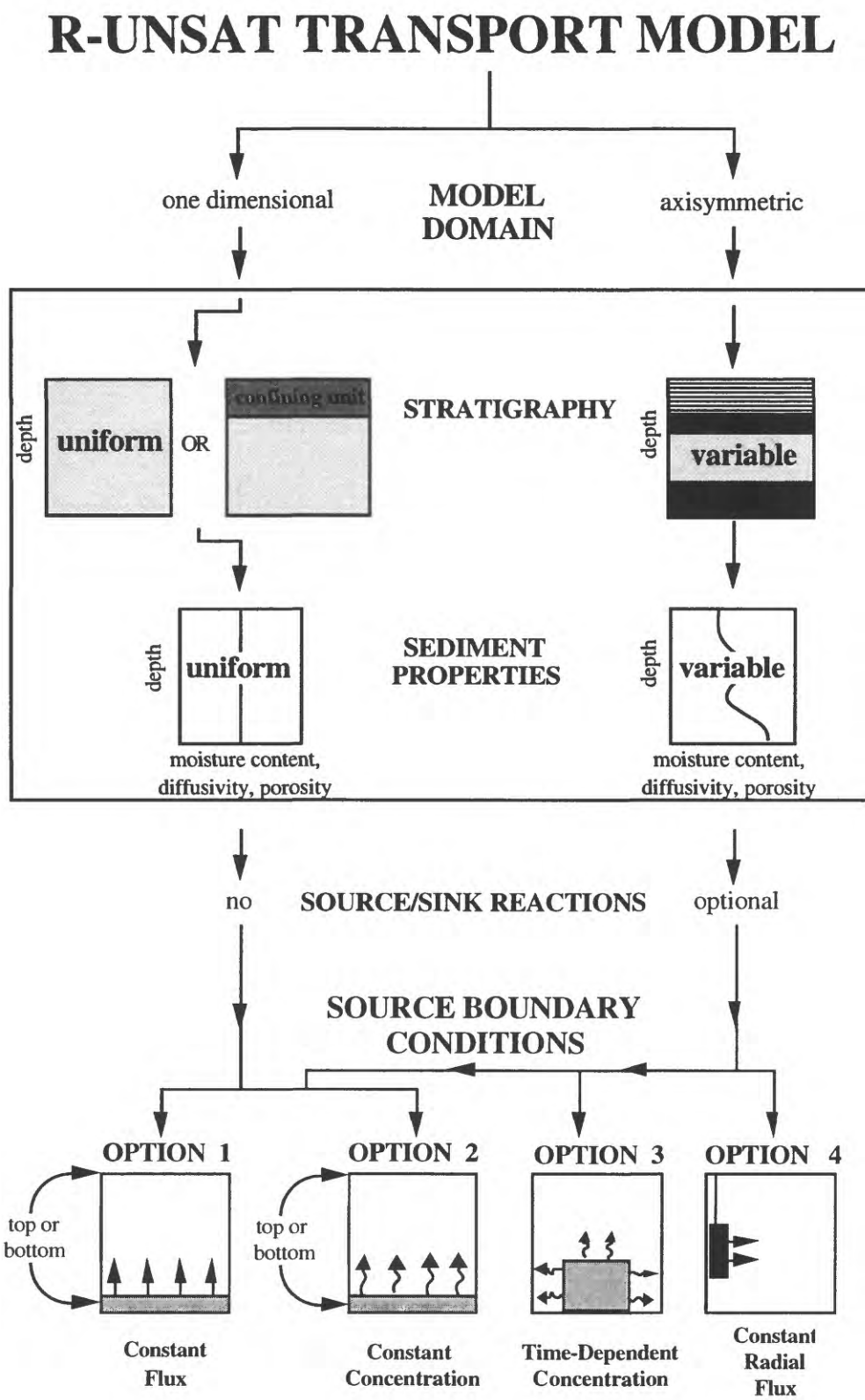

Figure 2. Flow chart of R-UNSAT software package.

SECTION 2.0--TRANSPORT-MODEL DEVELOPMENT

2.1 Derivation of the Governing Transport Equation

The unsaturated-zone transport model is based on the following conservation-of-mass equation, which applies to each constituent (k):

$$\frac{\partial}{\partial t}[G_k\theta_a + C_k\theta_w + S_k\rho_b] + \nabla \cdot [\mathbf{J}_{ka} + \mathbf{J}_{kw}] = R_k \quad (1)$$

where

G_k	=	concentration of the k^{th} constituent in the gaseous phase	[g/cm³]
C_k	=	concentration of the k^{th} constituent in the aqueous phase	[g/cm³]
S_k	=	mass of the k^{th} constituent adsorbed per unit mass of porous medium	[g/g]
θ_a	=	gaseous-phase porosity of the k^{th} constituent	[dimensionless]
θ_w	=	aqueous-phase porosity of the k^{th} constituent	[dimensionless]
ρ_b	=	bulk density	[g/cm³]
$\mathbf{J}_{ka}$	=	gaseous-phase flux vector of the k^{th} constituent	[g/cm²-s]
$\mathbf{J}_{kw}$	=	aqueous-phase flux vector of the k^{th} constituent	[g/cm²-s]
R_k	=	reaction rate (source/sink) of the k^{th} constituent	[g/cm³-s]

To derive (1), the immiscible phase is assumed to be stationary and is modeled as a boundary condition. This assumption implies that the immiscible phase is at residual saturations and (1) is applied to the spatial domain outside the zone of contamination.

The gaseous-phase mass flux ($\mathbf{J}_{ka}$) is related to the gaseous-phase concentration gradient according to Fick's Law:

$$J_{ka} = -D_{ka}\nabla G_k \quad (2)$$

where

D_{ka}	=	effective-diffusion coefficient of the k^{th} constituent in the gaseous phase	[cm²/s]
G_k	=	gaseous-phase concentration of the k^{th} constituent	[cm²/s]

Fick's Law (2) assumes that gaseous-phase advection is negligible. This assumption is generally valid in the absence of air pumping or a rapidly fluctuating water table (Kreamer and others, 1988; Massmann and Farrier, 1992). The implications of neglecting gaseous-phase advection are discussed further in Section 2.4.1.

The aqueous-phase mass flux ($\mathbf{J}_{kw}$) is defined according to the following advection-dispersion model:

$$\mathbf{J}_{kw} = \mathbf{q}_w C_k - (\boldsymbol{\delta} + D_{kw})\nabla C_k \quad (3)$$

where

$\mathbf{q}_w$ = specific-discharge vector for the aqueous phase [cm/s]
$\boldsymbol{\delta}$ = mechanical dispersivity [cm²/s]
D_{kw} = effective-diffusion coefficient of the k^{th} constituent in the aqueous phase [cm²/s]

In porous-media transport studies, $\boldsymbol{\delta}$ is the principal dispersion mechanism for the aqueous phase, and is assumed to be linearly related to the average fluid velocity as follows:

$$\boldsymbol{\delta} = \left(\frac{|\mathbf{q}_w|}{\theta_w} \right) \boldsymbol{\alpha} \tag{4}$$

where

$\boldsymbol{\alpha}$ = dispersivity tensor for the aqueous phase [cm]
$|\mathbf{q}_w|$ = magnitude of the specific-discharge vector [cm/s]

The effective-diffusion coefficients (D_{ka}) and (D_{kw}) of equations (2) and (3) are functions of the pore-space configuration and the fluid-phase composition as follows:

$$D_{ka} = d_{ka}\theta_a\tau_a \tag{5}$$

$$D_{kw} = d_{kw}\theta_w\tau_w \tag{6}$$

where

d_{ka} = diffusivity of the k^{th} constituent in the gaseous phase [cm²/s]
d_{kw} = diffusivity of the k^{th} constituent in the aqueous phase [cm²/s]
τ_a = gaseous-phase tortuosity of the k^{th} constituent [dimensionless]
τ_w = aqueous-phase tortuosity of the k^{th} constituent [dimensionless]

The reader is referred to Section 2.4.2 for a comprehensive discussion of the models used to define these parameters.

In the conservation-of-mass equation (1), the reaction term (R_k) represents the mass loss associated with aerobic biodegradation. The biodegradation model supplied in R-UNSAT is dependent on the availability of free oxygen (see Section 2.4.4). However, because several kinetic models are available to characterize biodegradation processes, R-UNSAT is also designed to accommodate a user-specified reaction-rate model.

Substituting the constitutive relations (2) through (4) into the conservation-of-mass equation (1) results in the following definition of mass transport:

$$\frac{\partial}{\partial t}[G_k\theta_a + C_k\theta_w + S_k\rho_b] + \nabla \cdot [\mathbf{q}_w C_k - (\boldsymbol{\delta} + D_{kw})\nabla C_k - D_{ka}\nabla G_k] = R_k \tag{7}$$

Equation (5) can be simplified further by applying equilibrium relations to describe the partitioning of the mass between phases (see Section 2.4.3). Substituting these relations into the conservation-of-mass equation (7) allows the mass to be written in terms of the gaseous-phase concentration (G_k) as follows:

$$a_k \frac{\partial G_k}{\partial t} + \nabla \cdot \left[\frac{\mathbf{q}_w}{H_k} G_k - D_k \nabla G_k \right] = R_k$$

$$\text{and} \quad a_k = \left(\theta_a + \frac{\theta_w}{H_k} + \frac{K_k \rho_b}{H_k} \right); \; D_k = \left(D_{ka} + \frac{D_{kw}}{H_k} + \frac{\boldsymbol{\delta}}{H_k} \right) \tag{8}$$

where

H_k = Henry's Law constant of the k^{th} constituent [dimensionless]
K_k = adsorption isotherm coefficient of the k^{th} constituent [cm^3/g]

In (6), the storage coefficient (a_k) and the diffusion coefficient (D_k) are spatially dependent parameters. Equation (8) is the governing transport equation in R-UNSAT.

2.2 Development of the Numerical Solutions

In cylindrical coordinates, (8) can be written for each constituent (k) as:

$$a_k \frac{\partial G_k}{\partial t} + b_{k1} \frac{\partial^2 G_k}{\partial r^2} + b_{k2} \frac{\partial^2 G_k}{\partial z^2} + c_{k1} \frac{1}{r} \frac{\partial G_k}{\partial r} + c_{k2} \frac{\partial G_k}{\partial z} = R_k \tag{9a}$$

where the coefficients are depth-dependent and are expressed as:

$$a_k = \theta_a + \frac{\theta_w}{H_k} + \frac{K_k \rho_b}{H_k} \tag{9b}$$

$$b_{k1} = -\left(\frac{D_{kw}}{H_k} + \frac{\boldsymbol{\delta}_{wT}}{H_k} + D_{ka} \right) \tag{9c}$$

$$b_{k2} = -\left(\frac{D_{kw}}{H_k} + \frac{\boldsymbol{\delta}_{wL}}{H_k} + D_{ka} \right) \tag{9d}$$

$$c_{k1} = b_{k1} \tag{9e}$$

$$c_{k2} = \frac{\mathbf{q}_{wz}}{H_k} - \frac{\partial}{\partial z} b_{k2} \tag{9f}$$

where

δ_{wT} = transverse component of hydrodynamic dispersion [cm^2/s]
δ_{wL} = longitudinal component of hydrodynamic dispersion [cm^2/s]
$\mathbf{q}_{wz}$ = recharge rate [cm/s]

To derive (9), the effective-diffusion coefficients (D_{ka} and D_{kw}) are assumed to be depth-dependent. The numerical solution to (9) is developed in Section 2.4 for various combinations of boundary and initial conditions by employing finite-difference techniques.

2.2.1 Boundary and Initial Conditions for the Numerical Solutions

Source Boundary Condition Ω_1:

The numerical solution incorporates four alternative boundary conditions (options) to selectively characterize the source (figs. 3-6).

Option 1: Specified-flux boundary

As shown in figure 3, Option 1 represents a specified-flux (J_{k_o}) boundary condition defined by Fick's Law as:

$$J_{k_o}(r) = -D_k \frac{dG_k}{dz} + \frac{q_w}{H_k} G_k \qquad \text{at } t \geq 0 \text{ on } \Omega_1 \tag{10a}$$

The diffusion coefficient (D_k) along Ω_1 is assumed to be constant and is computed on the basis of the initial gaseous-phase composition and sediment-transport properties specified at the source boundary. The magnitude of J_{k_o} can be varied along Ω_1 for two-dimensional model applications. In the application described in Section 3.4.1, Option 1 is employed to simulate the constant flux of oxygen and carbon dioxide associated with aerobic hydrocarbon biodegradation at the water table.

Option 2: Constant-concentration boundary

As shown in figure 4, Option 2 represents a constant-concentration (G_{k_o}) boundary condition given by:

$$G_{k_o}(r) = G_k(r) \qquad \text{at } t \geq 0 \text{ on } \Omega_1 \tag{10b}$$

The source concentration is the vapor-phase equivalent of the aqueous-phase concentration if equilibrium partitioning according to Henry's Law is assumed. As in Option 1, the gaseous-phase concentrations can be varied across the source boundary. This option has also been employed to simulate oxygen and carbon dioxide transport associated with hydrocarbon biodegradation at the water table (Lahvis, 1993).

Option 3: Time-dependent-concentration boundary

Option 3 represents the source boundary condition developed by Baehr (1987) to model multi-species transport of hydrocarbons from an immiscible plume located in the unsaturated zone. As shown in figure 5, the source is represented by a time-dependent boundary condition, where the gaseous phase is in equilibrium with the stationary immiscible plume with the assumption of Raoult's Law (see Section 2.4.3):

$$G_k(r,z,t) = H^o_{ka}\, \chi_k(t) \qquad \text{for } (r,z), \text{ at } t \geq 0 \text{ on } \Omega_1 \tag{10c}$$

where

$H_{ka}{}^o$ = saturated gaseous-phase concentration of the pure k^{th} constituent [g/cm^3]

$\chi_k(t)$ = time-dependent mole fraction of the k^{th} constituent in the immiscible phase [dimensionless]

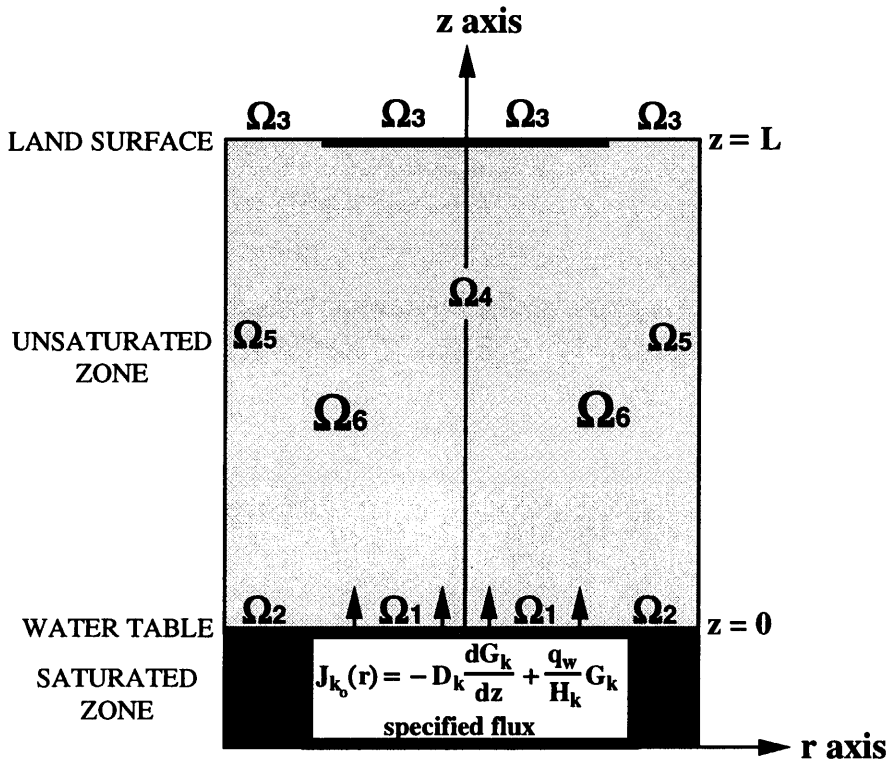

EXPLANATION

Ω_1	upper vertical source boundary
Ω_2	water-table boundary
Ω_3	upper vertical boundary
Ω_4	r = 0 axis of symmetry
Ω_5	outer radial boundary
Ω_6	model domain (r,z)
$J_{k_o}(r)$	specified-mass flux of kth constituent across upper vertical source boundary
D_k	effective-diffusion coefficient of kth constituent
G_k	gaseous-phase concentration of kth constituent
q_w	vertical recharge rate
H_k	Henry's Law constant of the kth constituent
L	length of model domain

Figure 3. Diagram showing model region and boundary conditions for Option 1.

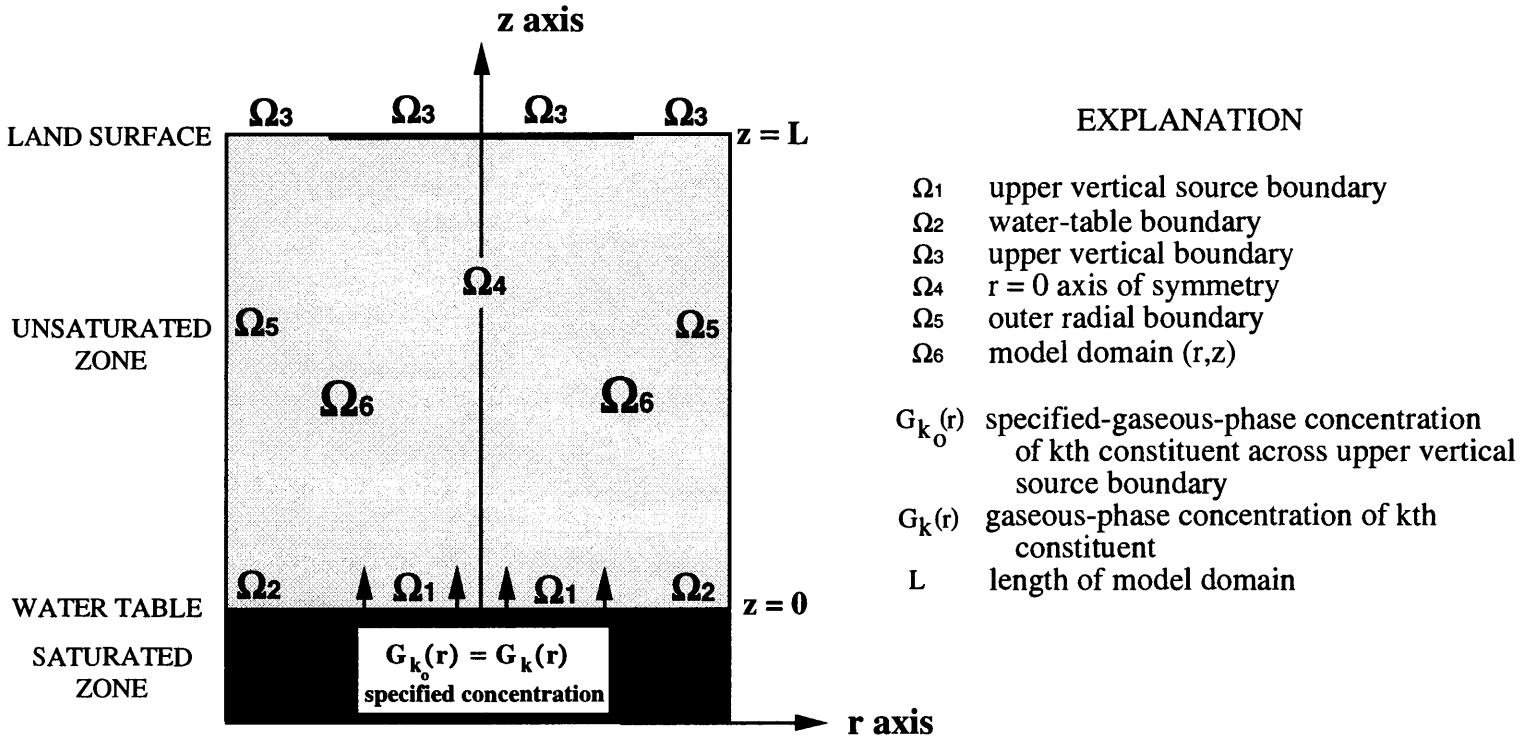

Figure 4. Diagram showing model region and boundary conditions for Option 2.

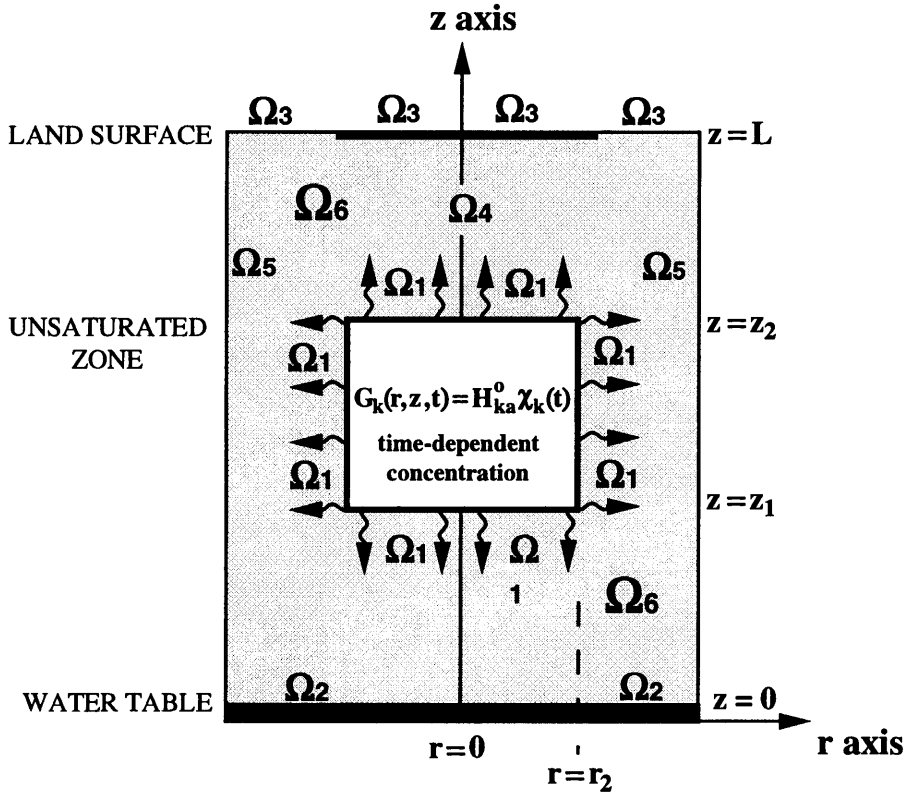

EXPLANATION

Ω_1	upper vertical source boundary
Ω_2	water-table boundary
Ω_3	upper vertical boundary
Ω_4	r = 0 axis of symmetry
Ω_5	outer radial boundary
Ω_6	model domain (r,z)
$G_k(r,z,t)$	time-dependent gaseous-phase concentration of kth constituent along source boundary
H^o_{ka}	saturated gaseous-phase concentration of the pure kth constituent
$\chi_k(t)$	time-dependent mole fraction of the kth constituent in the immiscible phase
r_2	radius of source
z_1	vertical location of lower source boundary
z_2	vertical location of upper source boundary
L	length of model domain

Figure 5. Diagram showing model region and boundary conditions for Option 3.

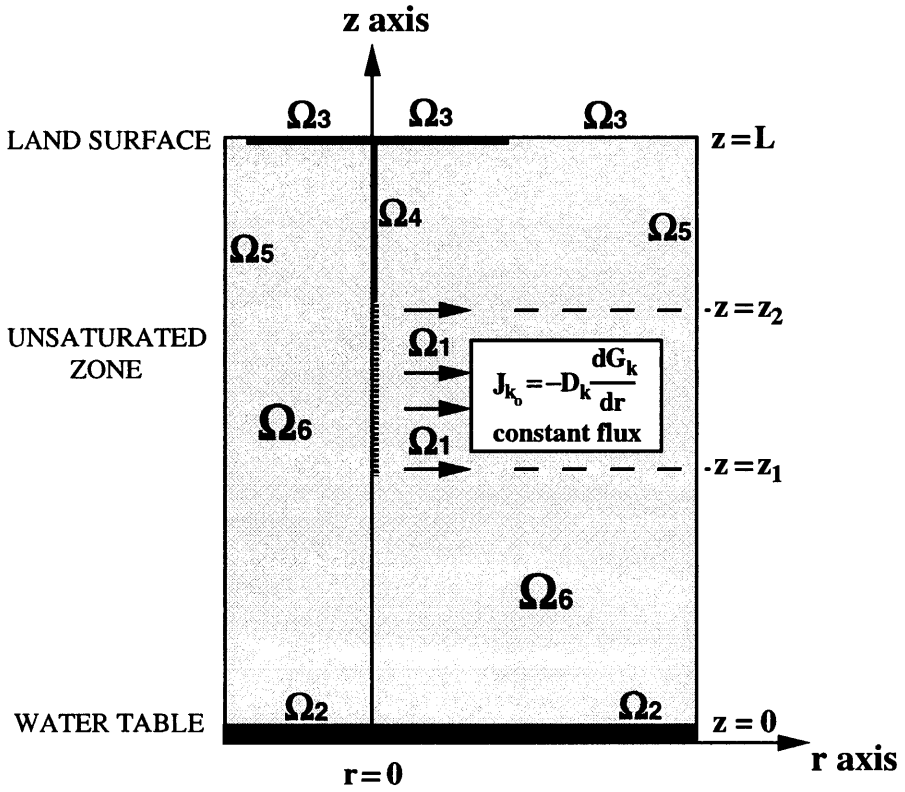

EXPLANATION

Ω_1	upper vertical source boundary
Ω_2	water-table boundary
Ω_3	upper vertical boundary
Ω_4	r = 0 axis of symmetry
Ω_5	outer radial boundary
Ω_6	model domain (r,z)
J_{k_o}	constant radial mass flux of the kth constituent across source boundary
D_k	effective-diffusion coefficient of the kth constituent
G_k	gaseous-phase concentration of the kth constituent
z_1	vertical location of lower source boundary
z_2	vertical location of upper source boundary
L	length of model domain

Figure 6. Diagram showing model region and boundary conditions for Option 4.

The immiscible plume as written in (10c) is assumed to be an ideal solution, with an activity coefficient equal to 1.0. In addition, the immiscible plume is assumed to be well-mixed, which implies that χ_k is spatially independent within the plume. For this boundary condition, $\chi_k(t)$ is algebraically readjusted at each time step by numerically evaluating the constituent-specific fluxes at the immiscible-plume boundary over the previous time step. Equation (10c) therefore accounts for coupled transport of the constituents. In Section 3.4.3, Option 3 is employed to simulate the selective transport of hydrocarbons from an immiscible plume located in the unsaturated zone.

Option 4: Constant-radial-flux boundary

As shown in figure 6, Option 4 was developed to simulate gas transport from a constant-flux source at r = 0. The constant flux is again defined according to Fick's Law, and is given by:

$$J_{k_o} = -D_k \frac{dG_k}{dr} \qquad \text{at } t \geq 0 \text{ on } \Omega_1 \tag{10d}$$

As in (10a), D_k is assumed to be constant along Ω_1 and is defined by the initial gaseous-phase composition and sediment-transport characteristics specified at the source boundary. In Section 3.4.4, (10d) is applied to simulate the constant release of a tracer gas from an injection probe located in the unsaturated zone.

Lower Boundary Condition Ω_2:

The lower boundary condition (Ω_2) (figs. 3-6) is modeled as a third-kind (Cauchy-type) boundary condition given by:

$$(1-\lambda_2)\,\Delta z \frac{dG_k(r,t)}{dz} + \lambda_2 G_k(r,t) = G_{k_{atm}} \qquad \text{at } t \geq 0 \text{ on } \Omega_2 \tag{11}$$

where ($0 \leq \lambda_2 \leq 1$). Setting $\lambda_2 = 0$ implies the existence of a no-flow boundary at Ω_2, characteristic of a water-table boundary impervious to gas transport. $\lambda_2 = 1$ implies the existence of a maximum mass-loss condition, which is appropriate for modeling highly soluble constituents subject to instantaneous mixing and dilution at the water table or modeling transport in deep unsaturated-zone systems where the lower model boundary is open to atmospheric gaseous-phase concentrations. The length over which λ_2 is applied can be varied along Ω_2.

Upper Boundary Condition Ω_3:

Likewise, the upper boundary (Ω_3) is modeled as:

$$(1-\lambda_3)\,\Delta z \frac{dG_k(r,t)}{dz} + \lambda_3 G_k(r,t) = G_{k_{atm}} \qquad \text{at } t \geq 0 \text{ on } \Omega_3 \tag{12}$$

where ($0 \leq \lambda_3 \leq 1$). $\lambda_3 = 0$ implies the existence of a no-flow boundary along Ω_3, which is indicative of a paved ground surface impervious to vertical gas transport. By contrast, $\lambda_3 = 1$ implies the existence of a constant-concentration boundary condition open to the atmosphere, where the constituent is subject to instantaneous mixing and dilution. Again, the length over which λ_3 is applied can be varied along Ω_3.

Inner-Radial Boundary Condition Ω_4:

The inner-radial boundary condition (Ω_4) is developed to establish radial symmetry in the model domain as follows:

$$\frac{dG_k}{dr} = 0 \qquad \text{on } \Omega_4 \tag{13}$$

Outer-Radial Boundary Condition Ω_5:

A third-kind (Cauchy-type) boundary condition is again used to model the outer-radial boundary Ω_5, and is given by:

$$(1-\lambda_5)\,\Delta r \frac{dG_k(z,t)}{dr} + \lambda_5 G_k(z,t) = G_{k_{atm}} \qquad \text{at } t \geq 0 \quad \text{on } \Omega_5 \tag{14}$$

where ($0 \leq \lambda_5 \leq 1$). Setting $\lambda_5 = 0$ implies the existence of a no-flow radial boundary representative of an impervious foundation or basement wall, whereas $\lambda_5 = 1$ implies the existence of a radial boundary open to the unsaturated zone and atmospheric gaseous-phase concentrations. The length over which λ_5 is applied can also be varied along Ω_5.

Initial Condition:

The initial condition can be specified as a constant concentration equal to the atmospheric concentration of the constituent or as a spatially dependent concentration given by:

$$G_k(r,z,t) = A_k(r,z) \qquad \text{for (r,z), at } t = 0 \quad \text{on } \Omega_6 \tag{15}$$

A_k can also be specified as a linear function in either the radial (r) or vertical (z) direction.

2.2.2 Finite-Difference Solution to Radially Symmetric Equations

The conservation-of-mass equation (9) is a linear and parabolic partial-differential equation that is solved numerically by employing finite-difference approximations. The following algorithm is applied to each constituent (here the subscript (k) has been dropped for notational simplification) at each node (r,z) in the model domain at time t_α:

$$a\frac{\partial G}{\partial t} + b_1\frac{\partial^2 G}{\partial r^2} + b_2\frac{\partial^2 G}{\partial z^2} + c_1\frac{1}{r}\frac{\partial G}{\partial r} + c_2\frac{\partial G}{\partial z} - R = 0$$
$$\text{for (r,z), } t > 0 \text{ on } \Omega_6 \tag{16}$$

Of the depth-dependent coefficients given in (16), only c_2 is differentiable (see Section 2.1). By applying the chain rule, the derivative term ($d/dz\ b_2$) in equation (9f) can be expanded as follows:

$$\frac{d}{dz}b_2 = -\frac{d}{dz}\left(D_{ka} + \frac{D_{kw}}{H_k} + \frac{\delta}{H_k}\right)$$

$$= -\left(d_{ka}\tau_a\frac{d\theta_a}{dz} + d_{ka}\frac{d\tau_a}{dz}\theta_a + \frac{dd_{ka}}{dz}\tau_a\theta_a\right) - \frac{\left(d_{kw}\tau_w\frac{d\theta_w}{dz} + d_{kw}\frac{d\tau_w}{dz}\theta_w + \frac{dd_{kw}}{dz}\tau_w\theta_w\right)}{H_k} - \frac{q_w\alpha_L}{H_k}\left[\frac{d}{dz}\left(\frac{1}{\theta_w}\right)\right] \quad (17)$$

The differentiation terms (17) can then be solved numerically by employing the following central-difference approximations:

$$\frac{d\Gamma}{dz} = \frac{\Gamma_{i,j+1} - \Gamma_{i,j-1}}{2\Delta z} \quad \text{where: } \Gamma = \theta_a, \theta_w, \tau_a, \tau_w, d_{ka}, d_{kw}, \frac{1}{\theta_w} \quad (18)$$

where the subscripts (i) and (j) represent the two-dimensional array indices.

The time-dependent partial derivatives in (16) can also be approximated numerically as follows:

$$\frac{\partial G}{\partial t} = \frac{G_{i,j}^{n+1} - G_{i,j}^{n}}{\Delta t} \quad (19a)$$

$$\frac{\partial^2 G}{\partial r^2} = \alpha\left[\frac{G_{i+1,j}^{n+1} - 2G_{i,j}^{n+1} + G_{i-1,j}^{n+1}}{(\Delta r)^2}\right] + (1-\alpha)\left[\frac{G_{i+1,j}^{n} - 2G_{i,j}^{n} + G_{i-1,j}^{n}}{(\Delta r)^2}\right] \quad (19b)$$

$$\frac{\partial^2 G}{\partial z^2} = \alpha\left[\frac{G_{i,j+1}^{n+1} - 2G_{i,j}^{n+1} + G_{i,j-1}^{n+1}}{(\Delta z)^2}\right] + (1-\alpha)\left[\frac{G_{i,j+1}^{n} - 2G_{i,j}^{n} + G_{i,j-1}^{n}}{(\Delta z)^2}\right] \quad (19c)$$

$$\frac{\partial G}{\partial r} = \alpha\left[\frac{G_{i+1,j}^{n+1} + G_{i-1,j}^{n+1}}{2(\Delta r)}\right] + (1-\alpha)\left[\frac{G_{i+1,j}^{n} + G_{i-1,j}^{n}}{2(\Delta r)}\right] \quad (19d)$$

$$\frac{\partial G}{\partial z} = \alpha\left[\frac{G_{i,j+1}^{n+1} + G_{i,j-1}^{n+1}}{2(\Delta z)}\right] + (1-\alpha)\left[\frac{G_{i,j+1}^{n} + G_{i,j-1}^{n}}{2(\Delta z)}\right] \quad (19e)$$

where (n) represents a time-step index. The time derivative t_α is approximated by:

$$t_\alpha = \alpha t^{n+1} + (1-\alpha)\, t^{n} \quad (20)$$

The coefficient value $\alpha = 0$ corresponds to an explicit approach and $\alpha = 1$ corresponds to a fully implicit approach. The nodal spacings Δr and Δz are constant, implying that nodes are equally spaced throughout the model domain.

Substituting the numerical approximations (equations 17-20) into the general conservation-of-mass equation (16) results in the following numerical expression:

$$\frac{a}{\Delta t} G_{i,j}^{n} + \frac{b_1(\alpha-1)}{(\Delta r)^2}\left[G_{i+1,j}^{n} - 2G_{i,j}^{n} + G_{i-1,j}^{n}\right] + \frac{b_2(\alpha-1)}{(\Delta z)^2}\left[G_{i,j+1}^{n} - 2G_{i,j}^{n} + G_{i,j-1}^{n}\right]$$

$$\frac{c_1\alpha}{2(\Delta r)}\left[G_{i+1,j}^{n+1} - G_{i-1,j}^{n+1}\right] + \frac{c_2\alpha}{2(\Delta z)}\left[G_{i,j+1}^{n+1} - G_{i,j-1}^{n+1}\right] = F^{n} \qquad (21a)$$

where F^n defines the explicit component and is given by:

$$F^{n} = \frac{a}{\Delta t} G_{i,j}^{n} + \frac{b_1(\alpha-1)}{(\Delta r)^2}\left[G_{i+1,j}^{n} - 2G_{i,j}^{n} + G_{i-1,j}^{n}\right] + \frac{b_2(\alpha-1)}{(\Delta z)^2}\left[G_{i,j+1}^{n} - 2G_{i,j}^{n} + G_{i,j-1}^{n}\right]$$

$$+ \frac{c_1(\alpha-1)}{2(\Delta r)}\left[G_{i+1,j}^{n} - G_{i-1,j}^{n}\right] + \frac{c_2(\alpha-1)}{2(\Delta z)}\left[G_{i,j+1}^{n} - G_{i,j-1}^{n}\right] + R \qquad (21b)$$

The implicit portion (21a) can be redefined as:

$$A\left[G_{i-1,j}^{n+1}\right] + B\left[G_{i+1,j}^{n+1}\right] + C\left[G_{i,j}^{n+1}\right] + D\left[G_{i,j-1}^{n+1}\right] + E\left[G_{i,j+1}^{n+1}\right] = F^{n} \qquad (22a)$$

where the coefficients are expressed numerically as:

$$A = \frac{b_1\alpha}{(\Delta r)^2} - \frac{c_1\alpha}{2(\Delta r)} = \frac{\alpha}{\Delta r}\left[\frac{b_1}{\Delta r} - \frac{c_1}{2}\right] \qquad (22b)$$

$$B = \frac{b_1\alpha}{(\Delta r)^2} - \frac{c_1\alpha}{2(\Delta r)} = \frac{\alpha}{\Delta r}\left[\frac{b_1}{\Delta r} - \frac{c_1}{2}\right] \qquad (22c)$$

$$C = \frac{a}{\Delta t} - \frac{2b_1\alpha}{(\Delta r)^2} - \frac{2b_2\alpha}{(\Delta z)^2} = \frac{a}{\Delta t} - 2\alpha\left[\frac{b_1}{(\Delta r)^2} + \frac{b_2}{(\Delta z)^2}\right] \qquad (22d)$$

$$D = \frac{b_2\alpha}{(\Delta z)^2} - \frac{c_2\alpha}{2(\Delta z)} = \frac{\alpha}{\Delta z}\left[\frac{b_2}{\Delta z} - \frac{c_2}{2}\right] \qquad (22e)$$

$$E = \frac{b_2\alpha}{(\Delta z)^2} - \frac{c_2\alpha}{2(\Delta z)} = \frac{\alpha}{\Delta z}\left[\frac{b_2}{\Delta z} - \frac{c_2}{2}\right] \qquad (22f)$$

The boundary conditions (10-14) can be approximated numerically as follows:

Option 1: Specified-flux source boundary (Ω_1):

$$G_{i,j}^{n+1} = \frac{\left\{ J_k - \left[\frac{D_k}{\Delta z} \right] G_{i+1,j}^{n+1} \right\}}{\left\{ \frac{q_{wz}}{H_k} - \left[\frac{D_k}{\Delta z} \right] \right\}} \qquad \text{for } t > 0 \text{ on } \Omega_1 \tag{23a}$$

Option 2: Constant-concentration source boundary (Ω_1):

$$G_{i,j}^{n+1} = H_k \, C_{i,j-1}^{n+1} \qquad \text{for } t > 0 \text{ on } \Omega_1 \tag{23b}$$

Option 3: Time-dependent-concentration source boundary (Ω_1):

$$G_{i,j}^{n+1} = H_{ka}^{o} \, \chi_{ki}^{n} \qquad \text{for } t > 0 \text{ on } \Omega_1 \tag{23c}$$

Option 4: Constant-radial-flux source boundary (Ω_1):

$$G_{i,j}^{n+1} = \frac{J_k \, \Delta r}{D_k} + G_{i+1,j}^{n+1} \qquad \text{for } t > 0 \text{ on } \Omega_1 \tag{23d}$$

Upper (m = 2), lower (m = 3), and outer-radial (m = 5) boundaries (Ω_m):

$$G_{i,j}^{n+1} = (1-\lambda_m) G_{i,j-1}^{n+1} + \lambda_m G_{i,j}^{n+1}\Big|_{atm} \qquad \text{for } (r,z),\ t \geq 0 \text{ on } \Omega_m \qquad m = 2,3,5 \tag{24}$$

Inner-radial boundary (Ω_4):

$$G_{i,j}^{n+1} = G_{i,j}^{n+1}\Big|_{atm} \qquad \text{for } t > 0 \text{ on } \Omega_4 \tag{25}$$

Substituting the appropriate boundary-condition approximations (23-25) into (22) results in a system of simultaneous equations for $G^{n+1}_{i,j}$ defined as the following function of α:

$$G_{i,j}^{n+1} = f_{i,j}(\alpha, G_{i-1,j}^{n+1}, G_{i+1,j}^{n+1}, G_{i,j-1}^{n+1}, G_{i,j+1}^{n+1}) + g_{i,j}(\alpha, G_{i-1,j}^{n}, G_{i+1,j}^{n}, G_{i,j-1}^{n}, G_{i,j+1}^{n}) \tag{26}$$

In R-UNSAT, the time derivative is approximated at its midpoint $\alpha = 0.5$ (Crank-Nicolson method). The advantage of this approach is that the algorithm is numerically stable at relatively large time steps (Δt) and has second-order (Δx^2) accuracy. A Gauss-Seidel iterative technique employed to solve the system of equations requires an initial estimate or approximation of $G^{n+1}{}_{i,j}$, given by $g_{i,j}(\alpha = 0)$. In effect, Gauss-Seidel iteration provides a second-order refinement to the first-order explicit projection $g_{i,j}(\alpha = 0)$. Additional projection schemes developed in the model include an implicit projection, $f_{i,j}(\alpha = 0)$, and a Taylor first-order projection, defined as:

$$G_{i,j}^{n+1} = f_{i,j}(\alpha = 1) + \Delta t \left[\frac{f_{i,j}(\alpha = 1) - g_{i,j}(\alpha = 1)}{2} \right] \tag{27}$$

Although this two-staged approach for solving a system of equations requires more mathematical computations than the conventional explicit or implicit approach, a larger time step Δt can be specified, which decreases the overall computer-processing time.

2.3 Development of the Analytical Solutions

For simulating nonreactive, vertical gas transport in a relatively uniform unsaturated zone, R-UNSAT implements the following one-dimensional (Cartesian) version of (8):

$$\frac{\partial G_k}{\partial t} = \frac{D_k}{a_k} \frac{\partial^2 G_k}{\partial z^2} \tag{28}$$

To derive (28), the coefficients D_k and a_k are assumed to be constant with respect to time and space, which in turn implies that the physical properties of the unsaturated-zone sediments (total porosity, moisture content, and tortuosity) are temporally and spatially constant. Analytical solutions were developed to solve (28) on the basis of the boundary and initial conditions presented in the following section.

2.3.1 Boundary and Initial Conditions for the Analytical Solutions

The analytical solution was developed for two source-boundary conditions located at the water table: Option 1--a constant-flux boundary (J_{k_o}) characterized by Fick's Law as:

$$J_{k_o} = -D_k \frac{dG_k}{dz} \qquad \text{at } z = 0 \tag{29a}$$

and Option 2--a constant-concentration boundary (G_{k_o}) defined as:

$$G_{k_o} = G_k \qquad \text{at } z = 0. \tag{29b}$$

The upper boundary (ground surface) can be specified as either a constant-concentration boundary condition given by:

$$G_k = G_{k_U} \qquad \text{at } z = L \qquad (30a)$$

or a third-kind boundary condition analogous to a leaky confining unit given by:

$$D\frac{dG}{dz} = D'\left(\frac{G_{atm} - G}{b'}\right) \qquad \text{at } z = L \qquad (30b)$$

where

D_k' = effective-diffusion coefficient of the confining unit [cm^2/s]
b' = thickness of the confining unit [cm]
G_{kU} = constant concentration of the k^{th} constituent on the upper side of the confining unit [g/cm^3]

The initial condition can be specified as a constant value for the entire domain equal to the atmospheric concentration of the constituent, or as a spatially dependent condition given by:

$$G_k(z,0) = A_k(z) \qquad \text{at } 0 \le z \le L \qquad (31)$$

where $A_k(z)$ represents a piecewise linear function of the gas-concentration data collected at time t = 0.

2.3.2 One-Dimensional Analytical Solutions

Analytical solutions to (26) subject to one of the following sets of boundary conditions

case (1): constant flux (J_{ko}) (29a) at z = 0; constant concentration (30a) at z = L
case (2): constant concentration (G_{ko}) (29b) at z = 0; constant concentration (30a) at z = L
case (3): constant flux (J_{ko}) (29a) at z = 0; leaky confining unit (30b) at z = L
case (4): constant concentration (G_{ko}) (29b) at z = 0; leaky confining unit (30b) at z = L

and the initial condition (31) are obtained by applying the following separation-of-variables technique:

$$G_k(z,t) = v(z,t) + K(z) \qquad (32)$$

where v(z,t) is the transient component of the solution:

$$v(z,t) = \left\{\sum_{n=0}^{\infty} T_n(t)\, \phi_n(z)\right\} \qquad (33)$$

where

$$T_n(t) = C_n \exp\left(-\lambda_n \frac{D_k}{a_k} t\right)$$

$$\phi_n = \cos\sqrt{\lambda_n}\, z \qquad \text{cases 1 and 3}$$

$$\phi_n = \sin\sqrt{\lambda_n}\, z \qquad \text{cases 2 and 4}$$

In general,

$$C_n = \frac{2}{L}\int_0^L [A_k(z) - K(z)]\, \phi_n\, dz$$

where $A_k(z)$ is the initial condition consisting of m components, given by:

$$A_k(z) = \sum_{i=1}^{m} M_{k_i}^o\, z + B_{k_i}^o \tag{34}$$

and K(z) is the steady-state solution defined as:

$$K(z) = -\left(\frac{J_{k_0}}{D_k} z\right) + \left[J_{k_0}\left(\frac{L}{D_k}\right) + G_{k_U}\right] \qquad \text{case 1} \tag{35a}$$

$$K(z) = \left\{\frac{(G_{k_U} - G_{k_0})}{L}\right\} z + G_{k_o} \qquad \text{case 2} \tag{35b}$$

$$K(z) = -\left(\frac{J_{k_0}}{D_k} z\right) + \left[J_{k_0}\left(\frac{b'}{D_k'} + \frac{L}{D_k}\right) + G_{k_U}\right] \qquad \text{case 3} \tag{35c}$$

$$K(z) = \left\{\frac{(G_{k_U} - G_{k_0})}{L + \frac{D_k}{D_k'} b'}\right\} z + G_{k_o} \qquad \text{case 4} \tag{35d}$$

For each case, the constants C_n are defined more specifically as:

$$C_n = \frac{2}{L}\sum_{i=1}^{m} \left\{\frac{M_i}{\lambda_n}\left[\cos L\sqrt{\lambda_n} + L\sqrt{\lambda_n} \sin L\sqrt{\lambda_n} - 1\right] + \frac{B_i}{\lambda_n} \sin L\sqrt{\lambda_n}\right\}$$

cases 1 and 3

$$C_n = \frac{2}{L}\sum_{i=1}^{m}\left\{\frac{M_i}{\lambda_n}\left[\sin L\sqrt{\lambda_n} + L\sqrt{\lambda_n}\cos L\sqrt{\lambda_n}\right] + \left[\frac{B_i}{\lambda_n}\cos L\sqrt{\lambda_n} - 1\right]\right\}$$

cases 2 and 4

where

$$M_i = M_{k_i}^o + \frac{J_k}{D_k}$$ cases 1 and 3

$$M_i = M_{k_i}^o - \left[\frac{(G_{k_U} - G_{k_0})}{L}\right]$$ case 2

$$M_i = M_{k_i}^o - \left[\frac{(G_{k_U} - G_{k_0})}{L + \frac{D_k}{D_k'}b'}\right]$$ case 4

$$B_i = B_{k_i}^o - \left[J_k\left(\frac{L}{D_k}\right) + G_{k_U}\right]$$ case 1

$$B_i = B_{k_i}^o - G_{k_0}$$ cases 2 and 4

$$B_i = B_{k_i}^o - \left\{\left[J_k\left(\frac{b'}{D_k'} + \frac{L}{D_k}\right)\right] + G_{k_U}\right\}$$ case 3

The eigenvalues (λ_n) in each case are given by:

$$\sqrt{\lambda_n} = (2n-1)\frac{\pi}{2L}$$ case 1

$$\tan L\sqrt{\lambda_n} = \frac{\frac{D_k'}{b'}}{D_k\sqrt{\lambda_n}}$$ case 2

$$\tan L\sqrt{\lambda_n} = \frac{-D_k\sqrt{\lambda_n}}{\frac{D_k'}{b'}}$$ case 3

$$\sqrt{\lambda_n} = \frac{n\pi}{L}$$ case 4

For cases 1 and 2, the eigenvalues are determined numerically by using the Newton-Raphson method.

2.4 Constitutive Relations

2.4.1 Fick's Law and its Limitations

The mathematical solutions developed in R-UNSAT are based on Fick's Law of gas diffusion. The use of R-UNSAT can therefore be inappropriate for certain gas-transport applications where gaseous-phase advection is significant. Gaseous-phase advection caused by atmospheric-pressure variations is therefore assumed to be negligible. This hypothesis is reasonable because atmospherically induced advection is significant only while the pressure is fluctuating (Massmann and Farrier, 1992). Therefore, atmospheric-pressure fluctuations would have little effect on the reliability of gas-concentration data collected over several barometric cycles.

Gaseous-phase advection can also be caused by the generation of gases from biochemical reactions. This phenomenon can occur in the absence of a measurable pressure gradient (Thorstenson and Pollock, 1989). The Stefan-Maxwell transport model (Curtiss and Hirschfelder, 1949) presented below provides a reference for evaluating these limitations for an ideal-gas mixture near atmospheric pressure:

$$\nabla \chi_{ka} = \sum_{i=1,\, i \neq k}^{M} \frac{1}{cD_{ki}} \left(\chi_{ka} \frac{J_i}{\omega_i} - \chi_{ia} \frac{J_k}{\omega_k} \right) \tag{36}$$

where

J_i, J_k	=	total flux of the i^{th} and k^{th} gaseous-phase constituents, respectively	[g/cm²-s]
D_{ki}	=	effective-diffusion coefficient of the k^{th} gaseous-phase constituent in the mixture of i gaseous-phase constituents	[cm²/s]
χ_{ia}, χ_{ka}	=	mole fraction of the i^{th} and k^{th} constituents in the gaseous phase, respectively	[dimensionless]
ω_i , ω_k	=	molecular weights of the i^{th} and k^{h} gaseous-phase constituents	[g/mol]
c	=	gaseous-phase molar density	[g/cm³]
M	=	total number of gaseous-phase constituents	[dimensionless]

This model, unlike Fick's Law (2), is fully compositional. Moreover, J_k in equation (34) represents a total flux, given by:

$$J_k = -c\omega_k D_{ki} \nabla \chi_k + \chi_k \sum_{i=1,\, i \neq k}^{M} J_i \qquad k = 1,2...N \tag{37}$$

where the diffusive and advective components of flux are represented by the first and second terms on the right-hand side of the equation, respectively. As expressed in (37), the accuracy of Fick's Law as an estimator of the total flux depends on the relative magnitude of the advective-flux component, which is a function of the concentration of the diffusing species (χ_k) and the total

bulk-gas flow (ΣJ).

Many of the biochemical reactions that generate gases in the subsurface consume gases in the process. For example, the aerobic biodegradation reaction involves both CO_2 production and O_2 utilization. The near-equimolar production and utilization of these gases prevents the establishment of significant pressure gradients. Fick's Law has been proven valid for such cases (Lahvis and Baehr, 1996). Fick's Law can degenerate, however, if the ratio of O_2 utilization to CO_2 production becomes increasingly disproportionate.

To gauge the adequacy of Fick's Law, the following definition of relative error was developed by assuming that the Stefan-Maxwell equations define the true estimate of flux (Lahvis and Baehr, 1996):

$$\varepsilon_J = \frac{J_{Fick} - J_{SM}}{J_{SM}} \tag{38}$$

where

ε_J	=	relative error	[dimensionless]
J_{SM}	=	total flux of the gaseous-phase constituent, respectively	[g/cm²-s]
J_{Fick}	=	diffusive flux of the gaseous-phase constituent, respectively	[g/cm²-s]

The relative error associated with Fick's Law for a range of flux values is shown in figure 7, where the diffusive flux is expressed as the following dimensionless parameter:

$$J^* = \frac{J_k L}{c\omega_k D_k} \tag{39}$$

In (39), the diffusion coefficient (D_k) is constant and is defined at the source ($z = 0$).

2.4.2 Diffusion-Coefficient Determination

In equation (5) in Section 2.1, the gaseous-phase diffusivity (d_{ka}) is a measure of the rate of gaseous diffusion into a bulk-gaseous phase and is defined as (Bird and others, 1960):

$$d_{ka} = \frac{1 - \chi_k}{\sum_{i=1,\, i \neq k}^{N} \frac{\chi_i}{d_{ki}}} \qquad k = 1,2...N \tag{40}$$

where

d_{ki}	=	binary diffusivity of the k^{th} and i^{th} constituents in a mixture of N gaseous-phase constituents	[cm²/s]

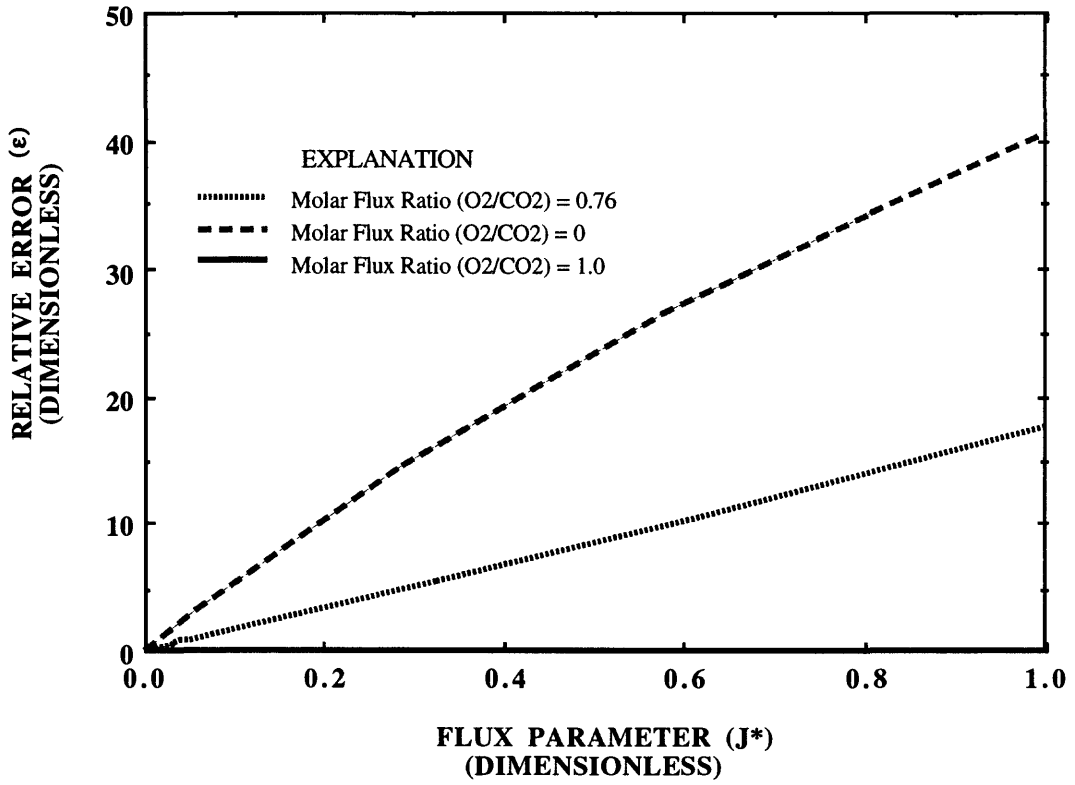

Figure 7. Nomograph of the relative error in the mass-flux estimate if Fick's Law is used to define reactive gas transport associated with aerobic biodegradation.

The binary diffusivity (d_{ka}) in the gaseous phase is temperature- and pressure-dependent and is modeled according to the following method described by Fuller and others (1966):

$$d_{ki} = \frac{0.00143\ T^{1.75}}{P(M_g)^{0.5}\ (\zeta^{1/3} + \zeta^{1/3})^2} \quad \text{and} \quad M_g = 2(\omega_k^{-1} + \omega_i^{-1})^{-1} \qquad k = 1,2...N \quad (41)$$

where

d_{ki}	=	binary gaseous-phase diffusivity	[cm^2/s]
T	=	temperature	[K]
P	=	pressure	[bars]
ω_i, ω_k	=	molecular weights of the i^{th} and k^{th} gaseous-phase constituents	[g/mol]
ζ_i, ζ_k	=	atomic diffusion volumes of the i^{th} and k^{th} gaseous-phase constituents (see table 1)	[dimensionless]

A compilation of atomic diffusion volume data is presented in table 1. These data can be summed to compute ζ for more complex constituents [for example, toluene (C_7H_8)] as follows:

$$\zeta_{C_7H_8} = 7(15.9) + 8(2.31) - 18.3 = 111.5 \quad (42)$$

For many applications, air is considered to be a chemical species for calculating d_{ki}. The ζ value reported for air in table 1 is based on a mole fraction composition of $N_2 = 0.79$ and $O_2 = 0.21$.

Table 1. Diffusion volumes and structural increments for selected compounds of environmental interest
[Data from Reid and others (1987)]

Chemical species	Diffusion volume
ζ_i for simple molecules	
N_2	18.5
O_2	16.3
CO	18.0
CO_2	26.9
NO	35.9
NH_3	20.7
H_20	13.1
air	19.7
$\Delta\zeta$ structural increments ($\zeta_i = \Sigma\ \Delta\zeta$)	
C	15.9
H	2.31
O	6.11
N	4.54
Aromatic ring	-18.3
Heterocyclic ring	-18.3
Cl	21.0
S	22.9

The tortuosity (τ) is a function of the fluid-phase saturation and can range over several orders of magnitude in unsaturated-zone sediments. No universal relation exists, however, to adequately define this parameter for natural sediments because of the complexity of the sediment-pore structures. In R-UNSAT, this parameter can be user-specified or, in the absence of tortuosity data, computed according to the following model developed by Millington (1959):

$$\tau = \frac{\theta_f^{7/3}}{\phi^2} \tag{43}$$

where

θ_f = fluid-filled porosity [dimensionless]
ϕ = total porosity [dimensionless]

Bruell and Hoag (1986) found that the Millington (1959) model best described gaseous-phase tortuosity for diffusion experiments conducted with gasoline-range hydrocarbons in sands near field-capacity moisture. These tortuosity relations can degenerate however, if applied to fine-grained or highly-saturated sediments (Reibel and Shair, 1982; Fischer and others, 1996).

Aqueous-phase diffusion is about four orders of magnitude less than gaseous-phase diffusion. Thus, aqueous-phase diffusivity (d_{kw}) is relatively insignificant unless the pore space is nearly saturated. In R-UNSAT, d_{kw} is modeled as a constant equal to 1.0E-05 cm^2/s. If aqueous-phase diffusion is important, the user can compute d_{kw} by employing the following correlation equation developed by Wilke and Chang (1955):

$$d_{kw} = \frac{3.14E{-}07\ T}{\eta\ V_k^{0.6}} \tag{44}$$

where

T	=	temperature	[Kelvin]
η	=	viscosity of water (see table 2)	[cP]
V_k	=	molar volume of the k^{th} constituent	[cm^3/mol]

The molar volume can be determined from critical-volume data by applying the following method developed by Tyn and Calus (1975):

$$V_k = 0.285\ V_c^{1.048} \tag{45}$$

where

V_c	=	critical volume (see table 3)	[cm^3/mol]

Table 2. Viscosity of water at temperatures from 0 to 25 degrees Celsius

Temperature (degrees Celsius)	Viscosity (centipoise)
0	1.73
5	1.50
10	1.31
15	1.15
20	1.02
25	.91

Table 3. Critical volumes for selected compounds of environmental interest

Chemical species	Critical volume (dimensionless)
O_2	73.4
N_2	89.8
CO_2	93.9
CH_4	99.2
Benzene	259
o-Xylene	369
Ethylbenzene	374
Tri-methylbenzene	490

2.4.3 Equilibrium Relations

Raoult's Law is used to describe the partitioning between the gaseous and immiscible phases. The law states that the partial pressure of a constituent in an ideal solution is linearly related to the vapor pressure of the pure constituent and its mole fraction in the immiscible phase as follows:

$$P_k = P_k^o \chi_k \qquad k = 1,2...N \qquad (46)$$

where

P_k = partial pressure of the k^{th} constituent [bars]
P_k^o = vapor pressure of the k^{th} constituent [bars]
χ_k = mole fraction of the k^{th} constituent in the immiscible phase [dimensionless]

Many correlation equations for estimating (P_k^o) are cited in the literature (for example, Antoine equation, Clapeyron equation). The partial pressure (P_k) can be expressed as an equivalent gaseous-phase concentration by applying the ideal-gas law,

$$G_k = \frac{\omega_k}{RT} P_k \qquad k = 1,2...N \qquad (47)$$

where

R = ideal gas law constant [atm-l/mol-K]
T = temperature [K]

Raoult's Law holds for any χ_k provided the solution remains ideal. Substituting (46) into (47) results in the boundary condition referred to as Option 3 (see Section 2.2.1).

$$G_k = H_k^o \chi_k(t) \text{ and } H_k^o = \frac{\omega_k}{RT} P_k^o \qquad k = 1,2...N \qquad (48)$$

where

H_k^o = saturated vapor concentration of the pure k^{th} constituent [g/cm³]

The mole fraction in the immiscible phase (χ_k) is defined as:

$$\chi_k(t) = \frac{\frac{1}{\omega_k} I_k(t)}{\sum_{j=1}^{N} \frac{1}{\omega_j} I_j(t)} \qquad (49)$$

where

I_j, I_k = time-dependent concentration of the j^{th} and k^{th} constituents in the immiscible phase [g/cm³]

Substituting (49) into (48) yields the desired relation between the gaseous- and immiscible-phase concentrations:

$$G_k(r,z,t) = \left[H_k^o \left(\frac{1}{\omega_k \sum_{j=1}^{N} \frac{1}{\omega_j} I_j(t)} \right) \right] I_k(t) \qquad (50)$$

Henry's Law is used to define equilibrium partitioning between the gaseous and aqueous phases, and is defined as:

$$G_k = H_k C_k \qquad k = 1,2...N \qquad (51)$$

where

H_k = Henry's Law constant of the k^{th} constituent [dimensionless]

Henry's Law adequately describes air/water partitioning for slightly soluble, non-electrolyte constituents up to a pressure ≈ 1 bar, assuming an ideal gas phase (Alberty, 1987). The equilibrium relation (51) is uncoupled (that is, independent of composition).

Equilibrium partitioning between the aqueous and solid phases is modeled by assuming a linear isotherm relation given by:

$$S_k = K_k C_k \qquad k = 1,2...N \qquad (52)$$

where

K_k = adsorption isotherm coefficient of the k^{th} constituent [cm^3/g]

Because the relative humidity of the bulk gaseous phase is generally between 98 and 100 percent (Hanks and Ashcroft, 1980), direct partitioning between the gaseous and solid phases is neglected. Gaseous/solid-phase partitioning is then described by the following coupled expression involving Henry's Law (51) and the linear isotherm (52):

$$S_k = K_k \frac{G_k}{H_k} \qquad k = 1,2...N \qquad (53)$$

2.4.4 Reaction-Rate Determination

The reaction term (R_k) in the conservation-of-mass equation (1) represents the gain or loss of mass resulting from biogeochemical reactions in the unsaturated zone. In R-UNSAT, these reactions can be simulated by assuming zero- or first-order kinetics. A single reactant can be rate-limiting or reaction rates can be coupled. For example, the production rate of one compound can be defined by the consumption rate of another. If the available kinetics models are not appropriate, the user may substitute his or her own model directly into the computer program. The modular format of the FORTRAN code easily accommodates this type of modification (see Section 3.2.1).

In hydrocarbon-transport investigations, R_k is customarily used to simulate the mass loss from biodegradation. Although the magnitude of R_k can vary depending on the supply of hydrocarbon (substrate) or biomass and nutrient concentrations; the availability of oxygen, the electron acceptor, generally governs the rate of the biotransformation (Borden and Bedient, 1986). The biodegradation of a generic hydrocarbon (C_nH_m) in the presence of oxygen (O_2) can be expressed as:

$$C_n H_m + (n + 0.25m) O_2 \rightarrow n CO_2 + (0.5m) H_2O \qquad (54)$$

By assuming that the aerobic-degradation reaction (54) goes to completion, the mass of O_2 consumed can be stoichiometrically related to the mass of hydrocarbon degraded as follows:

$$R_k = \frac{R_{O_2}}{r_{O_2}} \qquad (55)$$

where

r_{O2} = stoichiometric mass constant [dimensionless]

The coefficient (r_{O2}) is related to the dissolved-hydrocarbon composition and is relatively constant for a wide range of hydrocarbon compounds (see table 4). A first-order kinetics model is available in R-UNSAT to compute R_k by simulating O_2 transport independently and imposing an upper-bound estimate equal to the lesser of either the stoichiometric equivalent of available O_2 in the aqueous phase:

$$R_k = -\alpha \frac{C_{O_2}}{r_{O_2}} \tag{56}$$

where

α = first-order rate constant [1/s]

or a fraction of the hydrocarbon present in the aqueous phase:

$$R_k = -\alpha\, C_k \tag{57}$$

The value of α is defined by the user in the model input. A representative value for the mineralization of benzene, toluene, ethylbenzene, and xylenes (BTEX) compounds under aerobic conditions is α = 1.0E-6 1/s (Landmeyer and others, 1996).

Table 4. Stoichiometric constants (r_{O2}) for selected hydrocarbon compounds of environmental interest

Hydrocarbon compound	r_{O2} (dimensionless)
C_6 aromatics (for example, benzene)	3.08
C_7 aromatics (for example, toluene)	3.13
C_8 aromatics (for example, xylene)	3.17
C_9 - C_{11} aromatics (for example, trimethyl benzene)	3.22
C_5 - C_6 alkanes (for example, hexane)	3.43
C_7 - C_{11} alkanes (for example, octane, decane)	3.51
C_6 alkenes (for example, hexene)	3.43
C_6 napthenes	3.43

SECTION 3.0--R-UNSAT BASIC OPERATIONS AND DATA FILES

3.1 R-UNSAT Basic Operations

R-UNSAT is a computer program designed to implement the diffusive-transport model described in Section 2. The model can be used in a calibration mode to quantify gas fluxes from experimental gas-concentration data or in a predictive mode to estimate gas fluxes and gaseous-phase concentrations as a function of time and space within an aquifer system.

The computer code is written in FORTRAN 77 and runs on a variety of computer systems including mainframes and personal computers with only minor changes. R-UNSAT employs a modular structure, which facilitates modifications to the source code. Whenever these modifications are made, the program must be recompiled with a FORTRAN 77 compiler to incorporate the changes in the executable version of the program code. The commands needed to compile and link R-UNSAT depend on the computer system and the type of compiler being used. The procedures for mainframe and personal computers are given below:

1. Copy the files from the website address onto your computer.
2. Compile and execute the source code.

If a Microsoft®[2] FORTRAN compiler is used, the command is:

```
FL R-UNSAT.FOR
```

If a PRIME® 6450 mainframe computer is used, the sequence of commands is:

```
F77 R-UNSAT.F77  -BIG
&DATA SEG -LOAD
LOAD R-UNSAT
LI
SA
QU
&END
SEG R-UNSAT
```

To execute the program on a mainframe computer, type:

```
SEG R-UNSAT
```

To execute the program on an IBM® personal computer, enter the directory containing the executable or compiled version of the program (for example, R-UNSAT.EXE) and, at the prompt, type:

```
R-UNSAT
```

A menu appears prompting the user to select the appropriate application.

After R-UNSAT has been invoked, a menu will appear on the screen offering the following options:

[2] Use of trade names in this report is for identification purposes only and does not constitute endorsement by the U. S. Geological Survey.

```
-------------------------------------------------------------------------------------------------------------
      R-UNSAT: A COMPUTER MODEL FOR THE SIMULATION OF REACTIVE,
        MULTISPECIES TRANSPORT IN THE UNSATURATED ZONE (Ver 1.0)

              DEVELOPED BY:  MATTHEW A. LAHVIS
                             ARTHUR L. BAEHR
-------------------------------------------------------------------------------------------------------------


 SELECT:
              1:  TO CREATE NEW MODEL INPUT DATA
              2:  TO RUN R-UNSAT USING EXISTING MODEL INPUT
```

To execute R-UNSAT requires formatted input files, which can be created by selecting Option 1. Option 1 prompts the user to choose an appropriate mathematical solver and then to input the parameter values for the given model application and the names of any data files used for the entry of spatially dependent input data. These data are then incorporated into a main input file (MIF) and supplemental map files, formatted for use in R-UNSAT. Modifications to these formatted files can be achieved by invoking a system text editor, provided the file layouts and contents correspond to the formats discussed in the following section.

R-UNSAT can be executed by selecting Option 2 and specifying the name of the MIF. Depending on the mathematical solver, the complexity of the model application, and the computer's math coprocessing capabilities, execution times for model simulations can range from a few seconds to several hours. Analytical-solution applications generally last less than 1 minute. The run time for numerical-solution applications is a function of the time step, number of grid points, and error (tolerance) criterion. When model calibrations are conducted with the numerical solutions, use of a relatively large time step and a relaxed error criterion for the initial calibrations will reduce overall computation times. The results of these initial calibrations can then be used in subsequent simulations to refine the parameter search and thereby avoid the large computation times associated with poor initial estimates. In addition, all mathematical calculations are performed in double precision. This can become burdensome for small computing systems. The following statement can be removed from each subroutine or commented out to calculate in single precision:

```
IMPLICIT DOUBLE PRECISION (A-H, O-Z)
```

Output data are written as concentration as a function of time, concentration as a function of distance, and flux as a function of time. The names of all output files, with the exception of flux as a function of time files (for example, FLXDT.xx), are determined by the user.

3.2 R-UNSAT Input Files

Formatted input files are required to execute R-UNSAT. Details of the file format and contents for creating or modifying the input data are presented in this section.

3.2.1 Numerical Solution Input

If the numerical solver is chosen under Option 1, R-UNSAT will prompt the user to specify

model input for the MIF. The model input for the numerical solution falls into the following categories:

- model-domain parameters
- constituent properties
- boundary and initial conditions
- physical properties of the sediments
- algorithm parameters
- output parameters

A summary of the input variables for the numerical solutions is presented in appendix 1. All input variables are required to be in CGS units unless otherwise specified.

An example MIF input file is given below:

```
INPUT RECORDS

|----|----|----|----|----|----|----|----|----|----|----|----|----|----|----|----|
0    5   10   15   20   25   30   35   40   45   50   55   60   65   70   75   80

             1
********************************************************************************
                            NUMERICAL MODEL INPUT
********************************************************************************

TITLE -  TEST.NUMERICAL

  VALUE     MODEL CODE          DEFINITION        [cgs units]
            DESIGNATION
  -----     ----------          ----------        -----------

*************************** MODEL DOMAIN PARAMETERS ****************************

    1         (IDIM)           MODEL DIMENSIONALITY
                                 1: 1-D VERTICAL (z - DIRECTION)
                                 2: 1-D RADIAL (r - DIRECTION)
                                 3: 2-D (r,z DIRECTIONS)
0.1000E+07    (CSA)            CROSS-SECTIONAL AREA [cm]
0.1000E+03    (ZSURF)          LENGTH OF DOMAIN IN z - DIRECTION [cm]
   11         (NZ)             NUMBER OF NODES IN z - DIRECTION
0.1000E+02    (DZ)             NODAL SPACING IN THE VERTICAL DIRECTION [cm]
0.1000E+02    (TEMP)           UNSATURATED-ZONE TEMPERATURE [C]
0.1000E+01    (ATM)            UNSATURATED-ZONE PRESSURE [mm Hg]
0.1000E+01    (DARCY)          RECHARGE RATE [cm/yr]
    1         (IDISP)          AQUEOUS-PHASE DISPERSION OPTION
                                 0: NEGLECT AQUEOUS-PHASE DISPERSION
                                 1: ACCOUNT FOR AQUEOUS-PHASE DISPERSION

*************************** CONSTITUENT PROPERTIES *****************************

    2         (NK)             NUMBER OF MODEL CONSTITUENTS

------------------------------- CONSTITUENT  1 -------------------------------

    2         (ICON)           CONSTITUENT INDEX FOR: OXYGEN
```

```
0.3200E+02   (WK(IK))        MOLECULAR WEIGHT OF CONSTITUENT [g]
0.1630E+02   (DV(IK))        ATOMIC DIFFUSION VOLUME [dimensionless]
0.3160E+02   (HAW(IK))       HENRYS LAW PARTITION COEFFICIENT (air/water)
                               [dimensionless]
0.2790E-03   (ATCONC(IK))    GAS-PHASE CONCENTRATION ABOVE UPPER
                             BOUNDARY [g/cm3]

-------------------------------- CONSTITUENT  2 --------------------------------

    3        (ICON)          CONSTITUENT INDEX FOR: NITROGEN
0.2802E+02   (WK(IK))        MOLECULAR WEIGHT OF CONSTITUENT [g]
0.1850E+02   (DV(IK))        ATOMIC DIFFUSION VOLUME [dimensionless]
0.6000E+02   (HAW(IK))       HENRYS LAW PARTITION COEFFICIENT (air/water)
                               [dimensionless]
0.9100E-03   (ATCONC(IK))    GAS-PHASE CONCENTRATION ABOVE UPPER
                             BOUNDARY [g/cm3]

********************** BOUNDARY AND INITIAL CONDITIONS ***********************

    1        (IOPT)          SOURCE BOUNDARY CONDITION OPTION
                               1: SPECIFIED FLUX AT WATER TABLE
                               2: SPECIFIED CONCENTRATION AT WATER TABLE
                               3: HYDROCARBON PLUME ABOVE WATER TABLE
                               4: CONSTANT FLUX FROM INJECTION PROBE

-------------------------------- CONSTITUENT  1 --------------------------------

-.1000E-07   (FLX(IR,IK))    GAS FLUX ACROSS WATER TABLE [g/cm2-s]

-------------------------------- CONSTITUENT  2 --------------------------------

0.0000E+00   (FLX(IR,IK))    GAS FLUX ACROSS WATER TABLE [g/cm2-s]

--------------------------------------------------------------------------------

    0        (ISURF)         UPPER BOUNDARY CHARACTERIZATION
                               0: UNIFORM
                               1: VARIABLE
0.1000E+01   (AR2)           BOUNDARY CONDITION PARAMETER: GROUND SURFACE

*** DISCRETIZED INITIAL CONDITION DATA CONTAINED IN FILE-"IC.MAP"

***************************** SEDIMENT PROPERTIES ******************************

    0        (ISTRAT)        HOMOGENEOUS UNSATURATED ZONE
0.3800E+00   (POR(IL))       POROSITY OF UNSATURATED ZONE [dimensionless]
0.2200E+00   (THW(IL))       MOISTURE CONTENT OF UNSAT. ZONE [dimensionless]
0.5600E-01   (TA(IL))        TORTUOSITY [dimensionless]
0.1000E-09   (AL(IL))        LONGITUDINAL DISPERSIVITY [cm]
0.1000E-09   (ALT(IL))       TRANSVERSE DISPERSIVITY [cm]
0.1500E+01   (BD(IL))        BULK DENSITY [g/cm3]

***************************** MODELING PARAMETERS ******************************

    0        (ITIME)         TIME-STEP ADJUSTMENT OPTION
                               0: CONSTANT TIME-STEP
                               1: VARIABLE TIME-STEP
0.1000E+01   (DT1)           TIME-STEP [hrs]
0.1000E+04   (TEND)          ENDING TIME [hrs]
```

```
    0         (ISS)           STEADY-STATE DEFAULT OPTION
                                0: DO NOT ZERO-OUT STORAGE TERM
                                1: ZERO-OUT STORAGE TERM
  500         (NITER)         MAX. # OF ITERATIONS PER TIME STEP
0.1000E-02    (EPS)           CONVERGENCE CRITERIA - ACCEPTABLE MAX.
                                RELATIVE ERROR
    0         (IPROJ)         MATRIX-SOLVER SEED
                                0: PREVIOUS TIME-STEP
                                1: LINEAR PROJECTION FROM PREVIOUS TIME-STEP
                                2: DIRECT PROJECTION

****************************** OUTPUT PARAMETERS ********************************

    1         (IOUT)          OUTPUT OPTION
                                0: CONCENTRATION VS. TIME (breakthrough)
                                1: CONCENTRATION VS. DISTANCE (snapshot)
    0         (ISNAP)         SNAPSHOT OPTION
                                0: ENTIRE DOMAIN
                                1: AT SPECIFIC LOCATIONS
0.1000E+04    (TSNAP)         TIME [hrs] FOR SNAPSHOT

-------------------------------- CONSTITUENT  1 --------------------------------

    1         (IOUTOPT(IK))   OUTPUT OPTION
                                0: NO OUTPUT DATA REQUESTED
                                1: OUTPUT DATA REQUESTED

  *** OUTPUT DATA (t,G) [hrs,g/cm3] CONTAINED IN FILE-OUT.NUM

-------------------------------- CONSTITUENT  2 --------------------------------

    0         (IOUTOPT(IK))   OUTPUT OPTION
                                0: NO OUTPUT DATA REQUESTED
                                1: OUTPUT DATA REQUESTED

--------------------------------------------------------------------------------


************************** MODEL DOMAIN COORDINATES ***************************

  564         (R(NR))         r - COORDINATE: OUTER BOUNDARY [cm]
  564         (R(IRIM))       r - COORDINATE: RADIUS OF SOURCE [cm]g
  100         (Z(NZ))         z - COORDINATE: SURFACE BOUNDARY [cm]
    0         (Z(IZLOW))      z - COORDINATE: LOWER SOURCE BOUNDARY [cm]
   10         (Z(IZHI))       z - COORDINATE: UPPER SOURCE BOUNDARY [cm]
--------------------------------------------------------------------------------
```

Once the MIF has been created, the parameter values can be modified for subsequent model runs by overwriting the values formatted within the first 10 input records. A new MIF must be created if the model geometry is varied.

Data files can be used for the entry of spatially dependent input data in the following categories:

- source boundary condition [3]
- initial condition
- physical properties of the sediments
  - total porosity
  - moisture content
  - gaseous-phase tortuosity
  - bulk density

The file names of all raw input files are specified by the user in the MIF. The sequencing and arrangement of variables within the data file must comply with the designated model format. In addition, all input data are required to be in CGS units. Specifications for each data file are given below, and are followed by an example:

FILE: SOURCE BOUNDARY CONDITION

FILE NAME: user-specified (for example, BC.DAT)
UNIT NUMBER: 50
FILE DESCRIPTION: source boundary-condition data for Option 1 (constant flux) and Option 2 (constant concentration)

LINE NUMBER	VARIABLE	FORMAT	DEFINITION
1	ICOUNT, NDAT	free-formatted	constituent index, number of data points contained in data file
2... (NDAT+1)	XPT(IDAT), YPT(IDAT)	free-formatted	location of data point along radial axis, value of data point (for example, flux, concentration)

EXAMPLE FILE: BC.DAT (RIM = 50, NR = 6, ΔR = 10)

LINE NUMBER	VARIABLE	INPUT RECORDS
		|----|----|----|----|----|----|----|----|----|----|
		0 5 10 15 20 25 30 35 40 45 50
1	ICOUNT, NDAT---------	1 2
2	XPT(IDAT),YPT(IDAT)--	0 100E-6
3	----------	50 200E-6
4	ICOUNT,NDAT----------	2 4
5	XPT(IDAT),YPT(IDAT)--	0 5E-5
6	----------	14 150E-5
7	----------	32 250E-5
8	----------	50 300E-5

---

[3] Available only with source boundary condition Option 1 (specified flux) and Option 2 (constant concentration).

FILE: INITIAL CONDITION

FILE NAME: user-specified (for example, IC.DAT)
UNIT NUMBER: 51
FILE DESCRIPTION: initial-condition data (varying spatially in both the radial and vertical directions)

LINE NUMBER	VARIABLE	FORMAT	DEFINITION
1	ICOUNT	free-formatted	constituent index
2... NZ	Y0(IR,IZ,IK)	(10G10.4)	gaseous-phase concentration of constituent (ICOUNT). Data must be written in an array format of dimensions (NR,NZ) (for example, NR = 10, NZ = 4; see example below)

EXAMPLE FILE: IC.DAT (NR = 5, NZ = 4)

LINE NUMBER	VARIABLE	INPUT RECORDS |----|----|----|----|----|----|----|----|----|----| 0 5 10 15 20 25 30 35 40 45 50					
1	ICOUNT----------	1					
2	Y0(IR,IZ,IK)---------	20E-6	20E-6	10E-6	10E-6	10E-6	
3	----------	30E-6	20E-6	20E-6	10E-6	10E-6	
4	----------	30E-6	30E-6	20E-6	20E-6	10E-6	
5	----------	30E-6	30E-6	30E-6	20E-6	20E-6	
6	ICOUNT----------	2					
7	Y0(IR,IZ,IK)---------	20E-5	30E-5	30E-5	30E-5	30E-5	
8	----------	10E-5	20E-5	20E-5	30E-5	30E-5	
9	----------	10E-5	10E-5	20E-5	20E-5	30E-5	
10	----------	10E-5	10E-5	10E-5	20E-5	20E-5	

FILE: TOTAL POROSITY

FILE NAME: user-specified (for example, POR.DAT)
UNIT NUMBER: 52
FILE DESCRIPTION: total-porosity data

FILE: MOISTURE CONTENT

FILE NAME: user-specified (for example, WAT.DAT)
UNIT NUMBER: 53
FILE DESCRIPTION: moisture-content data

FILE: GASEOUS-PHASE TORTUOSITY

FILE NAME: user-specified (for example, TA.DAT)
UNIT NUMBER: 54
FILE DESCRIPTION: gaseous-phase-tortuosity data

FILE: BULK DENSITY

FILE NAME: user-specified (for example, BD.DAT)
UNIT NUMBER: 55
FILE DESCRIPTION: bulk-density data

NUMBER	VARIABLE	FORMAT	DEFINITION
1	NDAT	free-formatted	number of data points contained in data file
2... (NDAT+1)	XPT(IDAT), YPT(IDAT)	free-formatted	location of data point along vertical axis, value of data point (for example, porosity, moisture content, gaseous-phase tortuosity, bulk density)

EXAMPLE FILE: POR.DAT (ZSURF = 100, NZ = 6, ΔZ = 20)

```
LINE                                INPUT RECORDS
NUMBER    VARIABLE                  |----|----|----|----|----|----|----|----|----|----|
                                    0    5   10   15   20   25   30   35   40   45   50

   1      NDAT----------------- 6
   2      XPT(IDAT),YPT(IDAT)-- 0   0.380
   3      --------------------- 20  0.225
   4      --------------------- 40  0.334
   5      --------------------- 60  0.288
   6      --------------------- 80  0.380
   7      --------------------- 100 0.376
```

All files used to enter input data should be located in the same directory as the executable program file. Certain computer platforms can, however, allow data files to be accessed from sub-directories provided the full path name is specified.

The file names and unit numbers of formatted map files generated by execution of Option 1 are given in table 5. The formatted data are written in one- and two-dimensional (r,z) arrays for use in R-UNSAT. The following are examples of formatted map files created from the example input files presented above:

EXAMPLE FILE: BC.MAP

```
LINE      INPUT RECORDS
NUMBER    |----|----|----|----|----|----|----|----|----|----|----|----|----|----|----|----|
          0    5   10   15   20   25   30   35   40   45   50   55   60   65   70   75   80

   1                    1
   2       0.1000E-03 0.1000E-03 0.1000E-03 0.1000E-03 0.1000E-03 0.2000E-03
   3                    2
   4       0.5000E-04 0.1500E-02 0.1500E-02 0.2500E-02 0.2500E-02 0.3000E-02
```

Table 5. Summary of formatted data files and corresponding unit numbers for the computer model R-UNSAT

File name	File description	F77 Format	Unit number	Units
Z-SPACE	node locations in z direction	(10G11.4)	6	cm
R-SPACE	node locations in r direction	(10G11.4)	7	cm
BC.MAP	source boundary-condition data	(10G11.4)	60	g/cm^2 (Option 1) g/cm^3 (Option 2)
IC.MAP	initial-condition data	(10G11.4)	61	g/cm^3
DKA.MAP	gaseous-phase diffusivity data	(10G11.4)	62	cm^2/s
POR.MAP	total-porosity data	(10G11.4)	63	dimensionless
THW.MAP	aqueous-phase porosity data	(10G11.4)	64	dimensionless
THA.MAP	gaseous-phase porosity data	(10G11.4)	65	dimensionless
TA.MAP	gaseous-phase tortuosity data	(10G11.4)	66	dimensionless
TW.MAP	aqueous-phase tortuosity data	(10G11.4)	67	dimensionless
BD.MAP	bulk-density data	(10G11.4)	68	g/cm^3

EXAMPLE FILE: IC.MAP

```
LINE     INPUT RECORDS
NUMBER   |----|----|----|----|----|----|----|----|----|----|----|----|----|----|----|----|
         0    5   10   15   20   25   30   35   40   45   50   55   60   65   70   75   80

  1                 1
  2       0.2000E-04 0.2000E-04 0.1000E-04 0.1000E-04 0.1000E-04 0.1000E-04
  3       0.3000E-04 0.2000E-04 0.2000E-04 0.1000E-04 0.1000E-04 0.1000E-04
  4       0.3000E-04 0.3000E-04 0.2000E-04 0.2000E-04 0.1000E-04 0.1000E-04
  5       0.3000E-04 0.3000E-04 0.3000E-04 0.2000E-04 0.2000E-04 0.1000E-04
  6                 2
  7       0.2000E-03 0.2000E-03 0.3000E-03 0.3000E-03 0.3000E-03 0.3000E-03
  8       0.1000E-03 0.2000E-03 0.2000E-03 0.3000E-03 0.3000E-03 0.3000E-03
  9       0.1000E-03 0.1000E-03 0.2000E-03 0.2000E-03 0.3000E-03 0.3000E-03
 10       0.1000E-03 0.1000E-03 0.1000E-03 0.2000E-03 0.2000E-03 0.3000E-03
```

EXAMPLE FILE: POR.MAP

```
LINE     INPUT RECORDS
NUMBER   |----|----|----|----|----|----|----|----|----|----|----|----|----|----|----|----|
         0    5   10   15   20   25   30   35   40   45   50   55   60   65   70   75   80

  1       0.3800E-00 0.2250E-00 0.3340E-00 0.2880E-00 0.3800E-00 0.3760E-00
```

The data contained within these files can also be modified for subsequent model runs provided the modifications are consistent with the formats specified in table 5.

As stated previously in Section 2.4.4, the numerical solution incorporates a reaction-rate model (R_k) to simulate hydrocarbon-mass loss associated with biodegradation. In R-UNSAT, the magnitude of R_k is determined in the model subroutine BIO1. To apply this model, O_2 is modeled as an additional gaseous-phase constituent by assuming a conservation of mass and equilibrium partitioning according to Henry's Law. O_2 must be designated in the MIF as the last (n^{th}) modeled constituent. The user should note, however, that several reaction-rate models are available in the literature to characterize the biodegradation process. A subroutine BIO2 has been incorporated in the numerical algorithm to accommodate user-specified reaction-rate models. Within this subroutine, the user is required to develop the FORTRAN 77 code to define the variable RBIO(IR,IZ), which is passed between the subroutine and the main calling subroutine BIO. The indices IR and IZ imply that R_k is spatially dependent in the r and z directions, respectively.

3.2.2 Analytical Solution Input

Model input for the analytical solutions falls into the following categories:

- boundary and initial conditions
- constituent properties
- physical properties of the sediments
- output parameters

A summary of the input variables for the analytical solutions is presented in appendix 2. Again, all input variables are required to be in CGS units unless otherwise specified. As previously stated, once the MIF has been created, the parameter values can be modified for subsequent model runs by overwriting the values formatted within the first 10 input records.

The following is an example of an MIF input file for the analytical solutions:

```
INPUT RECORDS
|----|----|----|----|----|----|----|----|----|----|----|----|----|----|----|----|
0    5   10   15   20   25   30   35   40   45   50   55   60   65   70   75   80

            2
********************************************************************************
                              ANALYTICAL MODEL INPUT
********************************************************************************

TITLE -  TEST.ANALYTICAL

  VALUE     MODEL CODE          DEFINITION        [cgs units]
            DESIGNATION
  -----     ----------          ----------        ---------

************************ BOUNDARY AND INITIAL CONDITIONS ************************

    1         (IBC0)       BOUNDARY CONDITION OPTION
0.1000E-09    (FLUX)       GAS FLUX AT THE WATER TABLE (z = 0) [g/cm2-s]
0.3000E-01    (UP)         GAS-PHASE CONCENTRATION AT (z = L) [mg/l]
    1         (INOPT)      INITIAL CONDITION OPTION
                             0: CONSTANT
```

```
                              1: LINEARLY VARIABLE
                              2: INITIAL CONDITION SPECIFIED IN SEPARATE
                                 INPUT FILE OF TYPE: [z(cm),G(mg/l)]
0.5000E-01    (XB0)        INITIAL CONCENTRATION OF CONSTITUENT AT z = 0 [mg/l]

********************* PHYSICAL PROPERTIES OF THE CONSTITUENT *********************

0.1261E+00    (DBIN)       DIFFUSIVITY OF CONSTITUENT IN BULK GAS PHASE [cm2/s]
0.3030E+02    (HENRY)      HENRYS LAW PARTITION COEFFICIENT (air/water)
                             [dimensionless]
0.2000E-02    (SWPC)       ADSORPTION COEFFICIENT (soil/water) [dimensionless]

***************************** LITHOLOGIC PROPERTIES ******************************

0.1000E+03    (XL)         LENGTH OF MODEL DOMAIN [cm]
0.3300E+00    (VOID)       POROSITY [dimensionless]
0.2400E+00    (WAT)        AQUEOUS-PHASE POROSITY [dimensionless]
0.9000E-01    (AIR)        GASEOUS-PHASE POROSITY [dimensionless]
0.3333E-01    (TOR)        TORTUOSITY [dimensionless]
0.1400E+01    (BULK)       BULK DENSITY [dimensionless]
0.3783E-03    (DEFF)       EFFECTIVE-DIFFUSION COEFFICIENT [cm2/s]

****************************** OUTPUT PARAMETERS *******************************

    1         (IOUT)       OUTPUT OPTION
                             0: CONCENTRATION VS. TIME (breakthrough)
                             1: CONCENTRATION VS. DISTANCE (snapshot)
                             2: PARAMETER CALIBRATION
    1         (ISNAP)      SNAPSHOT OPTION
                             0: ENTIRE DOMAIN
                             1: AT A SPECIFIED POINT
0.1000E+04    (TSNAP)      TIME FOR SNAPSHOT [hrs]
   50         (ZOUT)       VERTICAL COORDINATE OF OUTPUT DATA [cm]

  *** OUTPUT DATA [t(hrs),G(mg/l)] CONTAINED IN FILE-OUT.ANAL
-------------------------------------------------------------------------------
```

The analytical solutions can incorporate a variable initial condition. The name of this input file is specified by the user in the MIF. Again, the sequencing and arrangement of variables within this data file must comply with a designated model format. Specifications for an initial-condition input file are given below, followed by an example:

FILE: INITIAL CONDITION

FILE NAME: user-specified (for example, IC.DAT)
UNIT NUMBER: 81
FILE DESCRIPTION: initial-condition data (varying spatially in vertical direction)

LINE NUMBER	VARIABLE	FORMAT	DEFINITION
1	NDATIN	free-formatted	number of data points contained in data file
2... (NDATIN+1)	XPT(IDAT), YPT(IDAT)	free-formatted	location of data point along vertical axis, value of data point (for example, initial condition)

EXAMPLE FILE: IC.DAT

```
LINE                                INPUT RECORDS
NUMBER   VARIABLE                   |----|----|----|----|----|----|----|----|----|----|
                                    0    5   10   15   20   25   30   35   40   45   50
  1      NDAT-----------------    4
  2      XPT(IDAT),YPT(IDAT)--  0   100E-6
  6      ----------------------  14  150E-6
  7      ----------------------  32  250E-6
  8      ----------------------  50  300E-6
```

This input file should be located in the same directory as the executable program file.

3.3 R-UNSAT Output Files

Output from R-UNSAT can be written as concentration as a function of time (breakthrough), concentration as a function of distance (snapshot), and flux as a function of time data. If the numerical solutions are applied, output data can be generated for a maximum of eight modeled gaseous-phase constituents. If the analytical solutions are applied, output data are written for only a single gaseous-phase constituent. The output criteria are defined by the user in the MIF as well as the output file names, with the exception of the flux as a function of time files, FLUX.DAT (analytical solution) and FLXDT.xx (numerical solution). Breakthrough data can be obtained at up to three output locations for each model execution. To obtain breakthrough data at additional output locations, the user must change the locations of output data within the MIF and reexecute the transport model. Examples of numerical-solution output files with corresponding unit numbers are given below:

FILE: BREAKTHROUGH DATA

FILE NAME: user-specified (for example, OUT.1)
UNIT NUMBERS: 15-19; 30-49
FILE DESCRIPTION: concentration as a function of time data

```
LINE     INPUT RECORDS
NUMBER   |----|----|----|----|----|----|----|----|----|----|----|----|----|----|----|----|
         0    5   10   15   20   25   30   35   40   45   50   55   60   65   70   75   80

  1       CONSTITUENT=  1  LOCATION : R-COORDINATE (CM)=  100   Z-COORDINATE (CM)=   10
  2
  3              TIME (HOURS)      CONCENTRATION (G/CM3)
  4              ------------      ---------------------
  5
  6                12.0000             1.839E-04
  7                24.0000             3.125E-04
  8                36.0000             4.521E-04
  9                48.0000             5.626E-04
 10                60.0000             6.487E-04
 11                72.0000             7.003E-04
```

FILE: SNAPSHOT DATA

FILE NAME: user-specified (for example, OUT.1)
UNIT NUMBERS: 15-19; 30-49
FILE DESCRIPTION: concentration as a function of distance data

```
LINE     INPUT RECORDS
NUMBER   |----|----|----|----|----|----|----|----|----|----|----|----|----|----|----|----|
         0    5   10   15   20   25   30   35   40   45   50   55   60   65   70   75   80

  1       TIME (HOURS)=        10.000    CONSTITUENT=  1
  2
  3       R-LOCATION (CM)     Z-LOCATION (CM)     CONCENTRATION (G/CM3)
  4       ---------------     ---------------     ---------------------
  5              100.0000            10.0000           3.1245E-04
  6              100.0000            20.0000           4.5399E-04
  7              100.0000            30.0000           5.1612E-04
  8              100.0000            40.0000           6.4349E-04
  9              100.0000            50.0000           7.0855E-04
 10              200.0000            10.0000           3.0867E-04
 11              200.0000            20.0000           4.4479E-04
 12              200.0000            30.0000           5.4145E-04
 13              200.0000            40.0000           6.1683E-04
 14              200.0000            50.0000           6.8885E-04
 15              300.0000            10.0000           2.4847E-04
 16              300.0000            20.0000           4.2758E-04
 17              300.0000            30.0000           5.2181E-04
 18              300.0000            40.0000           5.9311E-04
 19              300.0000            50.0000           6.5314E-04
```

FILE: FLUX.DAT

FILE NAME: FLUX.DAT
UNIT NUMBER: 80
FILE DESCRIPTION: flux as a function of time data for analytical solutions

```
LINE     INPUT RECORDS
NUMBER   |----|----|----|----|----|----|----|----|----|----|----|----|----|----|----|----|
         0    5   10   15   20   25   30   35   40   45   50   55   60   65   70   75   80

  1        TIME (HRS)        CONCENTRATION (mg/l)        FLUX (G/CM2-S)
  2        ----------        --------------------        --------------
  3
  4      0.100000E+03            0.967848E+01             0.796659E-09
  5      0.150000E+03            0.124734E+02             0.633361E-09
  6      0.200000E+03            0.147909E+02             0.542455E-09
  7      0.250000E+03            0.166960E+02             0.481372E-09
  8      0.300000E+03            0.182729E+02             0.436590E-09
  9      0.350000E+03            0.195874E+02             0.401693E-09
 10      0.400000E+03            0.206884E+02             0.373655E-09
```

FILE: FLXDT.xx

FILE NAME: FLXDT.xx (for example, FLXDT.1)
UNIT NUMBERS: 80-87
FILE DESCRIPTION: flux as a function of time data for numerical solutions

```
 LINE      INPUT RECORDS
NUMBER     |----|----|----|----|----|----|----|----|----|----|----|----|----|----|----|----|
           0    5   10   15   20   25   30   35   40   45   50   55   60   65   70   75   80

   1        CONSTITUENT=    1
   2
   3          TIME (HOURS)      FLUX (G/CM2-S)
   4          ------------      --------------
   5
   6            12.0000            1.265E-08
   7            24.0000            8.532E-09
   8            36.0000            6.216E-09
   9            48.0000            5.625E-09
  10            60.0000            4.212E-09
  11            72.0000            3.569E-09
```

In addition, R-UNSAT performs mass-balance calculations, which are contained in the output file FATE. These calculations are computed at each time step in accordance with the printout increment set by the user in the MIF. The constituent mass is partitioned into the following fates: mass remaining in immiscible phase (SOURCE), mass present in the unsaturated zone (INTERIOR), mass leached into the aquifer (AQUIFER), mass volatilized to the atmosphere (ATMOSPHERE), and mass biodegraded (BIODEGRADATION). An example of the output file FATE is given below:

FILE: FATE

FILE NAME: FATE
UNIT NUMBER: 11
FILE DESCRIPTION: describes the partitioning of mass

```
 LINE      INPUT RECORDS
NUMBER     |----|----|----|----|----|----|----|----|----|----|----|----|----|----|----|----|
           0    5   10   15   20   25   30   35   40   45   50   55   60   65   70   75   80

   1          TIME      SOURCE     INTERIOR  ATMOSPHERE    AQUIFER  FAR BOUND.    BIO
   2
   3          172800 0.3833E+06 0.7261E+03 0.0000E+00 0.0000E+00 0.0000E+00 0.0000E+00
   4         1728000 0.3801E+06 0.2619E+04 0.4129E+02 0.2877E+03 0.6155E-05 0.4770E+03
   5         3456000 0.3784E+06 0.2892E+04 0.1966E+03 0.7997E+03 0.3553E-03 0.1139E+04
   6         5184000 0.3769E+06 0.2960E+04 0.3793E+03 0.1342E+04 0.1518E-02 0.1829E+04
   7         6912000 0.3754E+06 0.2975E+04 0.5656E+03 0.1892E+04 0.3457E-02 0.2534E+04
   8         8640000 0.3739E+06 0.2971E+04 0.7515E+03 0.2444E+04 0.5799E-02 0.3242E+04
```

3.4 R-UNSAT Test Problems and Applications

This section treats four examples that demonstrate specific applications of R-UNSAT as well as test the code's performance on other computer systems. The website address contains input files that reproduce the results of the examples provided in this section. The input files are contained in the directory EXAMPLE.FIL on the website and are also shown below.

Test problems 1 (Section 3.4.1) and 2 (Section 3.4.2) demonstrate R-UNSAT model applications to compute site-specific rates of aerobic biodegradation associated with bioventing and passive remediation at gasoline-spill sites, respectively. The method for estimating biodegradation rates is discussed in detail by Lahvis and Baehr (1996). Section 3.4.3 presents a predictive-model application to simulate the selective transport of hydrocarbons from a gasoline plume in the unsaturated zone. In Section 3.4.4, R-UNSAT is applied to analyze results of a tracer-test experiment designed to estimate the effective-diffusion coefficient of unsaturated-zone sediment.

3.4.1 Test Problem 1--Quantification of the Aerobic Biodegradation Rate: Bioventing Application

Aerobic biodegradation of gasoline hydrocarbons in the subsurface by indigenous microorganisms results in oxygen (O_2) depletion and carbon dioxide (CO_2) production (see Section 2.4.4). The rate of aerobic degradation is linked to the availability of free O_2. This microbial degradation process can be inhibited or even halted if the O_2 availability is limited. The supply of O_2 in the subsurface can be maintained or increased artificially by applying bioventing, a remediation technique designed to deliver atmospheric O_2 to the contaminated region through vapor extraction. The vapor-extraction process can result in near-atmospheric concentrations of both O_2 and CO_2 throughout the unsaturated zone. If vapor extraction is terminated, the redistribution or rebound of these gases can be used as a signature of aerobic biodegradation as it occurred during bioventing, when O_2 transport is nonlimiting (Lahvis and Baehr, 1996). Model calibration to these gas-concentration data provides gas-flux estimates that are proportional to the aerobic-degradation rate when reaction stoichiometry (54) is assumed. This test problem presents a one-dimensional analytical model application to compute the flux of CO_2 in the unsaturated zone and the aerobic-biodegradation rate.

Table 6 contains a subset of rebound-CO_2 gas-concentration data (from Lahvis and Baehr, 1996) collected during a bioventing field experiment at a gasoline-spill site. CO_2 rebound was monitored over a 1,000-hour period after termination of vapor extraction at a vapor probe positioned about 56 cm above the water table. The unsaturated-zone stratigraphy in this area can be approximated by a homogeneous sand overlain by a thin clay layer, as shown in figure 8. The lower boundary condition at $z = 0$ (determined by model calibration) is represented by a constant-concentration boundary condition (27b) for CO_2. The thin clay layer at $z = L$ is represented by a third-kind or leaky boundary condition, given by (28b). The initial condition, which is given in table 7, represents the CO_2 gaseous-phase concentrations measured just prior to the termination of vapor extraction. These data are contained in the separate input file 'IVSX' on the website. This file was created according to the format specified in Section 3.2.2. One-dimensional gas-transport for this problem is described by (26) and is solved by employing the analytical solution Case 4 in Section 2.2.2.

Table 6. Rebound carbon dioxide gas concentrations at location [1]VW9-8.2, Galloway Township, New Jersey, November 1990

Time [2] (hours)	Concentration (milligrams per liter)
0	5.80
50	7.25
146	10.25
268	12.98
511	20.24
845	28.81

[1] Vapor probe located at z = 56 cm.
[2] Time after vapor-extraction termination.

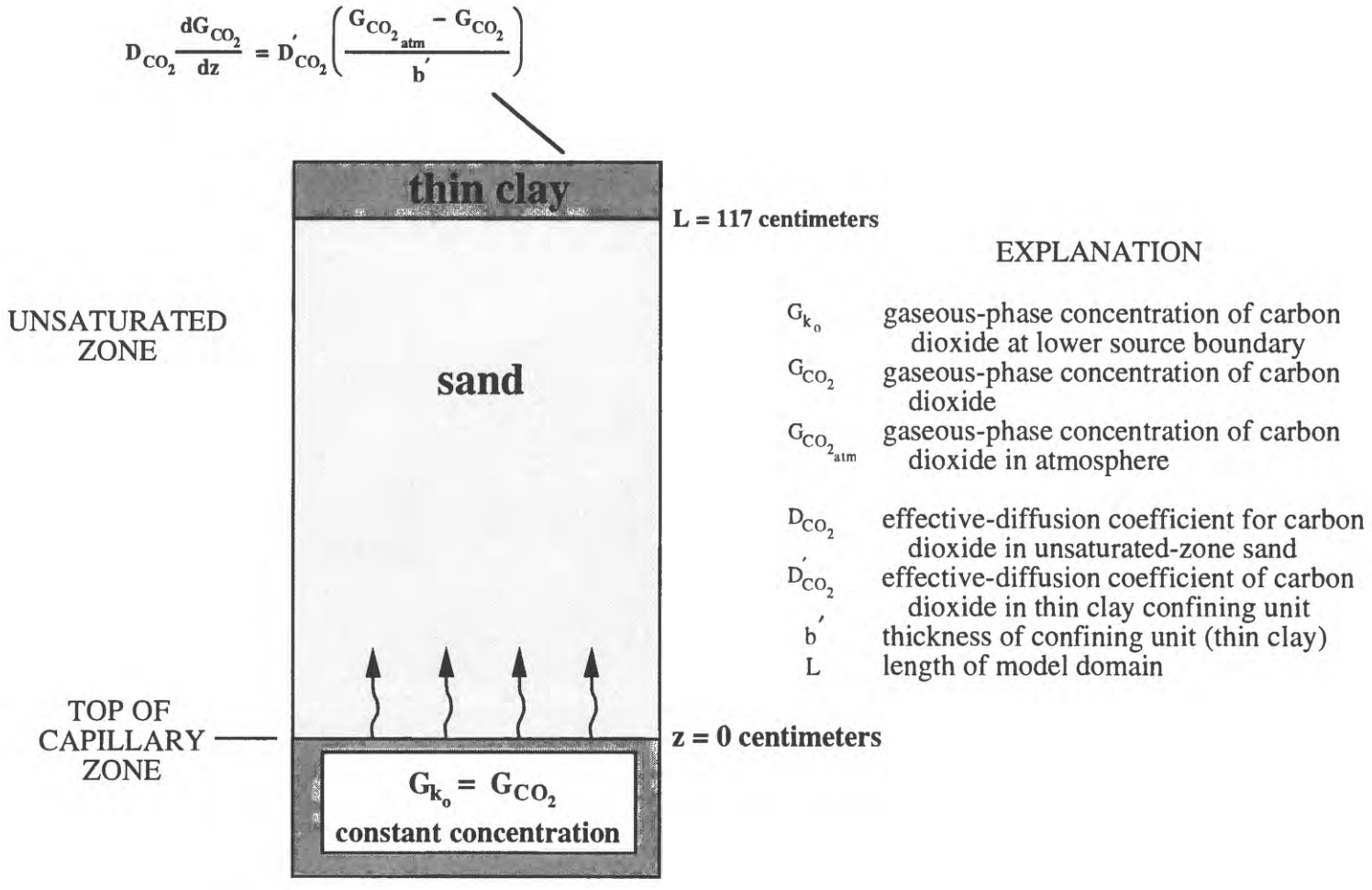

Figure 8. Diagram showing model geometry and boundary conditions used for a model application to quantify aerobic biodegradation rates associated with bioventing remediation.

Table 7. Model input for R-UNSAT computer model test problem 1: Quantification of the aerobic biodegradation rate associated with bioventing

Symbol	Definition	Value
	Physical properties of the sediments	
L	length of model domain	117 cm
b'	thickness of confining unit	6 cm
D_k'	effective-diffusion coefficient of confining unit (clay)	2.35E-04 cm^2/s
ϕ	total porosity (sand)	.350
θ_w	aqueous-phase porosity (sand)	.240
τ	gaseous-phase tortuosity (sand)	.042
ρ_b	bulk density (sand)	1.50 g/cm^3
	Constituent properties	
d_{ka}	gaseous-phase diffusivity	0.1520 cm^2/s
H_k	Henry's Law constant	.801
S_k	solid/water partition coefficient	0
	Boundary conditions	
G_{ko}	constant gaseous-phase concentration at water table (z = 0)	4.50E-05 g/cm^3
G_U	gaseous-phase concentration above confining unit (z = L)	6.39E-07 g/cm^3
	Initial conditions	
	z (cm) / carbon dioxide concentration (g/cm^3)	
	.01 / 42	
	56 / 5.8	
	116 / .64	
	Output parameters	
t_{end}	maximum time for breakthrough data	10,000 hr
Δt_b	time step for breakthrough data	50 hr
z_{vw}	output-data location in z-direction	56 cm

The following MIF was constructed by choosing to create new model input (Option 1--see Section 3.1), selecting the analytical solver (Option 2), and entering the required input parameters from table 7:

INPUT RECORDS

```
|----|----|----|----|----|----|----|----|----|----|----|----|----|----|----|----|
0    5   10   15   20   25   30   35   40   45   50   55   60   65   70   75   80

            2
*******************************************************************************
                    ANALYTICAL MODEL INPUT
*******************************************************************************

TITLE -  TEST.PROB. #1 ANALYSIS OF BIOVENTING EXPERIMENT (11/90)

  VALUE     MODEL CODE          DEFINITION        [cgs units]
            DESIGNATION
  -----     ----------          ----------        ---------

************************ BOUNDARY AND INITIAL CONDITIONS ************************

    4         (IBC0)       BOUNDARY CONDITION OPTION
0.4500E-04    (UW)         GAS-PHASE CONCENTRATION AT THE WATER TABLE
                             (z = 0) [mg/l]
0.6000E+01    (BP)         THICKNESS OF CONFINING UNIT AT (z = L)[cm]
0.2350E-03    (DP)         effective-diffusion COEFFICIENT OF CONFINING
                             UNIT AT (z = L) [cm2/s]
0.6390E-06    (UP)         GAS-PHASE CONCENTRATION ABOVE CONFINING UNIT
                             (z > L) [mg/l]
    2         (INOPT)      INITIAL CONDITION OPTION
                             0: CONSTANT
                             1: LINEARLY VARIABLE
                             2: INITIAL CONDITION SPECIFIED IN SEPARATE
                                INPUT FILE OF TYPE: [z(cm),G(mg/l)]

*** INITIAL CONDITION DATA [z(cm),G(mg/l)] CONTAINED IN FILE-IVSX

********************* PHYSICAL PROPERTIES OF THE CONSTITUENT ******************

0.1520E+00    (DBIN)       DIFFUSIVITY OF CONSTITUENT IN BULK GAS PHASE [cm2/s]
0.8010E+00    (HENRY)      HENRYS LAW PARTITION COEFFICIENT (air/water)
                             [dimensionless]
0.0000E+00    (SWPC)       ADSORPTION COEFFICIENT (soil/water) [dimensionless]

******************* PHYSICAL PROPERTIES OF THE POROUS MEDIA *******************

0.1170E+03    (XL)         LENGTH OF MODEL DOMAIN [cm]
0.3500E+00    (VOID)       POROSITY [dimensionless]
0.2400E+00    (WAT)        AQUEOUS-PHASE POROSITY [dimensionless]
0.1100E+00    (AIR)        GASEOUS-PHASE POROSITY [dimensionless]
0.4200E-01    (TOR)        TORTUOSITY [dimensionless]
0.1500E+01    (BULK)       BULK DENSITY [dimensionless]
0.7022E-03    (DEFF)       EFFECTIVE-DIFFUSION COEFFICIENT [cm2/s]

****************************** OUTPUT PARAMETERS ******************************

    0         (IOUT)       OUTPUT OPTION
                             0: CONCENTRATION VS. TIME (breakthrough)
                             1: CONCENTRATION VS. DISTANCE (snapshot)
0.1000E+04    (TMAX)       MAXIMUM TIME FOR BREAKTHROUGH DATA [hrs]
```

```
0.5000E+02    (DELT)       TIME INCREMENT FOR BREAKTHROUGH DATA [hrs]
   56         (ZOUT)       VERTICAL COORDINATE OF OUTPUT DATA [cm]

  *** OUTPUT DATA [t(hrs),G(mg/l)] CONTAINED IN FILE-OUT.CO2

  *** FLUX DATA AT THE WATER TABLE (z = 0) CONTAINED IN FILE "FLUX.DAT"
      [t(hrs),G(mg/l),J(g/cm2-s)]
-------------------------------------------------------------------------------
```

The gas concentration (G_o = 4.50E-05 g/cm^3) listed in the MIF was determined by a least-root-mean-squares fit of measured (table 6) and simulated gas-concentration data. The least-root-mean-squares fit of the rebound-CO_2 data is shown in figure 9. The constant-concentration boundary condition G_o = 4.50E-05 g/cm^3 implies a steady-state mass flux of J_o = 2.31E-10 g/cm^2-s across the water table, which was determined by increasing the maximum time length of the simulation to (TMAX = 1,000,000 hr) and the time-step size to (DELT = 10,000 hr). The flux as a function of time data across the source boundary (water table) is contained in the output file FLUX.DAT. The CO_2 flux, like the O_2 flux (see Section 2.4.4), can also be related to the hydrocarbon degradation rate by assuming reaction stoichiometry and applying the following expression (Lahvis and Baehr, 1996):

$$R_{bio} = \frac{J_{CO_2}}{r_k} \tag{58}$$

Applying (58) with the assumption of a stoichiometric-mass coefficient of r_{CO2} = 3.30 (mass of CO_2 produced per equivalent mass of hydrocarbon degraded) results in a biodegradation rate of R_{bio} = 8.43E-11 g/cm^2-s.

3.4.2 Test Problem 2--Quantification of the Aerobic Biodegradation Rate: Passive-Remediation Application

An analysis of the unsaturated-zone gas distribution prior to bioventing provides a method for assessing the natural rate of microbial degradation associated with a no-action or passive-remediation scenario (Lahvis and Baehr, 1996). For this analysis, the time scale over which the microbial community responds to physiochemical changes, such as substrate, electron acceptor, or nutrient availabilities, is assumed to be large relative to the time scale over which gases are physically redistributed in the unsaturated zone. Under this assumption, the microbial degradation rate can be estimated at the time of gas sampling on the basis of a steady-state gas distribution.

The following test problem illustrates a two-dimensional model application to simulate the steady-state CO_2 gas distribution shown in figure 10a. The data listed in table 8 were recorded prior to vapor extraction at a gasoline-spill site. Although the areal CO_2-concentration distribution in figure 10a is not quite radially symmetric, it is apparent that individual sectors can be approximated by two-dimensional axisymmetric boundaries. For this application, the CO_2

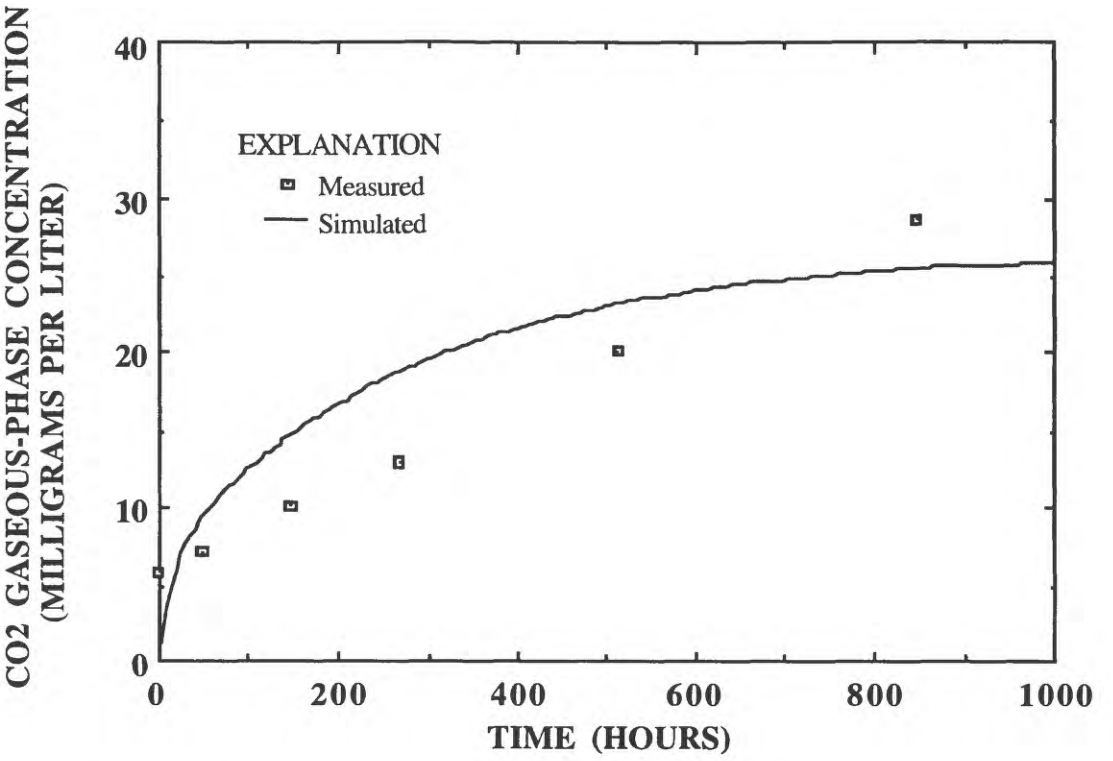

Figure 9. Graph showing results of model calibration to rebound-gas-concentration data following a period of vapor extraction.

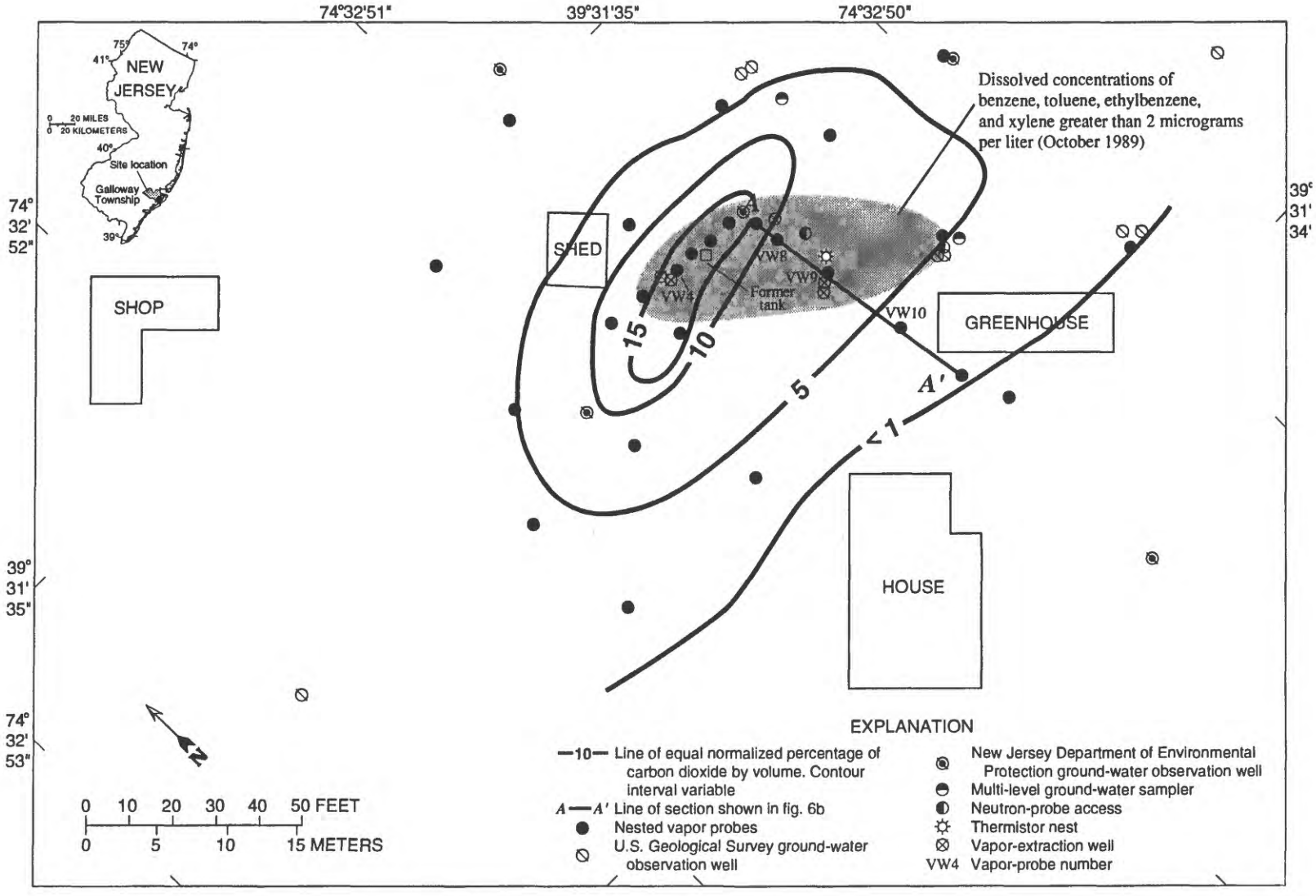

Figure 10a. Plot of the areal distribution of carbon dioxide as a percentage of unsaturated zone gas at a depth of 6 feet below land surface at Galloway Township, New Jersey, December 1989.

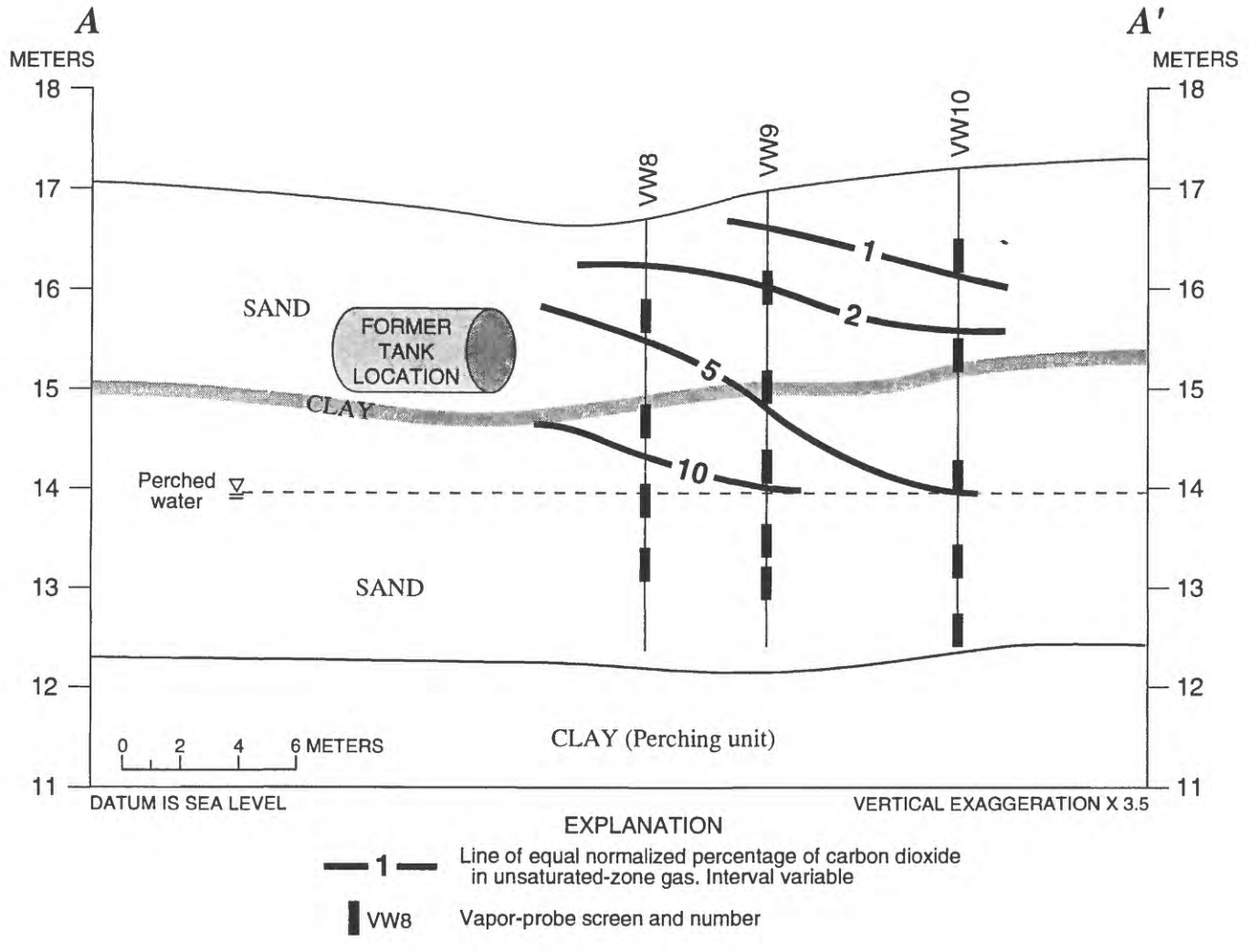

Figure 10b. Plot of the vertical distribution of carbon dioxide as a percentage of unsaturated-zone gas across section line A-A′ at Galloway Township, New Jersey.

distribution is analyzed from a single areal sector defined by the transect A - A′ and an area (A*) given by:

$$A^{*} = \pi r^{2}_{A-A'} \tag{59}$$

where

$r_{A-A'}$ = length of the transect A - A′ [cm]

Ideally the sitewide degradation rate would be defined by the summation of degradation rates calibrated for a composite of smaller sectors through reapplication of the transport model.

Figure 10b is a vertical transect through the unsaturated zone along A - A′. The unsaturated zone in this area consists of seven stratigraphic units whose transport properties are given in table 8. The test geometry and model boundary conditions are shown in figure 11. The lower boundary condition at z = 0 is represented by a specified-flux boundary for CO_2, described by (8a), where $J_k(r)$ is characterized by a linear relation defined as:

$$J_{CO_2}(r) = M_J r + B_J \tag{60}$$

where

M_J = specified-flux gradient [g/cm³-s]
B_J = specified flux at r = 0 [g/cm²-s]

The surface boundary is defined by a constant-atmospheric-concentration boundary condition given by (9) where $\lambda_2 = 1$, and the inner- and outer-radial boundaries are given by (11) and (12), respectively, where $\lambda_5 = 1$. Two-dimensional gas transport for this test problem is described by (7) and is solved numerically by employing source boundary condition Option 1 (see Section 2.2.1).

The aerobic biodegradation rate is determined by integrating (60) over the area (59), resulting in a total CO_2 mass flux for the sector given by:

$$Q_{CO_2} = \int_{A^*} J_{CO_2}\, dA = 2\pi \int_{r=r_1}^{r=r_2} (M_J r + B_J)\, r\, dr \tag{61}$$

where

Q_{CO2} = total CO_2 mass flux [g/s]

As in the previous section, reaction stoichiometry is assumed to relate the CO_2 flux to the sitewide hydrocarbon degradation rate (R_{bio}) as follows:

$$R_{bio} = \frac{Q_{CO_2}}{r_k} \tag{62}$$

Stratigraphic unit	Sediment description	Thickness (centimeters)
#1	off-white fine-grained sand	66
#2	orangish-brown clayey sand	13
#3	off-white fine-grained sand	38
#4	whitish-gray clay	6
#5	off-white fine-grained sand	61
#6	medium-brown clayey sand	102
#7	dark-brown clayey sand	46

EXPLANATION

$J_{k_o}(r)$	specified-mass flux of kth constituent across upper vertical source boundary
G_k	gaseous-phase concentration of kth constituent
$G_{k_{atm}}$	gaseous-phase concentration of kth constituent in atmosphere
D_k	effective-diffusion coefficient of kth constituent
q_w	vertical recharge rate
H_k	Henry's Law constant of the kth constituent
VW9-6.0	vapor-well number

VERTICAL SCALE

0 5 10 FEET

0 20 40 CENTIMETERS

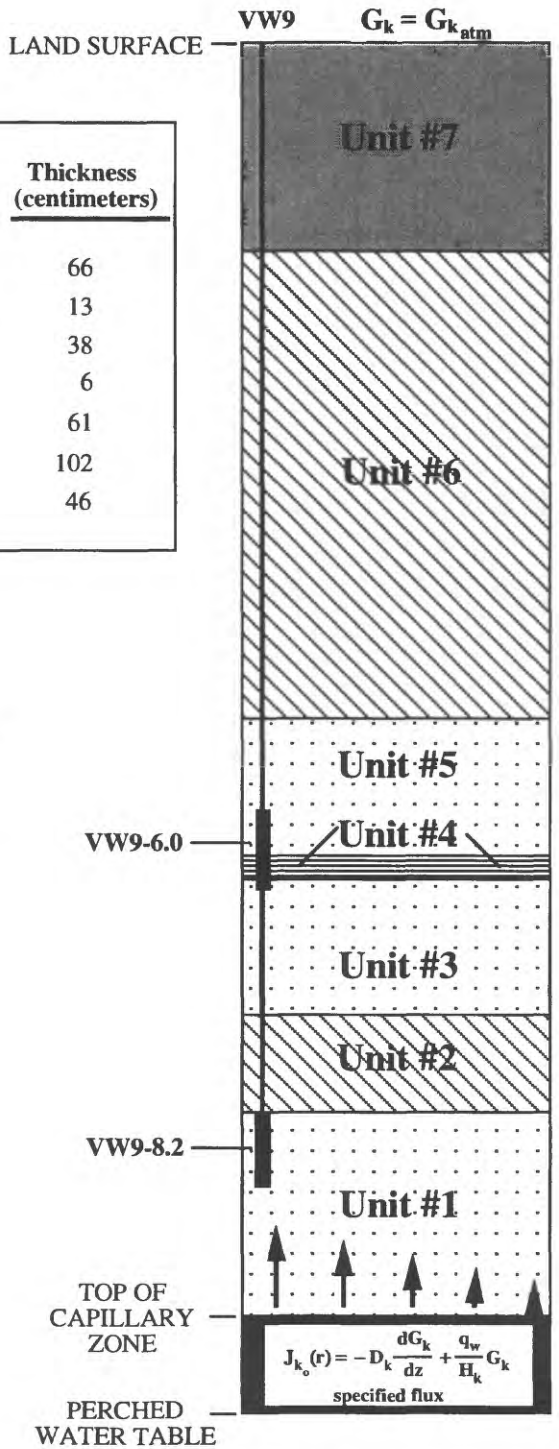

Figure 11. Diagram showing model geometry and boundary conditions used for a model application to analyze aerobic biodegradation rates associated with passive remediation.

Table 8. Carbon dioxide gas concentrations measured across unsaturated-zone transect A - A' during passive-remediation field experiment, Galloway Township, New Jersey, December 1989

Vapor probe	Radial coordinate (r) (cm)	Vertical coordinate (z) (cm)	Gaseous-phase concentration (mg/L)
VW8-6	637	100.2	183.6
VW8-3	637	191.2	86.91
VW9-8	974	56.0	169.3
VW9-6	974	117.0	106.9
VW9-3	974	215.5	44.41
VW10-10	1502	23.4	96.50
VW10-6	1502	145.9	85.50
VW10-3	1502	236.8	14.60

The MIF presented below was generated by choosing to create new model input (Option 1--see Section 3.1), selecting the numerical solver (Option 1), and entering the required input parameters from table 9. An input file containing boundary-condition data (designated in the MIF as BC.DAT) was also required for this analysis. An example of this input file is also given below.

The flux distribution $J_{CO2}(r)$ given in table 9 was determined by model calibration. Model calibration was again defined by a least-squares fit of measured (see table 10) and simulated gas-concentration data. The results of model calibration are shown in figure 12 and are listed in table 9. Applying (61) results in a total CO_2 mass flux of Q_{CO2} = 1.09E-03 g/s. This rate can be extrapolated to a sitewide estimate of pure hydrocarbon degradation R_{bio} = 3.31E-04 g/s (16.2 gal/yr) by applying (62), assuming r_{CO2} = 3.30, and assuming a hydrocarbon plume diameter (d) of 50 ft (1,524 cm) and an average hydrocarbon density (ρ) of 0.77 g/cm^3.

FILE: BC.DAT

```
LINE     INPUT RECORDS
NUMBER   |----|----|----|----|----|----|----|----|----|----|----|----|----|----|----|----|
         0    5    10   15   20   25   30   35   40   45   50   55   60   65   70   75   80
  1      1   2
  2      0  8.12E-09
  3      2000  0.00E-10
```

Table 9. Model input for R-UNSAT computer model test problem 2: Quantification of the aerobic biodegradation rate associated with passive remediation

Symbol	Definition	Value
	Model geometry	
R	length of model domain in r-direction	2000 cm
L	length of model domain in z-direction	300 cm
N_r	number of nodes in r-direction	21
N_z	number of nodes in z-direction	51
T	unsaturated-zone temperature	10 °C
P	unsaturated-zone pressure	760 mm Hg
q_{wz}	vertical recharge rate	0 cm/yr

Physical properties of the sediments

Sediment layer	Top of layer (cm)	Total porosity (dimensionless)	Moisture content (dimensionless)	Gaseous-phase tortuosity (dimensionless)	Bulk density (g/cm^3)
1	66.3	0.372	0.200	0.1192	1.66
2	79.4	.264	.130	.1321	1.88
3	117.2	.340	.160	.1583	1.74
4	124.2	.330	.180	.1100	1.81
5	152.7	.400	.155	.2347	1.59
6	254.3	.349	.157	.1745	1.41
7	300.0	.427	.165	.2408	1.39

	Constituent properties	
d_{ka}	gaseous-phase diffusivity	0.1520 cm^2/s
H_k	Henry's Law constant	.801
S_k	solid/water partition coefficient	0
	Boundary conditions	
	Carbon dioxide (CO_2) flux distribution along transect A - A′ $[J_{CO2}(r) = M_J r + B_J]$	
M_J	flux gradient	-4.06E-12 g/cm^3-s
B_J	specified flux at r = 0	8.12E-09 g/cm^2-s
G_U	gaseous-phase concentration above confining unit (z = L)	6.39E-07 g/cm^3
	Output parameters	
t_{snap}	time for snapshot data	30,000 hr

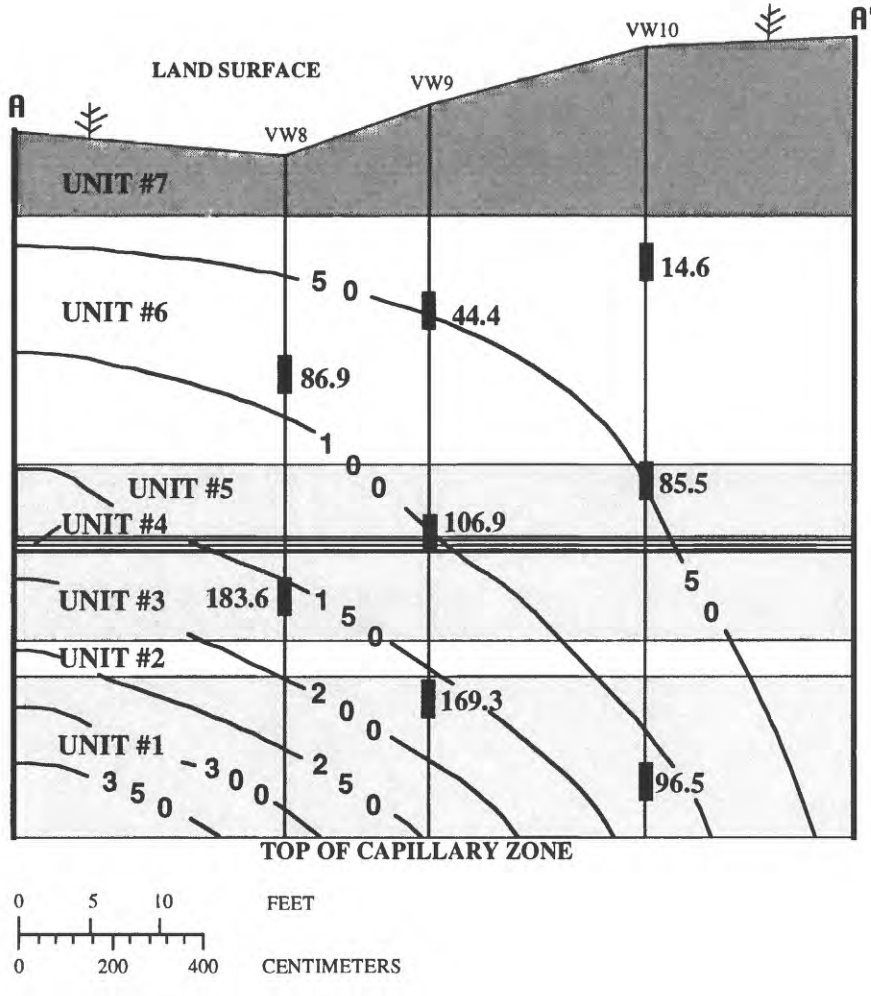

EXPLANATION

−50−	line of equal simulated carbon dioxide gaseous-phase concentration. Interval 50 milligrams per liter
86.9	measured carbon dioxide gaseous-phase concentration, in milligrams per liter
A - A'	vertical transect through the unsaturated zone shown in figure 10a
VW9	vapor-well number
▮	vapor probe

Stratigraphic unit	Sediment description	Thickness (centimeters)
#1	off-white fine-grained sand	66
#2	orangish-brown clayey sand	13
#3	off-white fine-grained sand	38
#4	whitish-gray clay	6
#5	off-white fine-grained sand	61
#6	medium-brown clayey sand	102
#7	dark-brown clayey sand	46

Figure 12. Plot of the results of model calibration to quasi-steady-state gas concentration along data section line A - A′ (figure 10a) through the unsaturated zone at Galloway Township, New Jersey.

INPUT RECORDS

```
|----|----|----|----|----|----|----|----|----|----|----|----|----|----|----|----|
0    5   10   15   20   25   30   35   40   45   50   55   60   65   70   75   80

            1
********************************************************************************
                          NUMERICAL MODEL INPUT
********************************************************************************

TITLE -  TEST.PROB. #2 ANALYSIS OF PASSIVE REMEDIATION EXPERIMENT (12/89)

  VALUE     MODEL CODE          DEFINITION        [cgs units]
            DESIGNATION
  -----     ----------          ----------        -----------

*************************** MODEL DOMAIN PARAMETERS ****************************

    3         (IDIM)            MODEL DIMENSIONALITY
                                  1: 1-D VERTICAL (z - DIRECTION)
                                  2: 1-D RADIAL (r - DIRECTION)
                                  3: 2-D (r,z DIRECTIONS)
0.2000E+04    (RF)              LENGTH OF MODEL DOMAIN IN r - DIRECTION [cm]
   21         (NR)              NUMBER OF NODES IN r - DIRECTION
0.3000E+03    (ZSURF)           LENGTH OF DOMAIN IN z - DIRECTION [cm]
   51         (NZ)              NUMBER OF NODES IN z - DIRECTION
0.1000E+03    (DR)              NODAL SPACING IN THE RADIAL DIRECTION [cm]
0.6000E+01    (DZ)              NODAL SPACING IN THE VERTICAL DIRECTION [cm]
0.1000E+02    (TEMP)            UNSATURATED-ZONE TEMPERATURE [C]
0.7600E+03    (ATM)             UNSATURATED-ZONE PRESSURE [mm Hg]
0.0000E+00    (DARCY)           RECHARGE RATE [cm/yr]

***************************** CONSTITUENT PROPERTIES ****************************

    1         (NK)              NUMBER OF MODEL CONSTITUENTS

-------------------------------- CONSTITUENT  1 --------------------------------

    1         (ICON)            CONSTITUENT INDEX FOR: CARBON DIOXIDE
0.4410E+02    (WK(IK))          MOLECULAR WEIGHT OF CONSTITUENT [g]
0.2690E+02    (DV(IK))          ATOMIC DIFFUSION VOLUME [dimensionless]
0.8010E+00    (HAW(IK))         HENRYS LAW PARTITION COEFFICIENT (air/water)
                                  [dimensionless]
0.6230E-06    (ATCONC(IK))      GAS-PHASE CONCENTRATION ABOVE UPPER
                                BOUNDARY [g/cm3]
              (DKA(IK))         GASEOUS-PHASE DIFFUSIVITY (** SEE MAP FILE - DKA.MAP)
0.1000E-04    (DKW(IK))         AQUEOUS-PHASE DIFFUSIVITY

********************** BOUNDARY AND INITIAL CONDITIONS **********************

    1         (IOPT)            SOURCE BOUNDARY CONDITION OPTION
                                  1: SPECIFIED FLUX AT WATER TABLE
                                  2: SPECIFIED CONCENTRATION AT WATER TABLE
                                  3: HYDROCARBON PLUME ABOVE WATER TABLE
                                  4: CONSTANT FLUX FROM INJECTION PROBE

-------------------------------- CONSTITUENT  1 --------------------------------
```

```
    1         (IBDRY)          BOUNDARY CONDITION OPTION
                                 0: BOUNDARY CONDITION IS CONSTANT
                                 1: BOUNDARY CONDITION VARIES

*** DISCRETIZED BOUNDARY CONDITION DATA CONTAINED IN FILE-"BC.MAP"

-------------------------------------------------------------------------------

0.0000E+00    (ZLOW)           LOWER SOURCE BOUNDARY: z - LOCATION [cm]
0.6000E+01    (ZHI)            UPPER SOURCE BOUNDARY: z - LOCATION [cm]
    0         (IFAR)           OUTER BOUNDARY CHARACTERIZATION
                                 0: UNIFORM
                                 1: VARIABLE
0.1000E+01    (AZ2)            BOUNDARY CONDITION PARAMETER: OUTER RADIAL BOUNDARY
    0         (ISURF)          UPPER BOUNDARY CHARACTERIZATION
                                 0: UNIFORM
                                 1: VARIABLE
0.1000E+01    (AR2)            BOUNDARY CONDITION PARAMETER: GROUND SURFACE

*** DISCRETIZED INITIAL CONDITION DATA CONTAINED IN FILE-"IC.MAP"

****************** PHYSICAL PROPERTIES OF THE POROUS MEDIA ********************

    2         (ISTRAT)         STRATIFIED UNSATURATED ZONE
    7         (NL)             NUMBER OF STRATIGRAPHIC UNITS

---------------------------------- LAYER  1 ----------------------------------

0.6630E+02    (ZLAY(IL))       TOP ELEVATION OF LAYER [cm]
0.3720E+00    (PORL(IL))       POROSITY OF LAYER [dimensionless]
0.2000E+00    (THWL(IL))       MOISTURE CONTENT OF LAYER [dimensionless]
0.1192E+00    (TAL(IL))        TORTUOSITY [dimensionless]
0.1660E+01    (BDL(IL))        BULK DENSITY [g/cm3]

---------------------------------- LAYER  2 ----------------------------------

0.7940E+02    (ZLAY(IL))       TOP ELEVATION OF LAYER [cm]
0.2640E+00    (PORL(IL))       POROSITY OF LAYER [dimensionless]
0.1300E+00    (THWL(IL))       MOISTURE CONTENT OF LAYER [dimensionless]
0.1321E+00    (TAL(IL))        TORTUOSITY [dimensionless]
0.1880E+01    (BDL(IL))        BULK DENSITY [g/cm3]

---------------------------------- LAYER  3 ----------------------------------

0.1162E+03    (ZLAY(IL))       TOP ELEVATION OF LAYER [cm]
0.3400E+00    (PORL(IL))       POROSITY OF LAYER [dimensionless]
0.1600E+00    (THWL(IL))       MOISTURE CONTENT OF LAYER [dimensionless]
0.1583E+00    (TAL(IL))        TORTUOSITY [dimensionless]
0.1740E+01    (BDL(IL))        BULK DENSITY [g/cm3]

---------------------------------- LAYER  4 ----------------------------------

0.1242E+03    (ZLAY(IL))       TOP ELEVATION OF LAYER [cm]
0.3300E+00    (PORL(IL))       POROSITY OF LAYER [dimensionless]
0.1800E+00    (THWL(IL))       MOISTURE CONTENT OF LAYER [dimensionless]
0.1100E+00    (TAL(IL))        TORTUOSITY [dimensionless]
0.1810E+01    (BDL(IL))        BULK DENSITY [g/cm3]
```

```
---------------------------------- LAYER  5 ----------------------------------

0.1527E+03   (ZLAY(IL))      TOP ELEVATION OF LAYER [cm]
0.4000E+00   (PORL(IL))      POROSITY OF LAYER [dimensionless]
0.1550E+00   (THWL(IL))      MOISTURE CONTENT OF LAYER [dimensionless]
0.2347E+00   (TAL(IL))       TORTUOSITY [dimensionless]
0.1590E+01   (BDL(IL))       BULK DENSITY [g/cm3]

---------------------------------- LAYER  6 ----------------------------------

0.2543E+03   (ZLAY(IL))      TOP ELEVATION OF LAYER [cm]
0.3490E+00   (PORL(IL))      POROSITY OF LAYER [dimensionless]
0.1570E+00   (THWL(IL))      MOISTURE CONTENT OF LAYER [dimensionless]
0.1745E+00   (TAL(IL))       TORTUOSITY [dimensionless]
0.1410E+01   (BDL(IL))       BULK DENSITY [g/cm3]

---------------------------------- LAYER  7 ----------------------------------

0.3000E+03   (ZLAY(IL))      TOP ELEVATION OF LAYER [cm]
0.4270E+00   (PORL(IL))      POROSITY OF LAYER [dimensionless]
0.1650E+00   (THWL(IL))      MOISTURE CONTENT OF LAYER [dimension1ess]
0.2408E+00   (TAL(IL))       TORTUOSITY [dimensionless]
0.1390E+01   (BDL(IL))       BULK DENSITY [g/cm3]

***************************** ALGORITHM PARAMETERS ******************************

    0        (ITIME)         TIME-STEP ADJUSTMENT OPTION
                               0: CONSTANT TIME-STEP
                               1: VARIABLE TIME-STEP
0.3000E+02   (DT1)           TIME-STEP [hrs]
0.3000E+05   (TEND)          ENDING TIME [hrs]
    0        (ISS)           STEADY-STATE DEFAULT OPTION
                               0: DO NOT ZERO-OUT STORAGE TERM
                               1: ZERO-OUT STORAGE TERM
  500        (NITER)         MAX. # OF ITERATIONS PER TIME STEP
0.1000E-02   (EPS)           CONVERGENCE CRITERIA - ACCEPTABLE MAX.
                               RELATIVE ERROR
    0        (IPROJ)         MATRIX-SOLVER SEED
                               0: PREVIOUS TIME-STEP
                               1: LINEAR PROJECTION FROM PREVIOUS TIME-STEP
                               2: DIRECT PROJECTION

***************************** OUTPUT PARAMETERS *****************************

    1        (IOUT)          OUTPUT OPTION
                               0: CONCENTRATION VS. TIME (breakthrough)
                               1: CONCENTRATION VS. DISTANCE (snapshot)
    0        (ISNAP)         SNAPSHOT OPTION
                               0: ENTIRE DOMAIN
                               1: AT SPECIFIC LOCATIONS
0.3000E+05   (TSNAP)         TIME [hrs] FOR SNAPSHOT

-------------------------------- CONSTITUENT  1 --------------------------------

    1        (IOUTOPT(IK))   OUTPUT OPTION
                               0: NO OUTPUT DATA REQUESTED
                               1: OUTPUT DATA REQUESTED

  *** OUTPUT DATA (t,G) [hrs,g/cm3] CONTAINED IN FILE-OUT1
```

```
------------------------------------------------------------------------------

************************** MODEL DOMAIN COORDINATES **************************

 2000        (R(NR))         r - COORDINATE: OUTER BOUNDARY [cm]
 2000        (R(IRIM))       r - COORDINATE: RADIUS OF SOURCE [cm]
    0        (Z(1))          z - COORDINATE: LOWER BOUNDARY [cm]
  300        (Z(NZ))         z - COORDINATE: SURFACE BOUNDARY [cm]
    0        (Z(IZLOW))      z - COORDINATE: LOWER SOURCE BOUNDARY [cm]
    6        (Z(IZHI))       z - COORDINATE: UPPER SOURCE BOUNDARY [cm]
   66        (ZLAY(IL))      z - COORDINATE: TOP OF LAYER  1  [cm]
   78        (ZLAY(IL))      z - COORDINATE: TOP OF LAYER  2  [cm]
  120        (ZLAY(IL))      z - COORDINATE: TOP OF LAYER  3  [cm]
  126        (ZLAY(IL))      z - COORDINATE: TOP OF LAYER  4  [cm]
  156        (ZLAY(IL))      z - COORDINATE: TOP OF LAYER  5  [cm]
  252        (ZLAY(IL))      z - COORDINATE: TOP OF LAYER  6  [cm]
  300        (ZLAY(IL))      z - COORDINATE: TOP OF LAYER  7  [cm]
------------------------------------------------------------------------------
```

3.4.3 Test Problem 3--Multispecies Hydrocarbon Transport and Biodegradation

Significant volumes of an organic liquid such as gasoline can remain immobilized within the pore spaces of the unsaturated zone after primary remediation ceases. These entrapped residuals can pose a long-term threat to ground-water resources. Specific hydrocarbon constituents emanating from the immiscible phase can volatilize or diffuse to the atmosphere, solubilize in ground water, be adsorbed to aquifer sediments, or undergo biochemical transformations (for example, biodegradation). The phase-partitioning properties of the constituents determine their fate and distribution in the subsurface. For example, aromatic constituents of gasoline such as benzene and toluene, which have relatively low air-water partition coefficients (H_k), tend to favor the aqueous phase, whereas alkanes such as n-octane, which have higher air-water partition coefficients, tend to favor the gaseous phase. Knowledge of the immiscible-phase composition is therefore extremely important in determining the environmental risk and consequences for remediation. The following test problem demonstrates a two-dimensional model application to simulate transport and biodegradation of two gasoline constituents with contrasting air/water partition coefficients (Henry's Law constants): o-xylene (k = 1), an aromatic hydrocarbon with $H_1 = 0.214$, and n-octane (k = 2), an alkane with $H_2 = 126.6$. The partitioning of mass (amount remaining in soil, leached into the ground water, diffused to the atmosphere, and biodegraded) is calculated as a function of time for the duration of the simulation (t_{end} = 4,000 days).

The model geometry and boundary conditions for this example problem are illustrated in figures 13 and 14, respectively. The immobilized immiscible phase exists in the region bounded by radial coordinates r_0 and r_1 and vertical coordinates z_1 and z_2. The immiscible phase is assumed to be a mixture of o-xylene and n-octane with an initial mole-fraction composition of $\chi_{1i} = 0.488$ and $\chi_{2i} = 0.309$, respectively (see table 10). The surface boundary is defined by a constant-atmospheric-concentration boundary condition given by (9) where $\lambda_2 = 1$, and the outer-radial boundary is defined as a constant-atmospheric-concentration boundary condition given by (11) where $\lambda_5 = 1$. These boundary conditions imply a maximum hydrocarbon-mass loss through diffusion. The water table is simulated as a no-flow boundary for the gaseous-phase constituents. Mass transfer across the water table is therefore caused solely by advection from recharging water.

An annual recharge rate of q_{wz} = 105.6 cm/yr is assumed. Hydrocarbon biodegradation (R_k) is simulated as a first-order reaction rate with decay constant α = 1.0E-6 1/s (see Section 2.4.4). Two-dimensional gas transport for this test problem is described by (7) and is solved numerically by employing source boundary condition Option 3 (see Section 2.2.1). The remaining model input for this test problem is contained in table 10.

The MIF presented below was generated by choosing to create new model input (Option 1--see Section 3.1), selecting the numerical solver (Option 1), and entering the required input parameters from table 10.

Figures 15a-b illustrate the partitioning of mass to various fates as a function of time for o-xylene and n-octane, respectively. The curves labeled "unsaturated zone" represent the fraction of the initial mass remaining in the unsaturated zone as a function of time. The curves labeled "atmosphere," "ground water,"and "biodegradation" represent the percentage of initial mass in the atmosphere, in ground water, and biodegraded. The distribution of the initial mass of o-xylene after 4,000 days (fig. 15a) was as follows: 47 percent remained in the unsaturated zone, 29 percent was biodegraded, 18 percent entered the ground water, and 4 percent entered the atmosphere. The distribution of the initial mass of n-octane after 4,000 days (fig. 15b) was as follows: 43 percent remained in the unsaturated zone, 53 percent entered the atmosphere, 3 percent was biodegraded, and <1 percent entered the ground water. Unlike o-xylene, most of the n-octane mass diffuses to the atmosphere. This process leaves behind aromatic-enriched immiscible phases. As shown in figure 15a, these residual volumes can pose a long-term threat to ground-water resources. As shown in figure 15a-b, the principal hydrocarbon-attenuation mechanisms also differ. For o-xylene, biodegradation is the principal mass-loss mechanism, whereas for n-octane, diffusion to the atmosphere is the favored mechanism. Minimal biodegradation of the alkane occurs because the hydrocarbon strongly partitions to the gaseous phase. Monitoring and remediation of the saturated zone beneath a gasoline spill would therefore be most effective if focused on the aromatic constituents.

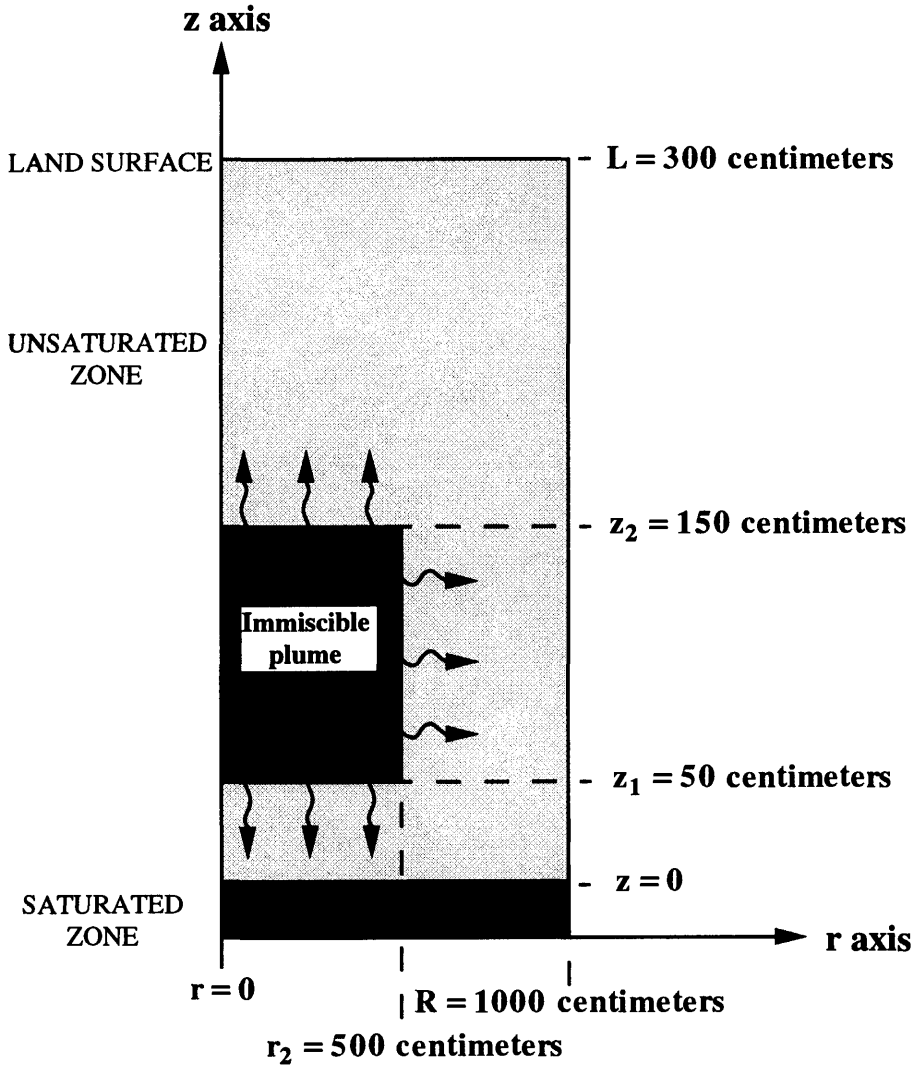

EXPLANATION

r_2	radius of source
z_1	vertical location of lower source boundary
z_2	vertical location of upper source boundary
R	radius of model domain
L	length of model domain

Figure 13. Diagram showing model geometry used for a model application to predict multispecies hydrocarbon transport and biodegradation.

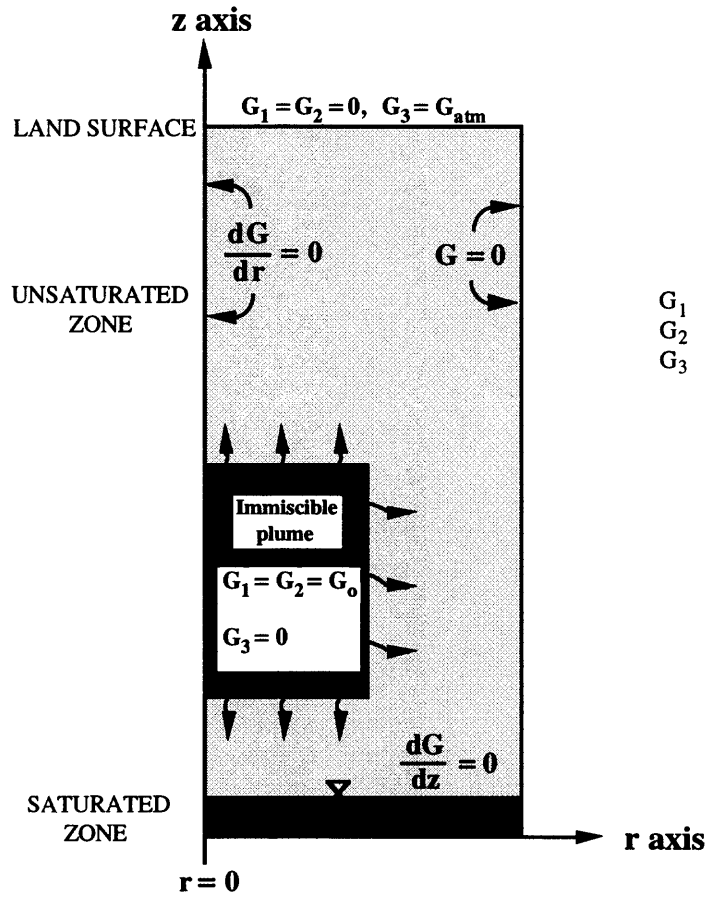

EXPLANATION

G_1 gaseous-phase concentration of o-xylene
G_2 gaseous-phase concentration of n-octane
G_3 gaseous-phase concentration of oxygen

Figure 14. Diagram showing model boundary conditions used for model application to predict multispecies hydrocarbon transport and biodegradation.

Table 10. Model input for R-UNSAT computer model test problem 3: Multispecies hydrocarbon transport and biodegradation

Symbol	Definition	Value
	Model geometry	
R	length of model domain in r - direction	1,000 cm
L	length of model domain in z - direction	300 cm
N_r	number of nodes in r - direction	21
N_z	number of nodes in z - direction	31
r_2	radius of source	500 cm
z_1	vertical location of lower source boundary (Ω_1)	50 cm
z_2	vertical location of upper source boundary (Ω_1)	150 cm
T	unsaturated-zone temperature	10 °C
P	unsaturated-zone pressure	760 mm Hg
q_{wz}	vertical recharge rate	105.6 cm/yr
	Constituent properties	
	o-Xylene (k = 1)	
H_1	Henry's Law constant	0.214
K_1	adsorption isotherm	.01
r_1	stoichiometric coefficient relating mass of oxygen utilized to unit mass of hydrocarbon degraded	3.17
G_{1latm}	gaseous-phase concentration at (Ω_2), (Ω_3) and (Ω_5)	0 g/cm³
	n-Octane (k = 2)	
H_2	Henry's Law constant	126.6
K_2	adsorption isotherm	.01
r_2	stoichiometric coefficient relating mass of oxygen utilized to unit mass of hydrocarbon degraded	3.51
$G_{2\,latm}$	gaseous-phase concentration at (Ω_2), (Ω_3) and (Ω_5)	0 g/cm³
	Oxygen (k = 3)	
H_3	Henry's Law constant	31.6
K_3	adsorption isotherm	0
$G_{2\,latm}$	gaseous-phase concentration at (Ω_2), (Ω_3) and (Ω_5)	279.0E-06 g/cm³

Table 10. Model input for R-UNSAT computer model test problem 3: Multispecies hydrocarbon transport and biodegradation--continued

	Boundary conditions	
I_1	initial concentration of o-xylene (k = 1) in immiscible plume (Ω_1)	0.488 g/cm^3
I_2	initial concentration of n-octane (k = 2) in immiscible plume (Ω_1)	.309 g/cm^3
I_3	initial concentration of oxygen (k = 3) in immiscible plume (Ω_1)	0 g/cm^3
θ_i	immiscible plume volumetric content	.01
λ_3	boundary-condition parameter: upper vertical boundary (Ω_3) (0 < z < R)	1.0
λ_5	boundary-condition parameter: outer radial boundary (Ω_5) (0 < z < L)	1.0
λ_2	boundary-condition parameter: lower vertical boundary (Ω_2) (0 < z < R)	0
A_1	initial gaseous-phase concentration in model domain	0 g/cm^3
A_2	initial gaseous-phase concentration in model domain	0 g/cm^3
A_3	initial gaseous-phase concentration in model domain	279.0E-06 g/cm^3
	Physical properties of the sediments	
ϕ	total porosity	0.400
θ_w	aqueous-phase porosity	.200
τ	gaseous-phase tortuosity	.200
ρ_b	bulk density	1.50 g/cm^3
	Algorithm parameters	
Δt	time step	96 hr
t_{end}	ending time	96,000 hr
$iter_{max}$	maximum number of iterations per time step	300
eps	convergence criteria (acceptable maximum relative error)	.001

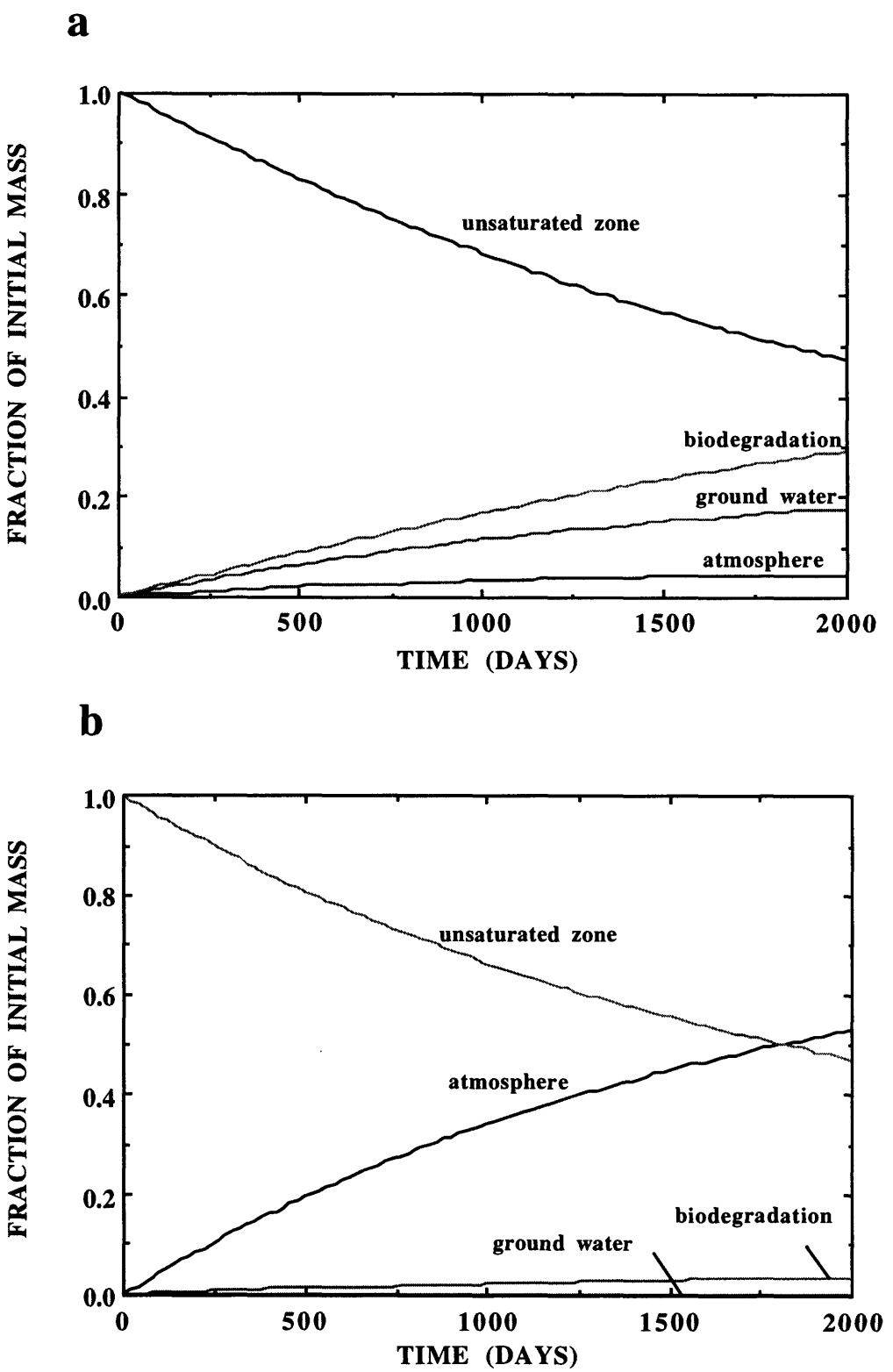

Figure 15. Example plot of the predicted long-term distribution of (a) o-xylene and (b) n-octane in the subsurface.

```
             1
********************************************************************************
                            NUMERICAL MODEL INPUT
********************************************************************************

TITLE - MULTISPECIES HYDROCARBON TRANSPORT AND BIODEGRADATION

  VALUE      MODEL CODE          DEFINITION          [cgs units]
             DESIGNATION
  -----      ----------          ----------          -----------

*************************** MODEL DOMAIN PARAMETERS ****************************

    3        (IDIM)              MODEL DIMENSIONALITY
                                   1: 1-D VERTICAL (z - DIRECTION)
                                   2: 1-D RADIAL (r - DIRECTION)
                                   3: 2-D (r,z DIRECTIONS)
0.1000E+04   (RF)                LENGTH OF MODEL DOMAIN IN r - DIRECTION [cm]
   21        (NR)                NUMBER OF NODES IN r - DIRECTION
0.3000E+03   (ZSURF)             LENGTH OF DOMAIN IN z - DIRECTION [cm]
   31        (NZ)                NUMBER OF NODES IN z - DIRECTION
0.5000E+02   (DR)                NODAL SPACING IN THE RADIAL DIRECTION [cm]
0.1000E+02   (DZ)                NODAL SPACING IN THE VERTICAL DIRECT ION [cm]
0.1000E+02   (TEMP)              UNSATURATED-ZONE TEMPERATURE [C]
0.7600E+03   (ATM)               UNSATURATED-ZONE PRESSURE [mm Hg]
0.1056E+03   (DARCY)             RECHARGE RATE [cm/yr]
    0        (IDISP)             AQUEOUS-PHASE DISPERSION OPTION
                                   0: NEGLECT AQUEOUS-PHASE DISPERSION
                                   1: ACCOUNT FOR AQUEOUS-PHASE DISPERSION

***************************** CONSTITUENT PROPERTIES ***************************

    3        (NK)                NUMBER OF MODEL CONSTITUENTS

--------------------------------- CONSTITUENT  1 ---------------------------------

   10        (ICON)              CONSTITUENT INDEX FOR: C8 AROMATIC
0.1062E+03   (WK(IK))            MOLECULAR WEIGHT OF CONSTITUENT [g]
0.1320E+03   (DV(IK))            ATOMIC DIFFUSION VOLUME [dimensionless]
0.2140E+00   (HAW(IK))           HENRYS LAW PARTITION COEFFICIENT (air/water)
                                   [dimensionless]
0.1000E-01   (HSW(IK))           ADSORPTION COEFFICIENT (soil/water) [dimensionless]
    1        (IBIO(IK))          BIODEGRADATION OPTION
                                   0: NO BIODEGRADATION
                                   1: AEROBIC DEGRADATION LINKED TO OXYGEN TRANSPORT
                                   2: BIODEGRADATION MODEL (subroutine "BIO2")
                                      SUPPLIED BY USER
0.3170E+01   (RK(IK))            STOICHIOMETRIC CONSTANT (rk) [dimensionless]
0.0000E+00   (ATCONC(IK))        GAS-PHASE CONCENTRATION ABOVE UPPER
                                 BOUNDARY [g/cm3]
             (DKA(IK))           GASEOUS-PHASE DIFFUSIVITY (** SEE MAP FILE - DKA.MAP)
0.1000E-04   (DKW(IK))           AQUEOUS-PHASE DIFFUSIVITY

--------------------------------- CONSTITUENT  2 ---------------------------------

   15        (ICON)              CONSTITUENT INDEX FOR: C8 ALKANE
0.1142E+03   (WK(IK))            MOLECULAR WEIGHT OF CONSTITUENT [g]
0.1688E+03   (DV(IK))            ATOMIC DIFFUSION VOLUME [dimensionless]
0.1266E+03   (HAW(IK))           HENRYS LAW PARTITION COEFFICIENT (air/water)
```

```
                                [dimensionless]
0.1000E-01    (HSW(IK))         ADSORPTION COEFFICIENT (soil/water) [dimensionless]
    1         (IBIO(IK))        BIODEGRADATION OPTION
                                  0: NO BIODEGRADATION
                                  1: AEROBIC DEGRADATION LINKED TO OXYGEN TRANSPORT
                                  2: BIODEGRADATION MODEL (subroutine "BIO2")
                                     SUPPLIED BY USER
0.3510E+01    (RK(IK))          STOICHIOMETRIC CONSTANT (rk) [dimensionless]
0.0000E+00    (ATCONC(IK))      GAS-PHASE CONCENTRATION ABOVE UPPER
                                BOUNDARY [g/cm3]
              (DKA(IK))         GASEOUS-PHASE DIFFUSIVITY (** SEE MAP FILE - DKA.MAP)
0.1000E-04    (DKW(IK))         AQUEOUS-PHASE DIFFUSIVITY

-------------------------------- CONSTITUENT  3 --------------------------------

    2         (ICON)            CONSTITUENT INDEX FOR: OXYGEN
0.3200E+02    (WK(IK))          MOLECULAR WEIGHT OF CONSTITUENT [g]
0.1630E+02    (DV(IK))          ATOMIC DIFFUSION VOLUME [dimensionless]
0.3160E+02    (HAW(IK))         HENRYS LAW PARTITION COEFFICIENT (air/water)
                                  [dimensionless]
0.2790E-03    (ATCONC(IK))      GAS-PHASE CONCENTRATION ABOVE UPPER
                                BOUNDARY [g/cm3]
              (DKA(IK))         GASEOUS-PHASE DIFFUSIVITY (** SEE MAP FILE - DKA.MAP)
0.1000E-04    (DKW(IK))         AQUEOUS-PHASE DIFFUSIVITY

********************** BOUNDARY AND INITIAL CONDITIONS ************************

    3         (IOPT)            SOURCE BOUNDARY CONDITION OPTION
                                  1: SPECIFIED FLUX AT WATER TABLE
                                  2: SPECIFIED CONCENTRATION AT WATER TABLE
                                  3: HYDROCARBON PLUME ABOVE WATER TABLE
                                  4: CONSTANT FLUX FROM INJECTION PROBE

-------------------------------- CONSTITUENT  1 --------------------------------

0.4880E+00    (XIK0(IK))        INITIAL IMMISCIBLE-PHASE CONCENTRATION [g/cm3]
0.1520E-03    (HWIK(IK))        SOLUBILITY [g/cm3]
0.1150E+01    (VK(IK))          SPECIFIC VOLUME [cm3/g]

-------------------------------- CONSTITUENT  2 --------------------------------

0.3090E+00    (XIK0(IK))        INITIAL IMMISCIBLE-PHASE CONCENTRATION [g/cm3]
0.6600E-06    (HWIK(IK))        SOLUBILITY [g/cm3]
0.1420E+01    (VK(IK))          SPECIFIC VOLUME [cm3/g]

-------------------------------- CONSTITUENT  3 --------------------------------

0.0000E+00    (XIK0(IK))        INITIAL IMMISCIBLE-PHASE CONCENTRATION [g/cm3]
0.0000E+00    (HWIK(IK))        SOLUBILITY [g/cm3]
0.9010E+00    (VK(IK))          SPECIFIC VOLUME [cm3/g]

--------------------------------------------------------------------------------

0.1000E-01    (THI0)            IMMISCIBLE PLUME VOLUMETRIC CONTENT [dimensionless]
0.5000E+03    (RIM)             RADIUS OF SOURCE [cm]
0.5000E+02    (ZLOW)            LOWER SOURCE BOUNDARY: z - LOCATION [cm]
0.1500E+03    (ZHI)             UPPER SOURCE BOUNDARY: z - LOCATION [cm]
    0         (IFAR)            OUTER BOUNDARY CHARACTERIZATION
                                  0: UNIFORM
```

```
                                1: VARIABLE
0.1000E+01    (AZ2)             BOUNDARY CONDITION PARAMETER: OUTER RADIAL BOUNDARY
    0         (ISURF)           UPPER BOUNDARY CHARACTERIZATION
                                0: UNIFORM
                                1: VARIABLE
0.1000E+01    (AR2)             BOUNDARY CONDITION PARAMETER: GROUND SURFACE
0.0000E+00    (AR3)             BOUNDARY CONDITION PARAMETER: WATER TABLE

*** DISCRETIZED INITIAL CONDITION DATA CONTAINED IN FILE-"IC.MAP"

****************** PHYSICAL PROPERTIES OF THE POROUS MEDIA ******************

    0         (ISTRAT)          HOMOGENEOUS UNSATURATED ZONE
0.4000E+00    (POR(NZ))         POROSITY OF UNSATURATED ZONE [dimensionless]
0.2000E+00    (THW(NZ))         MOISTURE CONTENT OF UNSAT. ZONE [dimensionless]
0.2000E+00    (TAL(IL))         TORTUOSITY [dimensionless]
0.1500E+01    (BDL(IL))         BULK DENSITY [g/cm3]

***************************** ALGORITHM PARAMETERS ****************************

    0         (ITIME)           TIME-STEP ADJUSTMENT OPTION
                                0: CONSTANT TIME-STEP
                                1: VARIABLE TIME-STEP
0.9600E+02    (DT1)             TIME-STEP [hrs]
0.9600E+05    (TEND)            ENDING TIME [hrs]
    0         (ISS)             STEADY-STATE DEFAULT OPTION
                                0: DO NOT ZERO-OUT STORAGE TERM
                                1: ZERO-OUT STORAGE TERM
  300         (NITER)           MAX. # OF ITERATIONS PER TIME STEP
0.1000E-02    (EPS)             CONVERGENCE CRITERIA - ACCEPTABLE MAX.
                                RELATIVE ERROR
    0         (IPROJ)           MATRIX-SOLVER SEED
                                0: PREVIOUS TIME-STEP
                                1: LINEAR PROJECTION FROM PREVIOUS TIME-STEP
                                2: DIRECT PROJECTION

***************************** OUTPUT PARAMETERS *****************************

    0         (IOUT)            OUTPUT OPTION
                                0: CONCENTRATION VS. TIME (breakthrough)
                                1: CONCENTRATION VS. DISTANCE (snapshot)
0.4800E+03    (YPR1)            PRINTOUT INCREMENT FOR BREAKTHROUGH DATA [hrs]
    1         (NW)              # OF LOCATIONS FOR OUTPUT DATA

------------------------------ OUTPUT LOCATION 1 ------------------------------

0.7500E+03    (RVW(IW))         RADIAL LOCATION FOR OUTPUT DATA [cm]
0.1500E+03    (ZVW(IW))         VERTICAL LOCATION FOR OUTPUT DATA [cm]

-------------------------------- CONSTITUENT  1 --------------------------------

    1         (IOUTOPT(IK))     OUTPUT OPTION
                                0: NO OUTPUT DATA REQUESTED
                                1: OUTPUT DATA REQUESTED

  *** OUTPUT DATA (t,G) [hrs,g/cm3] CONTAINED IN FILE-OUT1

-------------------------------- CONSTITUENT  2 --------------------------------
```

```
   1        (IOUTOPT(IK))   OUTPUT OPTION
                              0: NO OUTPUT DATA REQUESTED
                              1: OUTPUT DATA REQUESTED

  *** OUTPUT DATA (t,G) [hrs,g/cm3] CONTAINED IN FILE-OUT2

------------------------------ CONSTITUENT  3 -------------------------------

   1        (IOUTOPT(IK))   OUTPUT OPTION
                              0: NO OUTPUT DATA REQUESTED
                              1: OUTPUT DATA REQUESTED

  *** OUTPUT DATA (t,G) [hrs,g/cm3] CONTAINED IN FILE-OUT3

--------------------------------------------------------------------------------


************************** MODEL DOMAIN COORDINATES ***************************

 1000        (R(NR))         r - COORDINATE: OUTER BOUNDARY [cm]
  500        (R(IRIM))       r - COORDINATE: RADIUS OF SOURCE [cm]
    0        (Z(1))          z - COORDINATE: LOWER BOUNDARY [cm]
  300        (Z(NZ))         z - COORDINATE: SURFACE BOUNDARY [cm]
   50        (Z(IZLOW))      z - COORDINATE: LOWER SOURCE BOUNDARY [cm]
  150        (Z(IZHI))       z - COORDINATE: UPPER SOURCE BOUNDARY [cm]
  750        (R(IRVW(IW)))   r - COORDINATE: OUTPUT LOCATION  1 [cm]
  150        (Z(IZVW(IW)))   z - COORDINATE: OUTPUT LOCATION  1 [cm]
--------------------------------------------------------------------------------
```

3.4.4 Test Problem 4--Diffusion-Coefficient Determination

The effective-diffusion coefficient governs the rate of gaseous diffusion through the unsaturated zone. As described in Section 2.4.2, the diffusion coefficient is defined by gaseous-phase composition and the moisture-saturation properties of the unsaturated-zone sediments. Because of the complexity of natural sediment pore structure, the diffusion coefficient or, more specifically, τ, is commonly determined experimentally (Fischer and others, 1996; Kreamer and others, 1988). An experimental procedure for quantifying τ is outlined in the following test problem with the assumption that the effective-diffusion coefficient is described by (38).

Figures 16 and 17 illustrate the geometry and boundary conditions for this problem, respectively. A tracer gas, sulfur hexafluoride (SF_6), is injected at a constant rate (J_{k0} = 1.0E-08 g/cm^2-s) from an injection probe installed to a depth 155 cm below land surface. The probe has a 10-cm opening, bounded by vertical coordinates z_1= 145 cm and z_2 = 155 cm. Breakthrough (concentration as a function of time) data were recorded at a monitoring probe positioned 500 cm from the probe and 100 cm below land surface. These data are contained in table 11. Results of unsaturated-zone sampling revealed that the aquifer is homogeneous and isotropic, with a total porosity (ϕ) of 0.40 and a moisture content (θ_w) of 0.10. Temperatures within the unsaturated zone are constant (T = 10 °C). The surface boundary is defined by a constant-atmospheric-concentration boundary condition given by (9), where λ_2 = 1, and the outer-radial boundary is defined as a constant-atmospheric-concentration boundary condition given by (11), where λ_5 = 1. Two-dimensional gas transport for this test problem is described by (7) and is solved numerically by employing source boundary condition Option 4 (see Section 2.2.1). The remaining model input for this test problem is contained in table 12. The gaseous-phase tortuosity (τ) is unknown

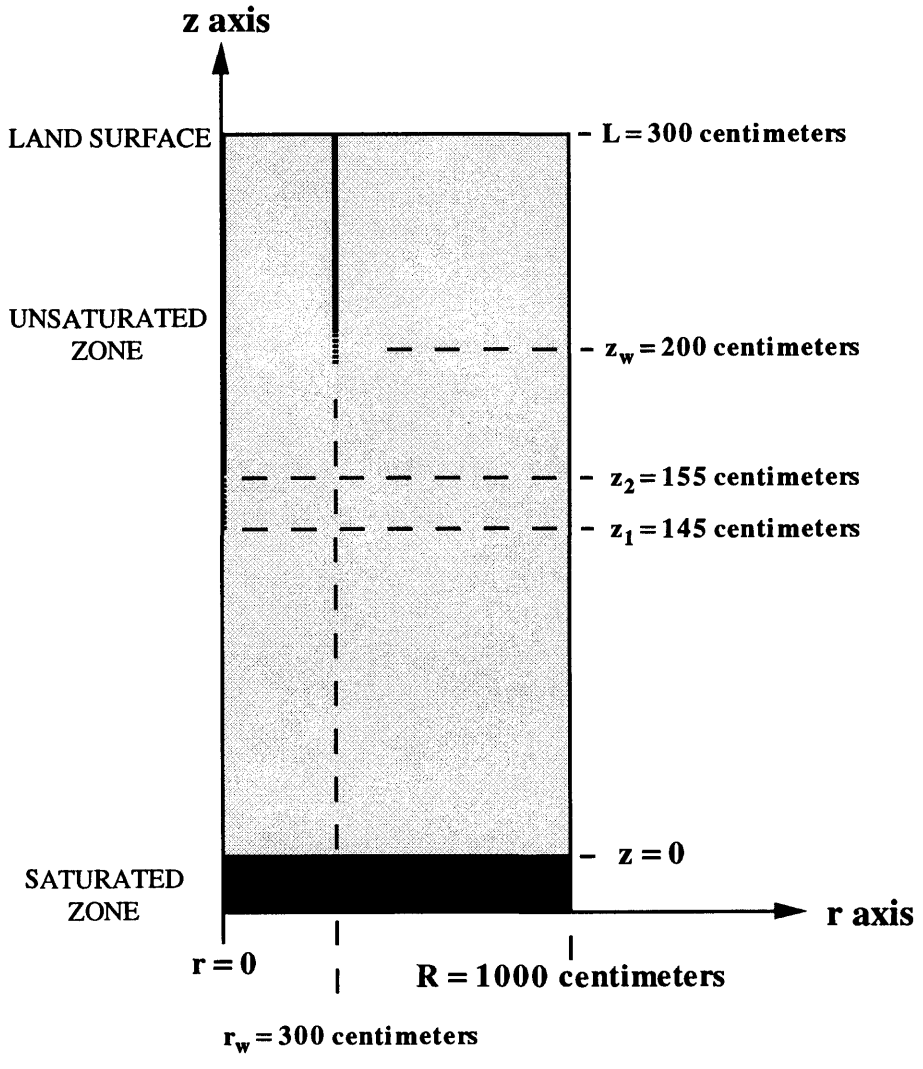

EXPLANATION

r_w	monitoring-well location in r-direction
z_w	monitoring-well location in z-direction
z_1	vertical location of lower source boundary
z_2	vertical location of upper source boundary
R	radius of model domain
L	length of model domain

Figure 16. Diagram showing model geometry used for model application to estimate the effective-diffusion coefficient.

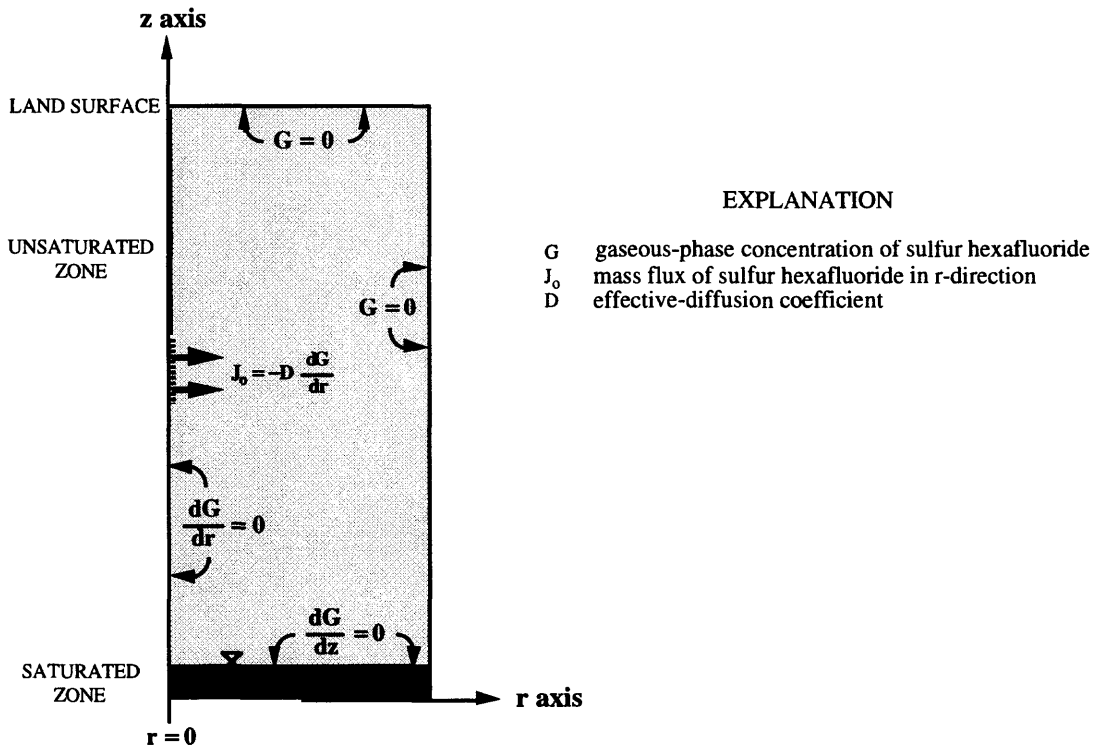

Figure 17. Diagram showing boundary conditions used for model application to estimate the effective-diffusion coefficient.

Table 11. Example of sulfur hexafluoride gas concentrations at the monitor probe location

Time (hours)	Concentration (milligrams per liter)
0	0.000E-00
90	2.304E-02
188	5.202E-02
242	8.901E-02
400	1.758E-01
430	1.827E-01

and is determined by model calibration. The MIF presented below was generated by choosing to create new model input (Option 1--see Section 3.1), selecting the numerical solver (Option 1), and entering the required input parameters from table 11.

Model calibration to the data contained in table 11 is obtained by a least-root-mean-squares fit of the simulated and measured gas-concentration data. The results of model calibration (fig. 18) yielded a τ estimate of $\tau_a = 0.340$. Substituting $d_{ka} = 0.07132$ cm^2/s, $\tau_a = 0.340$, and $\theta_a = 0.30$ (where $\theta_a = \phi - \theta_w$) into (38) results in an effective-diffusion-coefficient estimate of $D_{ka} = 7.37E\text{-}03$ cm^2/s. Because the effective porosity of natural sediments can be highly variable, this in situ approach yields a better estimate of D_{ka} than a standard laboratory approach, provided gaseous-phase diffusion is the dominant transport mechanism. The use of diffusion coefficients based on theoretical tortuosity relations such as that given by Millington (1959, equation 43) could lead to a significant error in gas-flux calculations (Lahvis and Baehr, 1996).

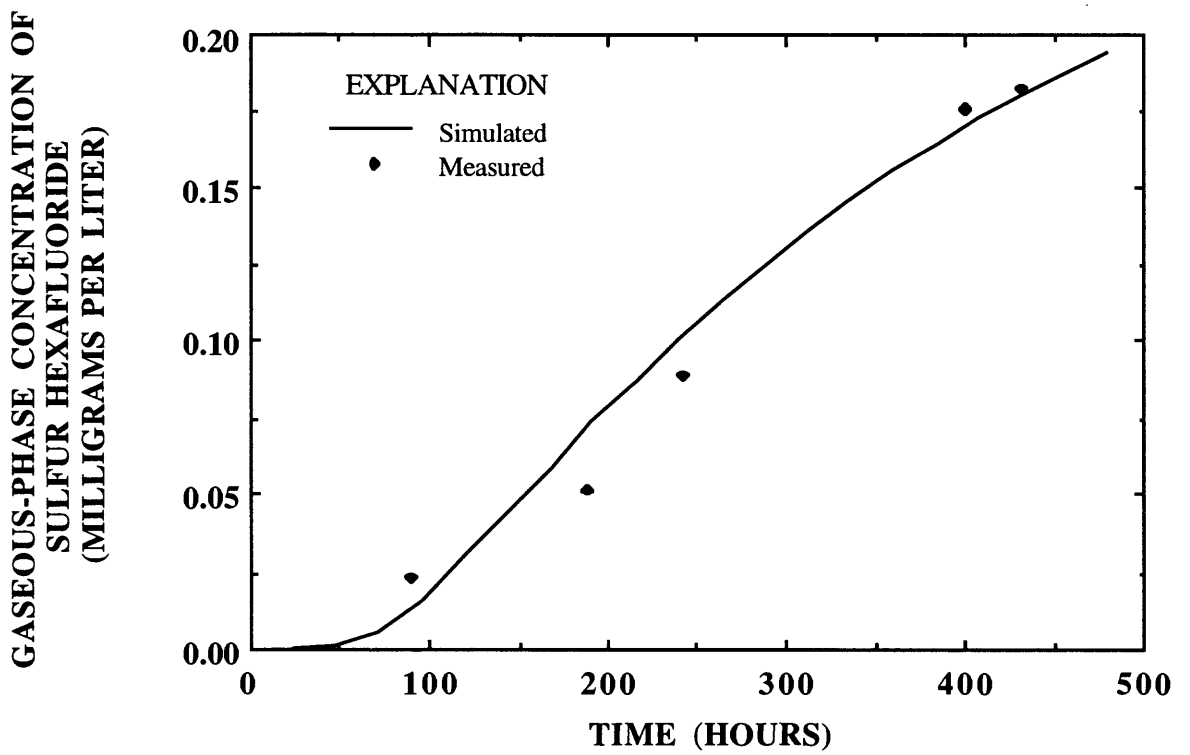

Figure 18. Example plot of the results of model calibration to tracer-gas-concentration data.

Table 12. Model input for R-UNSAT computer model test problem 4: Diffusion-coefficient determination

Symbol	Definition	Value
	Model geometry	
R	length of model domain in r-direction	1,000 cm
L	length of model domain in z-direction	300 cm
N_r	number of nodes in r-direction	101
N_z	number of nodes in z-direction	61
z_1	vertical location of lower source boundary (Ω_1)	145 cm
z_2	vertical location of upper source boundary (Ω_1)	155 cm
T	unsaturated-zone temperature	10 °C
P	unsaturated-zone pressure	760 mm Hg
q_{wz}	vertical recharge rate	0 cm/yr
	Constituent properties	
ω	molecular weight	146.0 g/cm^3
ζ	atomic diffusion volume	111.1
H	Henry's Law constant	123.4
S	solid/water partition coefficient	0
G_{1atm}	gaseous-phase concentration at (Ω_2), (Ω_3) and (Ω_5)	0 g/cm^3
	Physical properties of the unsaturated-zone sediments	
ϕ	total porosity	0.400
θ_w	aqueous-phase porosity	.100
τ	gaseous-phase tortuosity (calibrated)	.340
ρ_b	bulk density	1.50 g/cm^3
	Boundary condition	
J_o	constant gaseous-phase flux at injection probe ($z_1 < z < z_2$)	1.0E-09 g/cm^3
	Initial condition	
A	initial concentration of sulfur hexafluoride in unsaturated zone	0 g/cm^3
	Output parameters	
t_{end}	maximum time for breakthrough data	500 hr
Δt_b	time step for breakthrough data	2.4 hr
r_{vw}	output-data location in r-direction	300 cm
z_{vw}	output-data location in z-direction	200 cm
$iter_{max}$	maximum number of iterations per time-step	300
eps	convergence criteria (acceptable maximum relative error)	.001

```
             1
*******************************************************************************
                            NUMERICAL MODEL INPUT
*******************************************************************************

TITLE -  DIFFUSION COEFFICIENT DETERMINATION

  VALUE      MODEL CODE          DEFINITION         [cgs units]
             DESIGNATION
  -----      ----------          ----------         -----------

*************************** MODEL DOMAIN PARAMETERS ***************************

    3        (IDIM)          MODEL DIMENSIONALITY
                               1: 1-D VERTICAL (z - DIRECTION)
                               2: 1-D RADIAL (r - DIRECTION)
                               3: 2-D (r,z DIRECTIONS)
0.1000E+04   (RF)            LENGTH OF MODEL DOMAIN IN r - DIRECTION [cm]
  101        (NR)            NUMBER OF NODES IN r - DIRECTION
0.3000E+03   (ZSURF)         LENGTH OF DOMAIN IN z - DIRECTION [cm]
   61        (NZ)            NUMBER OF NODES IN z - DIRECTION
0.1000E+02   (DR)            NODAL SPACING IN THE RADIAL DIRECTION [cm]
0.5000E+01   (DZ)            NODAL SPACING IN THE VERTICAL DIRECTION [cm]
0.1000E+02   (TEMP)          UNSATURATED-ZONE TEMPERATURE [C]
0.7600E+03   (ATM)           UNSATURATED-ZONE PRESSURE [mm Hg]
0.0000E+00   (DARCY)         RECHARGE RATE [cm/yr]

***************************** CONSTITUENT PROPERTIES *****************************

    1        (NK)            NUMBER OF MODEL CONSTITUENTS

-------------------------------- CONSTITUENT  1 --------------------------------

    7        (ICON)          CONSTITUENT INDEX FOR: OTHER
0.1460E+03   (WK(IK))        MOLECULAR WEIGHT OF CONSTITUENT [g]
0.1111E+03   (DV(IK))        ATOMIC DIFFUSION VOLUME [dimensionless]
0.1234E+03   (HAW(IK))       HENRYS LAW PARTITION COEFFICIENT (air/water)
                               [dimensionless]
0.0000E+00   (HSW(IK))       ADSORPTION COEFFICIENT (soil/water) [dimensionless]
    0        (IBIO(IK))      BIODEGRADATION OPTION
                               0: NO BIODEGRADATION
                               1: AEROBIC DEGRADATION LINKED TO OXYGEN TRANSPORT
                               2: BIODEGRADATION MODEL (subroutine "BIO2")
                                  SUPPLIED BY USER
0.0000E+00   (ATCONC(IK))    GAS-PHASE CONCENTRATION ABOVE UPPER
                             BOUNDARY [g/cm3]
             (DKA(IK))       GASEOUS-PHASE DIFFUSIVITY (** SEE MAP FILE - DKA.MAP)
0.1000E-04   (DKW(IK))       AQUEOUS-PHASE DIFFUSIVITY

********************** BOUNDARY AND INITIAL CONDITIONS **********************

    4        (IOPT)          SOURCE BOUNDARY CONDITION OPTION
                               1: SPECIFIED FLUX AT WATER TABLE
                               2: SPECIFIED CONCENTRATION AT WATER TABLE
                               3: HYDROCARBON PLUME ABOVE WATER TABLE
                               4: CONSTANT FLUX FROM INJECTION PROBE

-------------------------------- CONSTITUENT  1 --------------------------------
```

```
0.1000E-07   (FLX(1,IK))        GAS FLUX ACROSS RADIAL BOUNDARY [g/cm2-s]

--------------------------------------------------------------------------------

0.1450E+03   (ZLOW)          LOWER SOURCE BOUNDARY: z - LOCATION [cm]
0.1550E+03   (ZHI)           UPPER SOURCE BOUNDARY: z - LOCATION [cm]
    0        (IFAR)          OUTER BOUNDARY CHARACTERIZATION
                               0: UNIFORM
                               1: VARIABLE
0.1000E+01   (AZ2)           BOUNDARY CONDITION PARAMETER: OUTER RADIAL BOUNDARY
    0        (ISURF)         UPPER BOUNDARY CHARACTERIZATION
                               0: UNIFORM
                               1: VARIABLE
0.1000E+01   (AR2)           BOUNDARY CONDITION PARAMETER: GROUND SURFACE
0.0000E+00   (AR3)           BOUNDARY CONDITION PARAMETER: WATER TABLE

*** DISCRETIZED INITIAL CONDITION DATA CONTAINED IN FILE-"IC.MAP"

****************** PHYSICAL PROPERTIES OF THE POROUS MEDIA ******************

    0        (ISTRAT)        HOMOGENEOUS UNSATURATED ZONE
0.4000E+00   (POR(NZ))       POROSITY OF UNSATURATED ZONE [dimensionless]
0.1000E+00   (THW(NZ))       MOISTURE CONTENT OF UNSAT. ZONE [dimensionless]
0.3400E+00   (TAL(IL))       TORTUOSITY [dimensionless]
0.1500E+01   (BDL(IL))       BULK DENSITY [g/cm3]

***************************** ALGORITHM PARAMETERS *****************************

    0        (ITIME)         TIME-STEP ADJUSTMENT OPTION
                               0: CONSTANT TIME-STEP
                               1: VARIABLE TIME-STEP
0.2400E+01   (DT1)           TIME-STEP [hrs]
0.5000E+03   (TEND)          ENDING TIME [hrs]
    0        (ISS)           STEADY-STATE DEFAULT OPTION
                               0: DO NOT ZERO-OUT STORAGE TERM
                               1: ZERO-OUT STORAGE TERM
  300        (NITER)         MAX. # OF ITERATIONS PER TIME STEP
0.1000E-02   (EPS)           CONVERGENCE CRITERIA - ACCEPTABLE MAX.
                               RELATIVE ERROR
    0        (IPROJ)         MATRIX-SOLVER SEED
                               0: PREVIOUS TIME-STEP
                               1: LINEAR PROJECTION FROM PREVIOUS TIME-STEP
                               2: DIRECT PROJECTION

***************************** OUTPUT PARAMETERS ******************************

    0        (IOUT)          OUTPUT OPTION
                               0: CONCENTRATION VS. TIME (breakthrough)
                               1: CONCENTRATION VS. DISTANCE (snapshot)
0.2400E+02   (YPR1)          PRINTOUT INCREMENT FOR BREAKTHROUGH DATA [hrs]
    1        (NW)            # OF LOCATIONS FOR OUTPUT DATA

------------------------------ OUTPUT LOCATION 1 -------------------------------

0.3000E+03   (RVW(IW))       RADIAL LOCATION FOR OUTPUT DATA [cm]
0.2000E+03   (ZVW(IW))       VERTICAL LOCATION FOR OUTPUT DATA [cm]

-------------------------------- CONSTITUENT  1 --------------------------------
```

```
   1        (IOUTOPT(IK))   OUTPUT OPTION
                              0: NO OUTPUT DATA REQUESTED
                              1: OUTPUT DATA REQUESTED

  *** OUTPUT DATA (t,G) [hrs,g/cm3] CONTAINED IN FILE-OUT1

-------------------------------------------------------------------------------


************************** MODEL DOMAIN COORDINATES ***************************

 1000        (R(NR))         r - COORDINATE: OUTER BOUNDARY [cm]
   10        (R(IRIM))       r - COORDINATE: RADIUS OF SOURCE [cm]
    0        (Z(1))          z - COORDINATE: LOWER BOUNDARY [cm]
  300        (Z(NZ))         z - COORDINATE: SURFACE BOUNDARY [cm]
  145        (Z(IZLOW))      z - COORDINATE: LOWER SOURCE BOUNDARY [cm]
  155        (Z(IZHI))       z - COORDINATE: UPPER SOURCE BOUNDARY [cm]
  500        (R(IRVW(IW)))   r - COORDINATE: OUTPUT LOCATION  1 [cm]
  200        (Z(IZVW(IW)))   z - COORDINATE: OUTPUT LOCATION  1 [cm]
-------------------------------------------------------------------------------
```

SECTION 4.0--MODEL VERIFICATION

The numerical algorithm was verified by comparing numerical solutions to known steady-state analytical solutions for simplified one-dimensional test cases. The algorithm was verified for the applications of constant-flux and constant-concentration boundary conditions at r = 0 and z = 0 and the ability to simulate aquifer heterogeneity and biogeochemical reactions.

4.1 Model Testing of the Source Boundary Conditions

4.1.1 Constant-Flux Source at r = 0

Figure 19 illustrates the one-dimensional model geometry used for a radial-transport test of the numerical algorithm when a constant-flux boundary is applied at r = 0. The steady-state mathematical equation describing transport for this geometry is given by:

$$\frac{\partial^2 G}{\partial r^2} + \left(\frac{1}{r}\right)\frac{\partial G}{\partial r} = 0 \tag{63}$$

with boundary conditions:

$$J_o = -D\frac{dG}{dr} \qquad \text{at } r = r_2 \tag{64}$$

$$G = 0 \qquad \text{at } r = R \tag{65}$$

to which the solution is

$$G = \frac{J_o}{D} r_2 \ln\left(\frac{R}{r}\right) \tag{66}$$

Transient solutions advance to the steady-state solution for the input data listed in table 13, as shown in figure 20.

4.1.2 Constant-Flux Source at z = 0

Figure 21 represents the one-dimensional model geometry used for a vertical-transport test of the numerical algorithm when a constant-flux boundary is applied at z = 0. The steady-state distribution corresponding to this geometry satisfies the following:

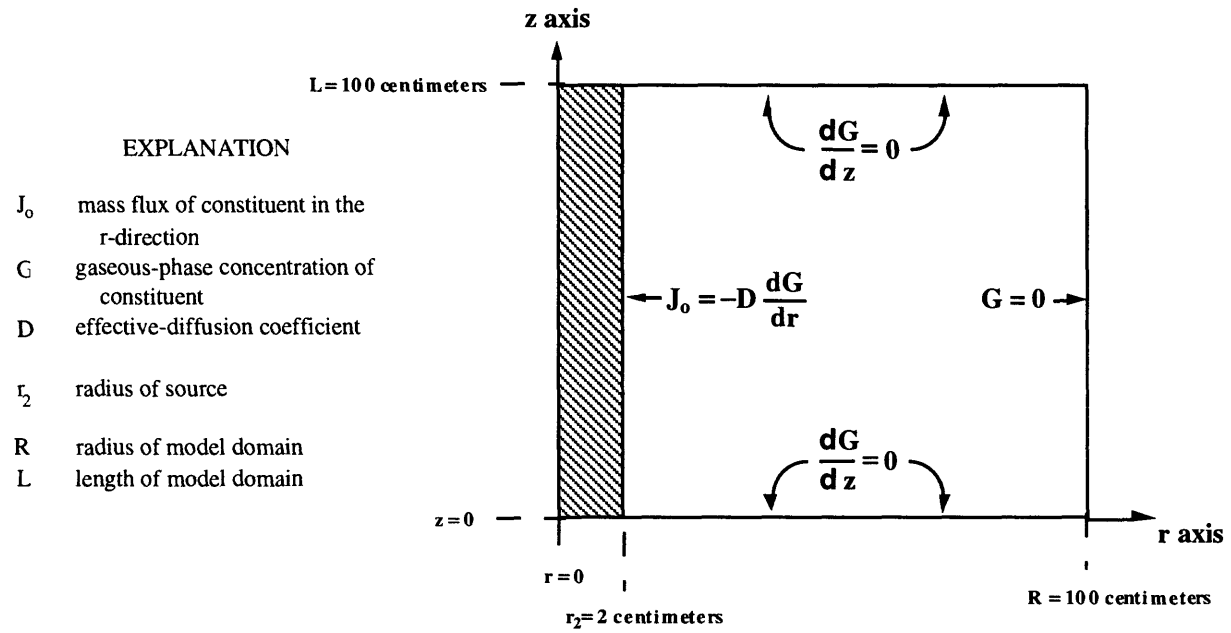

Figure 19. Diagram showing model geometry and boundary conditions used for the radial transport test of algorithm when a constant-flux boundary is applied at r = 0.

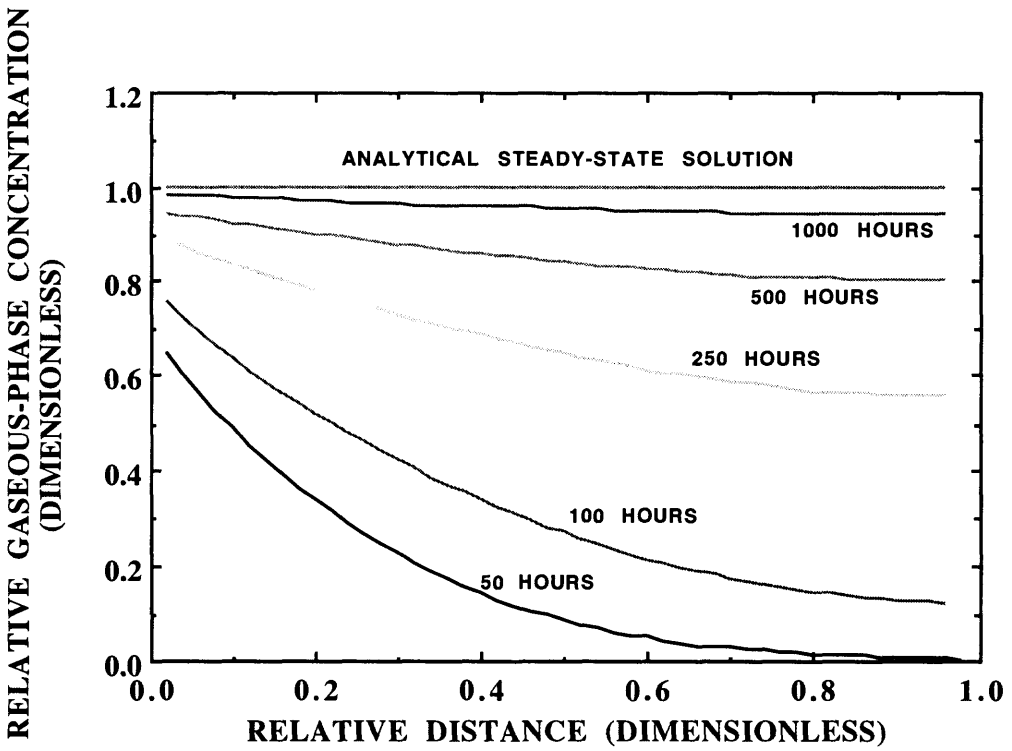

Figure 20. Plot of the transient approach to steady state for the radial-transport test of algorithm when a constant-flux boundary is applied at r = 0.

Table 13. Input parameters used for radial-transport test of a constant-flux boundary at r = 0

Symbol	Definition	Model code designation	Value
R	length of model domain in r-direction	RF	100 cm
L	length of model domain in z-direction	ZSURF	100 cm
Nr	number of nodes in r-direction	NR	51
J_o	gas flux across source boundary ($r = r_2$)	FLX(IRIM,IK)	1.0E-9 g/cm²-s
D	effective-diffusion coefficient		1.9E-4 cm²/s
r_2	radius of source	RIM	2 cm
z_1	vertical location of lower source boundary	ZLOW	0 cm
z_2	vertical location of upper source boundary	ZHI	100 cm
Δt	time step	DT	1 hr

$$\frac{d^2G}{dz^2} = 0 \tag{67}$$

with boundary conditions:

$$J_o = -D\frac{dG}{dz} \qquad \text{at } z = z_2 \tag{68}$$

$$G = 0 \qquad \text{at } z = L \tag{69}$$

to which the solution is

$$G = \frac{J_o}{D}(L - z_2) \tag{70}$$

Transient solutions advance to the steady-state solution for the input data listed in table 14, as shown in figure 22.

4.1.3 Constant-Concentration Source at r = 0

The one-dimensional model geometry used for a radial-transport test of the numerical algorithm when a constant-concentration boundary is applied at r = 0 is illustrated in figure 23. The steady-state mathematical equation describing transport for this geometry satisfies (63) for the boundary conditions:

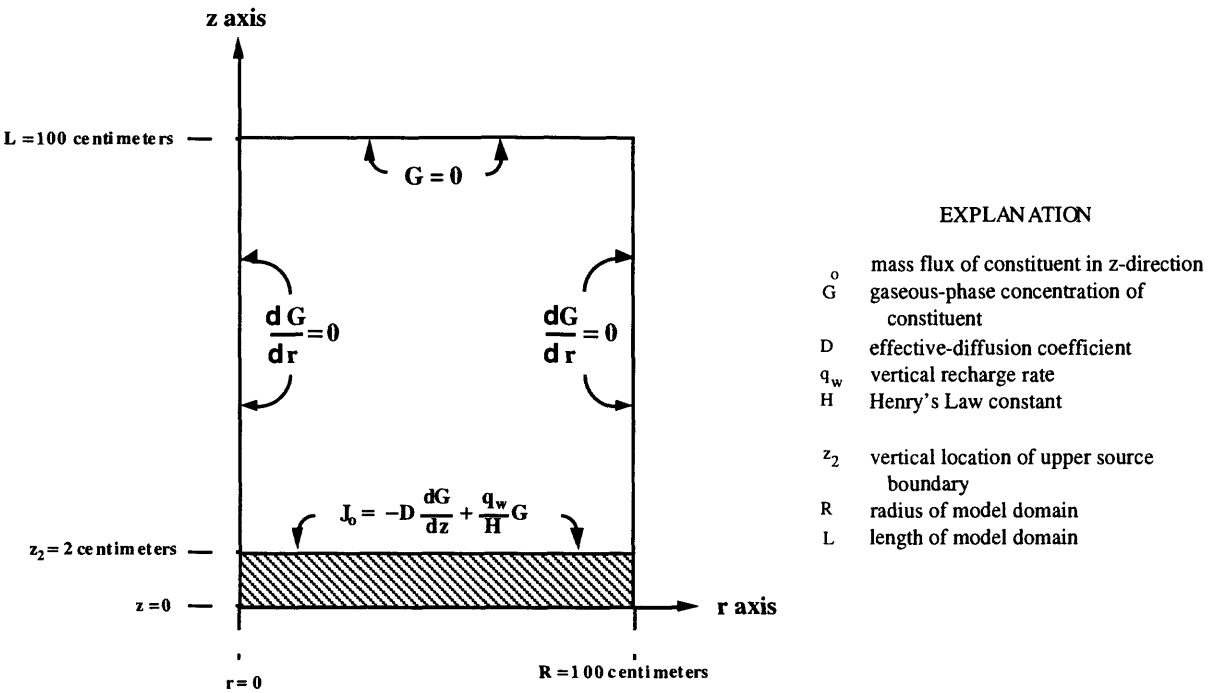

Figure 21. Diagram showing model geometry and boundary conditions used for the vertical transport test of algorithm when a constant-flux boundary is applied at z = 0.

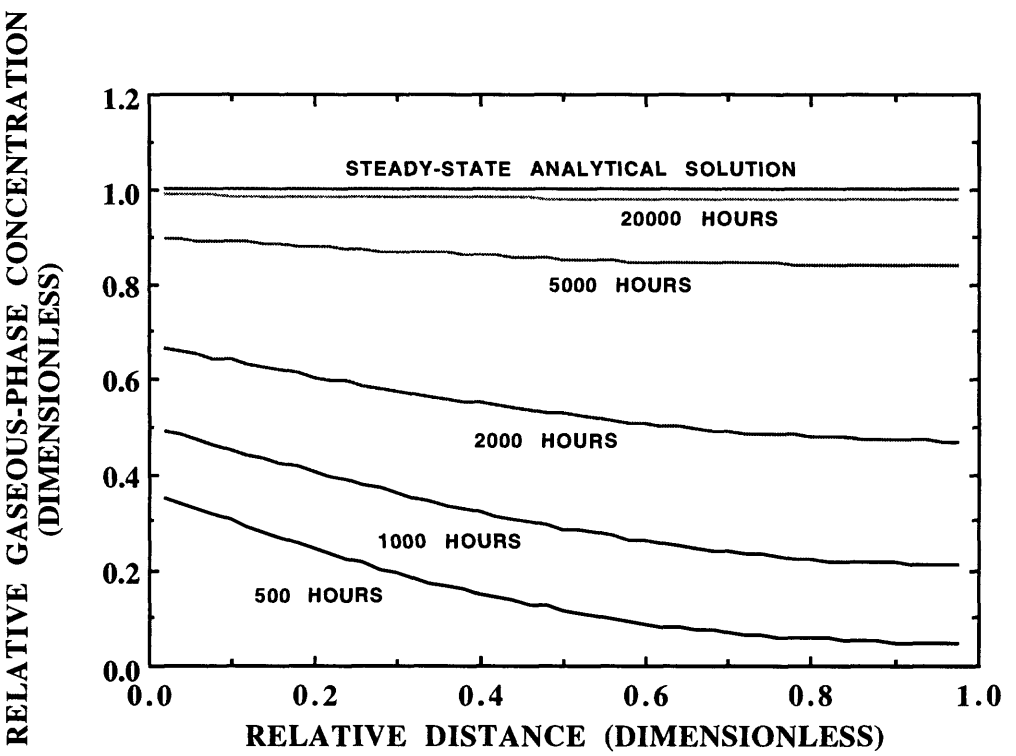

Figure 22. Plot of the transient approach to steady state for the vertical-transport test of algorithm when a constant-flux boundary is applied at z = 0

Table 14. Input parameters used for vertical-transport test of a constant-flux boundary at z = 0

Symbol	Definition	Model code designation	Value
L	length of model domain in z-direction	ZSURF	100 cm
Nz	number of nodes in z-direction	NZ	51
CSA	cross-sectional area of model domain	CSA	1.0E6 cm^2
J_o	gas flux across source boundary ($z = z_2$)	FLX(IR,IK)	1.0E-9 g/cm^2-s
D	effective-diffusion coefficient		1.9E-4 cm^2/s
z_1	vertical location of lower source boundary	ZLOW	0 cm
z_2	vertical location of upper source boundary	ZHI	2 cm
Δt	time step	DT	1 hr

$$G = G_o \quad \text{at } r = r_2 \tag{71}$$

$$G = 0 \quad \text{at } r = R \tag{72}$$

to which the solution is

$$G = G_o \left[\frac{\ln\left(\frac{r}{R}\right)}{\ln\left(\frac{r_2}{R}\right)} \right] \tag{73}$$

Transient solutions advance to the steady-state solution for the input data listed in table 15, as shown in figure 24.

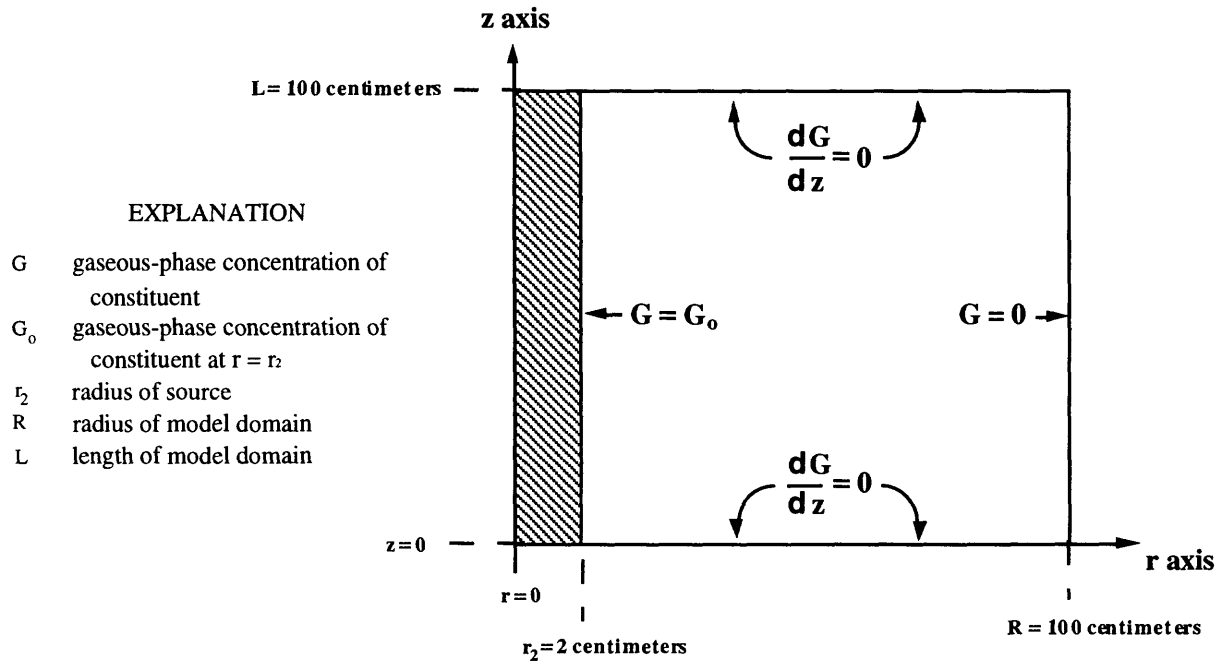

Figure 23. Diagram showing model geometry and boundary conditions used for the radial transport test of algorithm when a constant-concentration boundary is applied at r = 0.

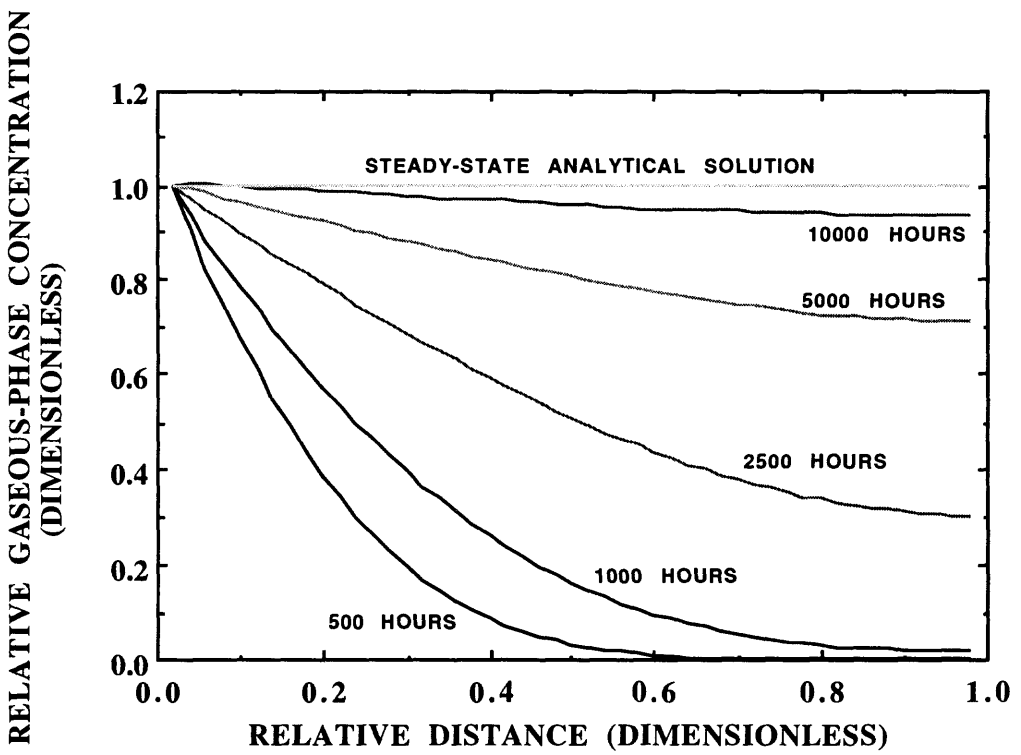

Figure 24. Plot of the transient approach to steady state for the radial-transport test of algorithm when a constant-concentration boundary is applied at r = 0.

Table 15. Input parameters used for radial-transport test of a constant-concentration boundary at r = 0

Symbol	Definition	Model code designation	Value
R	length of model domain in r-direction	RF	100 cm
L	length of model domain in z-direction	ZSURF	100 cm
Nr	number of nodes in r-direction	NR	51
G_o	gaseous-phase concentration at source boundary ($r = r_2$)	Y0(IRIM, IZ, IK)	5.15E3 g/cm^3
D	effective-diffusion coefficient		1.9E-4 cm^2/s
r_2	radius of source	RIM	2 cm
z_1	vertical location of lower source boundary	ZLOW	0 cm
z_2	vertical location of upper source boundary	ZHI	100 cm
Δt	time step	DT	1 hr

4.1.4 Constant-Concentration Source at z = 0

Figure 25 represents the one-dimensional model geometry used for a vertical-transport test of the numerical algorithm when a constant-concentration boundary is applied at z = 0. The steady-state distribution for this geometry satisfies (67) for the boundary conditions:

$$G = G_o \quad \text{at } z = z_2 \tag{74}$$

$$G = 0 \quad \text{at } z = L \tag{75}$$

to which the solution is

$$G = G_o \frac{(L - z)}{(L - z_2)} \tag{76}$$

Transient solutions advance to the steady-state solution for the input data listed in table 16, as shown in figure 26.

Table 16. Input parameters used for vertical-transport test of a constant-concentration boundary at z = 0

Symbol	Definition	Model code designation	Value
L	length of model domain in z-direction	ZSURF	100 cm
Nz	number of nodes in z-direction	NZ	51
CSA	cross-sectional area of model domain	CSA	1.0E6 cm^2
G_o	gaseous-phase concentration at source boundary ($z = z_2$)	Y0(IR, IZHI, IK)	1.0E-7 g/cm^3
D	effective-diffusion coefficient		1.9E-4 cm^2/s
z_1	vertical location of lower source boundary	ZLOW	0 cm
z_2	vertical location of upper source boundary	ZHI	2 cm
Δt	time step	DT	1 hr

4.2 Model Testing of Aquifer Heterogeneity

The verification of aquifer heterogeneity consisted of testing the numerical algorithm's ability to simulate sediment layering and a spatially variable diffusion coefficient [$D_k(z)$]. The ability to simulate sediment layering was verified by comparing steady-state transport in a two-sediment-layer aquifer to steady-state transport in an aquifer with a third-kind or leaky-confining-unit boundary condition applied at z = L. The ability to simulate diffusion-coefficient heterogeneity was verified by comparing numerical and steady-state analytical solutions for unsaturated-zone sediments exhibiting constant and linear moisture distributions.

4.2.1 Sediment-Layering Heterogeneity

Figure 27 depicts the model geometry used to verify the numerical algorithm for the sediment-layering ability when boundary conditions (74) and (75) are applied for the vertical-transport test case defined by (67) (see Section 4.1.2). The confining unit at z = L was modeled as a separate sediment layer whose thickness (b′) and diffusivity (D′) are specified in table 17. Verification was achieved by comparing the steady-state numerical solution for this geometry to the one-dimensional analytical-model solution referred to in Section 2.2.2 as case 4: constant concentration ($G = G_o$) at z = 0; leaky confining unit at z = L. Transient solutions advance to the steady-state solution for the input data listed in table 17, as shown in figure 28.

The numerical algorithm will fail if the effective-diffusion coefficients of bordering sediment layers differ significantly. Failure occurs as a result of the sharp diffusion-coefficient gradient (dD_k/dz) created between the nodes marking the lithologic contact. The maximum allowable difference that can be specified is a function of the grid spacing (Δz) and time-step increment (Δt). The maximum allowable difference in effective-diffusion coefficients with the assumption that

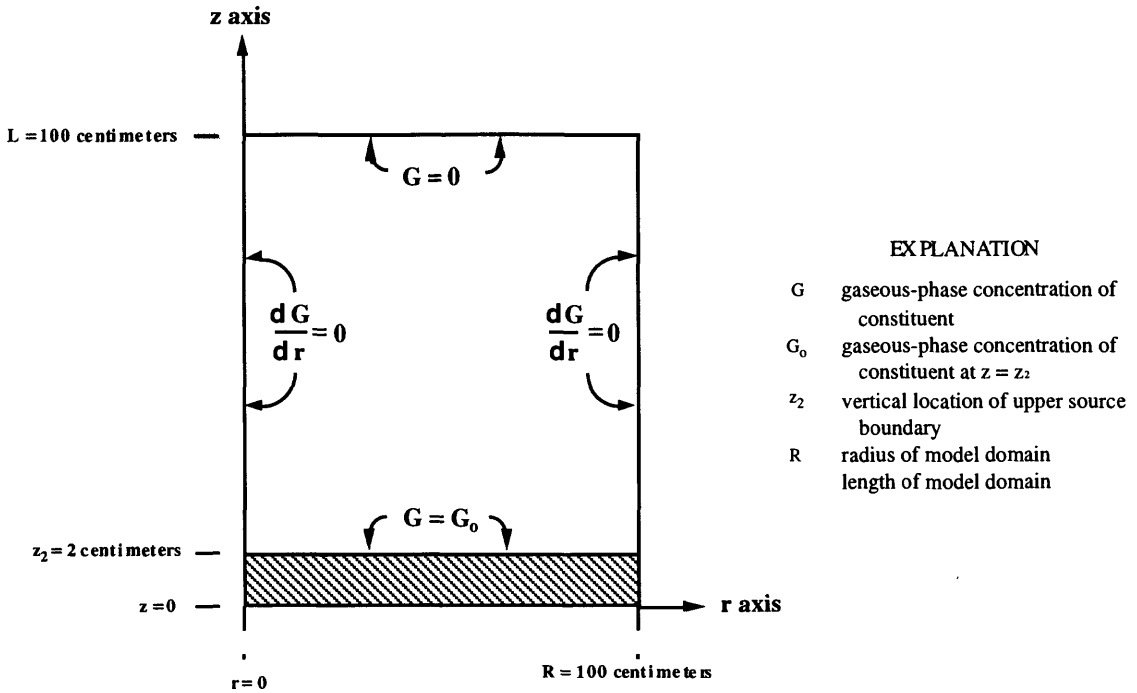

Figure 25. Diagram showing model geometry and boundary conditions used for the vertical transport test of algorithm when a constant-concentration boundary is applied at z = 0.

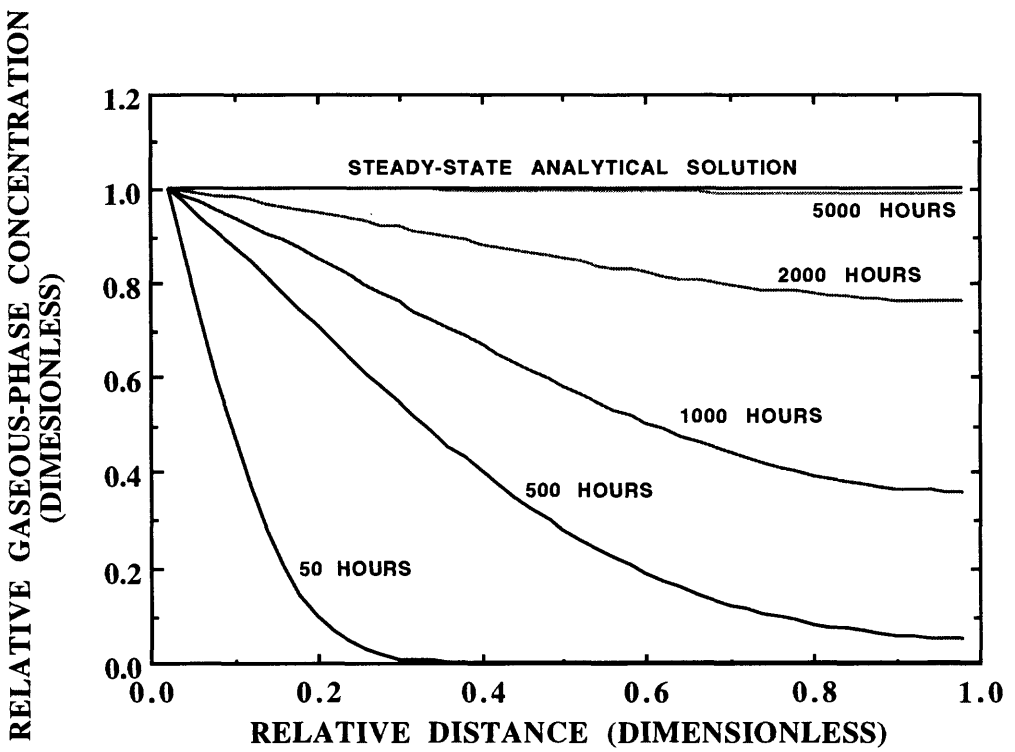

Figure 26. Plot of the transient approach to steady state for the vertical-transport test of algorithm when a constant-concentration boundary is applied at z = 0.

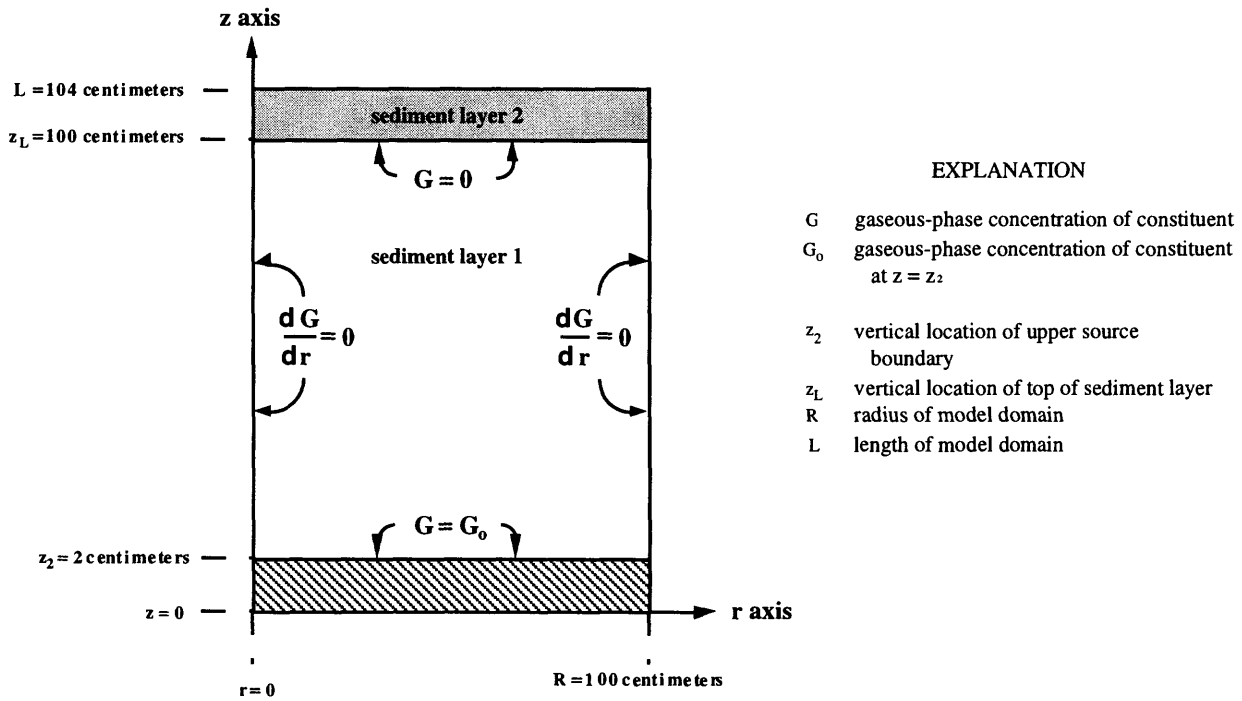

Figure 27. Diagram showing model geometry and boundary conditions used for the vertical transport test of sediment-layering heterogeneity.

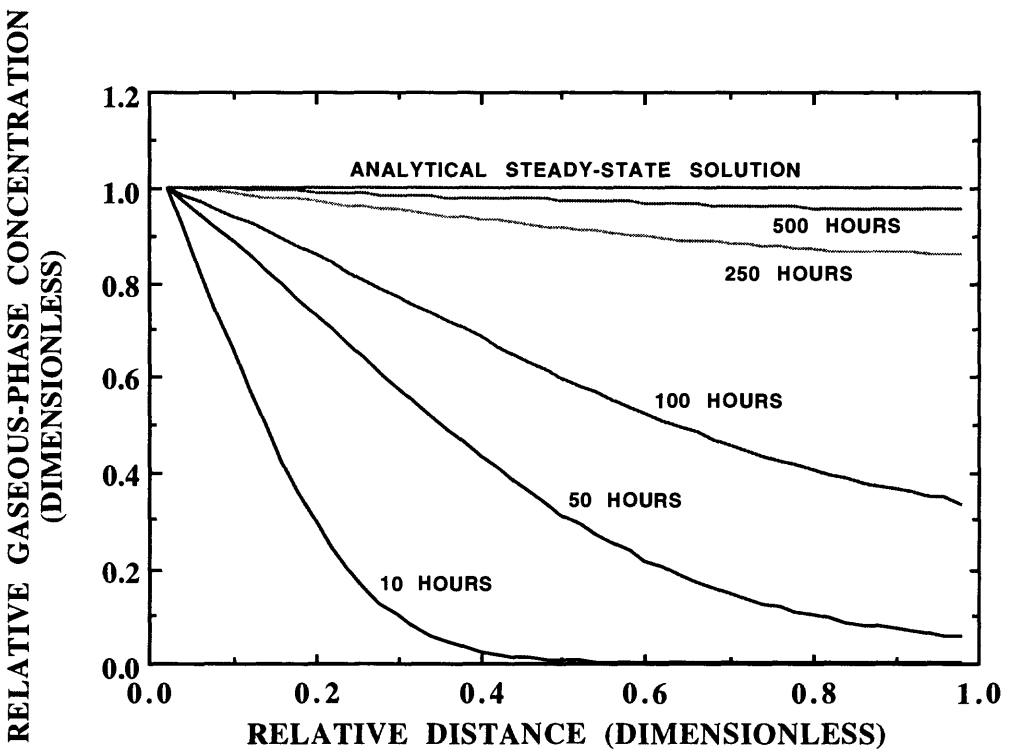

Figure 28. Plot of the transient approach to steady state for the vertical-transport test of sediment-layering heterogeneity.

Table 17. Input parameters used for vertical-transport test of sediment-layering heterogeneity

Symbol	Definition	Model code designation	Value
L	length of model domain in z-direction	ZSURF	104 cm
Nz	number of nodes in z-direction	NZ	53
CSA	cross-sectional area of model domain	CSA	1.0E6 cm^2
G_o	gaseous-phase concentration at source boundary ($z = z_2$)	Y0(IR, IZHI, IK)	1.0E-7 g/cm^3
D	effective-diffusion coefficient of sediment layer 1		1.0E-3 cm^2/s
D′	effective-diffusion coefficient of sediment layer 2		1.0E-4 cm^2/s
z_1	vertical location of lower source boundary	ZLOW	0 cm
z_2	vertical location of upper source boundary	ZHI	100 cm
z_{11}	vertical location of top of sediment layer 1	ZLAY(1)	100 cm
z_{12}	vertical location of top of sediment layer 2	ZLAY(2)	104 cm
Δt	time step	DT	1 hr

Δz = 2 cm and Δt = 360 s is about two orders of magnitude. This difference can be exceeded either by reducing Δt and/or increasing Δz, or by modeling the discontinuity as a gradual change over several nodes.

4.2.2 Diffusion-Coefficient Heterogeneity

The model geometry shown in figure 25 was used to test the algorithm for the ability to simulate diffusion-coefficient heterogeneity. Verification is achieved through a comparison of steady-state numerical and analytical solutions for unsaturated-zone sediments exhibiting a linear diffusion-coefficient distribution given by:

$$D(z) = d_a \tau_a \theta_a(z) \qquad \text{where} \quad \frac{d\theta_a}{dz} = -Az + \theta^o_a \tag{77}$$

where A is the gaseous-phase porosity gradient (A = 0.002 cm^{-1}) and θ^o_a is the gaseous-phase porosity at z = 0 (θ^o_a = 0.080). The steady-state analytical solution that corresponds to this distribution satisfies the following:

$$\frac{d}{dz}\left[-D(z)\frac{dG}{dz}\right]=0 \tag{78}$$

for the boundary conditions (74) and (75), to which the solution is

$$G = G_o - G_o\left[\frac{\ln\left(\frac{\theta_a^o}{Az+\theta_a^o}\right)}{\ln\left(\frac{\theta_a^o}{AL+\theta_a^o}\right)}\right] \tag{79}$$

Transient solutions advance to the steady-state solution for the input data listed in table 18, as shown in figure 29.

4.3 Model Testing of Reaction-Rate Model

The model geometry and boundary conditions shown in figure 30 were used to test the numerical algorithm for the ability to simulate a first-order reaction rate (R_k) (see equation 1). The following steady-state model was employed to simulate toluene (k = 1) gas diffusion and mass loss due to aerobic biodegradation:

$$-D_1\frac{d^2G_1}{dz^2}=R_1 \qquad \text{where} \quad R_1=-\alpha C_1=-\alpha\frac{G_1}{H_1} \tag{80}$$

where

α	=	rate constant	[1/s]
D_1	=	effective-diffusion coefficient	[cm²/s]
G_1	=	gaseous-phase concentration of toluene	[g/cm³]
C_1	=	aqueous-phase concentration of toluene	[g/cm³]
R_1	=	reaction rate (source/sink) of toluene	[g/cm³-s]
H_1	=	Henry's Law constant	[dimensionless]

The steady-state transport and aerobic biodegradation of toluene (80) are coupled to the diffusion and mass loss of oxygen (k = 2) as follows:

$$-D_2\frac{d^2G_2}{dz^2}=-r_1R_1 \tag{81}$$

Table 18. Input parameters used for vertical-transport test of diffusion-coefficient heterogeneity

Symbol	Definition	Model code designation	Value
L	length of model domain in z-direction	ZSURF	100 cm
Nz	number of nodes in z-direction	NZ	101
CSA	cross-sectional area of model domain	CSA	1.0E6 cm^2
G_o	gaseous-phase concentration at source boundary ($z = z_2$)	Y0(IR, IZHI, IK)	1.0E-4 g/cm^3
D_o	effective-diffusion coefficient at z = 0		1.13E-3 cm^2/s
H	Henry's Law constant	HAW(IK)	.801
z_1	vertical location of lower source boundary	ZLOW	0 cm
z_2	vertical location of upper source boundary	ZHI	2 cm
Δt	time step	DT	1 hr

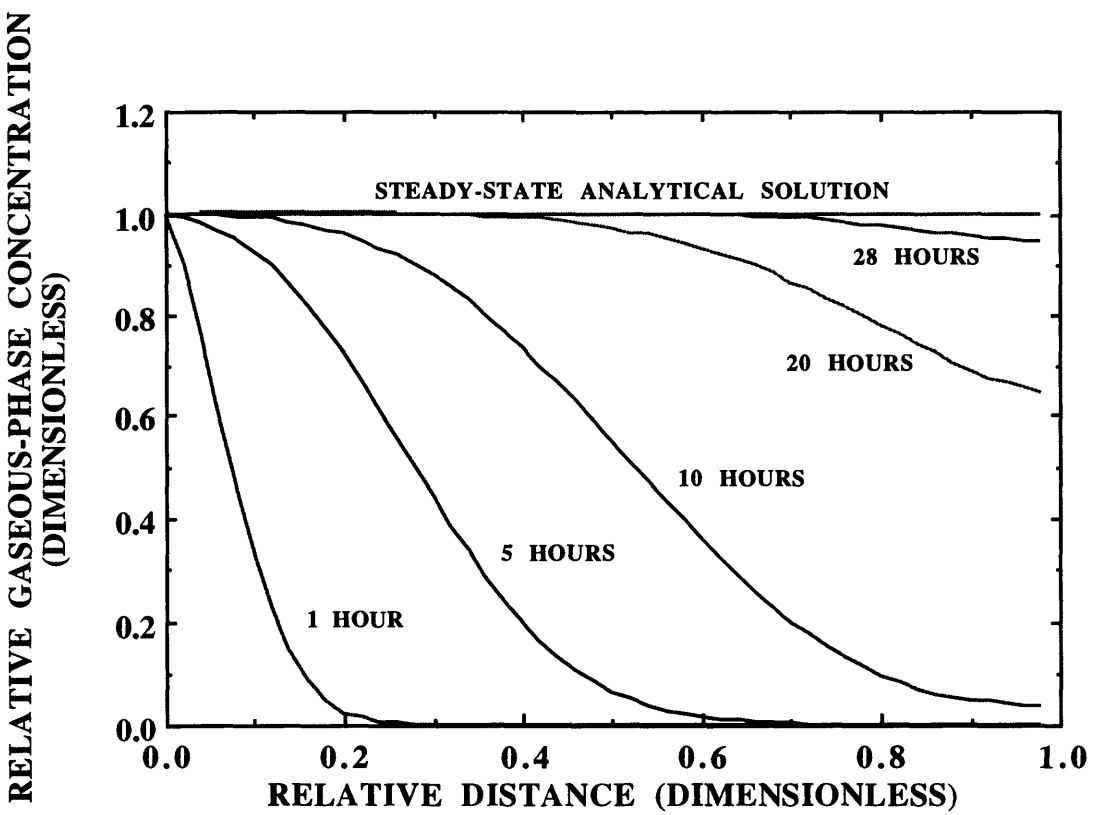

Figure 29. Plot of the transient approach to steady state for the vertical-transport test of diffusion-coefficient heterogeneity.

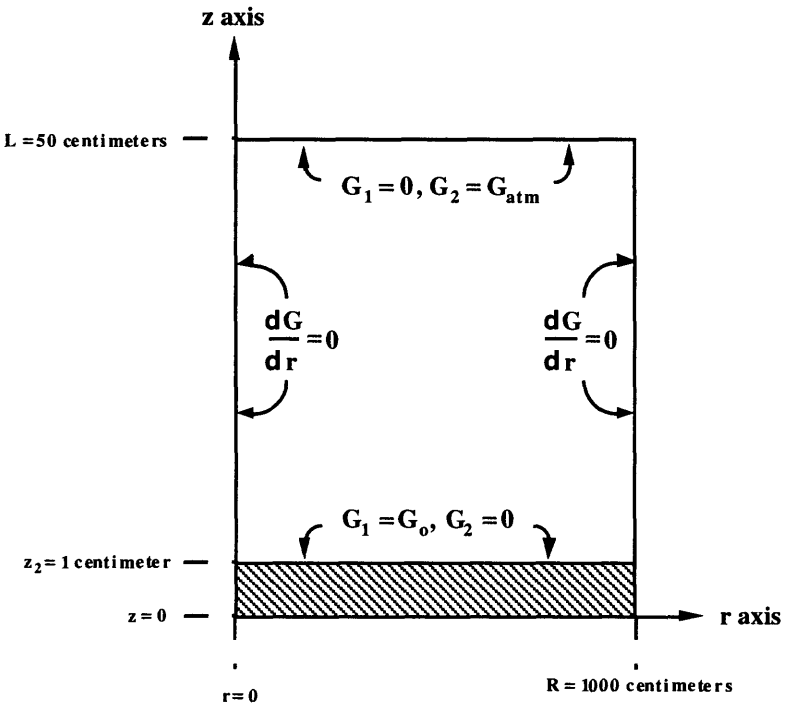

Figure 30. Diagram showing model geometry and boundary conditions used for verification of the reaction-rate model.

where

r_1 = stoichiometric mass constant (see Section 2.4.4) [dimensionless]

Coupling the mass-loss expressions (80) and (81) yields the following expression, which describes the coupled balance of diffusion and biological degradation:

$$\frac{d^2G_1}{dz^2} = \frac{1}{r_1}\left(\frac{D_2}{D_1}\right)\frac{d^2G_2}{dz^2} \tag{82}$$

The steady-state distribution for the geometry depicted in figure 31 satisfies (67) for the boundary conditions:

$$G_1 = G_0 \quad \text{at } z = 0 \tag{83}$$
$$G_1 = 0 \quad \text{at } z = L \tag{84}$$
$$G_2 = 0 \quad \text{at } z = 0 \tag{85}$$
$$G_2 = G_{atm} \quad \text{at } z = L \tag{86}$$

to which the solution for toluene is

$$G_1 = G_0\left[\cosh \omega z - \frac{\sinh \omega z}{\tanh \omega L}\right] \tag{87}$$

and for oxygen is

$$G_2 = r_1\left(\frac{D_1}{D_2}\right)G_1 + b_1 z + b_2 \quad \text{where} \quad b_1 = \frac{1}{L}\left[G_{atm} + r_1\left(\frac{D_1}{D_2}\right)G_0\right]$$
$$b_2 = -r_1\left(\frac{D_1}{D_2}\right)G_0 \tag{88}$$

Transient solutions advance to the steady-state solution for the input data listed in table 19, as shown in figure 32.

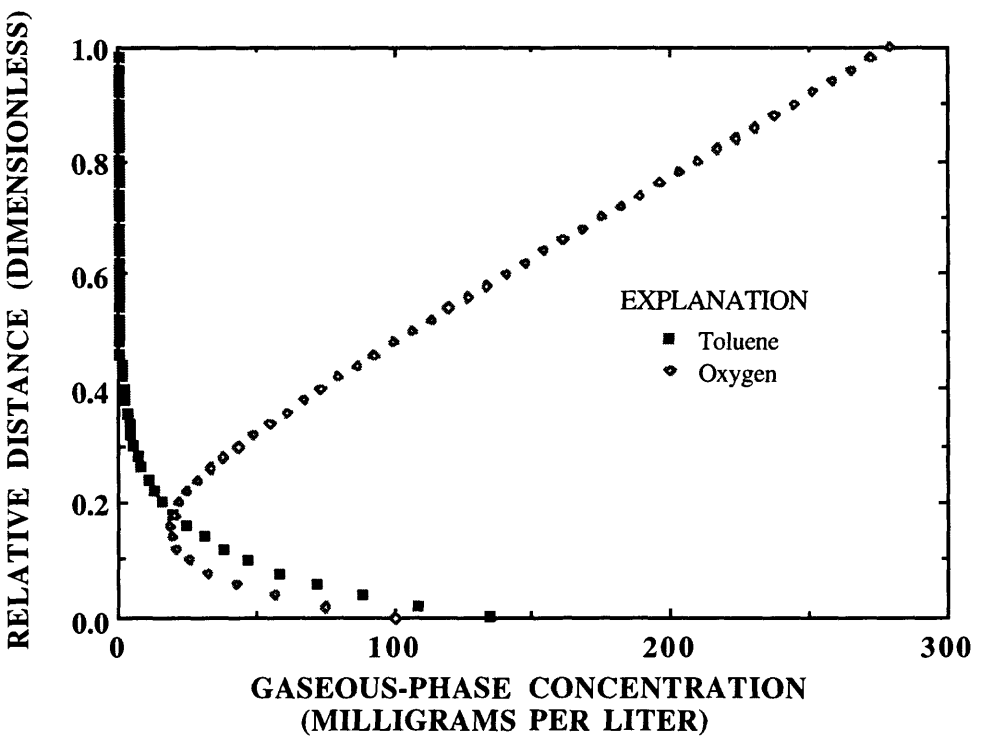

Figure 31. Plot of the steady-state gas distribution corresponding to the model geometry and boundary conditions illustrated in figure 30.

Table 19. Input parameters used to test reaction-rate model

Symbol	Definition	Model code designation	Value
L	length of model domain in z-direction	ZSURF	50 cm
Nz	number of nodes in z-direction	NZ	51
CSA	cross-sectional area of model domain	CSA	1.0E6 cm^2
	Constituent 1 (toluene)		
G_o	gaseous-phase concentration at source boundary ($z = z_2$)	Y0(IR, IZHI, IK)	1.34E-4 g/cm^3
G_o	gaseous-phase concentration at upper model boundary ($z = L$)	ATCONC(IK)	0 g/cm^3
D_o	effective-diffusion coefficient at $z = 0$		1.53E-3 cm^2/s
H_1	Henry's Law constant	HAW(IK)	.26
r_1	stoichiometric coefficient	RK(IK)	3.13
	Constituent 2 (oxygen)		
G_o	gaseous-phase concentration at source boundary ($z = z_2$)	Y0(IR, IZHI, IK)	1.00E-4 g/cm^3
G_o	gaseous-phase concentration at upper model boundary ($z = L$)	ATCONC(IK)	2.79E-4 g/cm^3
D_o	effective-diffusion coefficient at $z = 0$		3.81E-3 cm^2/s
H_2	Henry's Law constant	HAW(IK)	31.60
λ	biodegradation-rate constant	ALPHA	1.75E-05 1/s
z_1	vertical location of lower source boundary	ZLOW	0 cm
z_2	vertical location of upper source boundary	ZHI	1 cm
Δt	time step	DT	1 hr

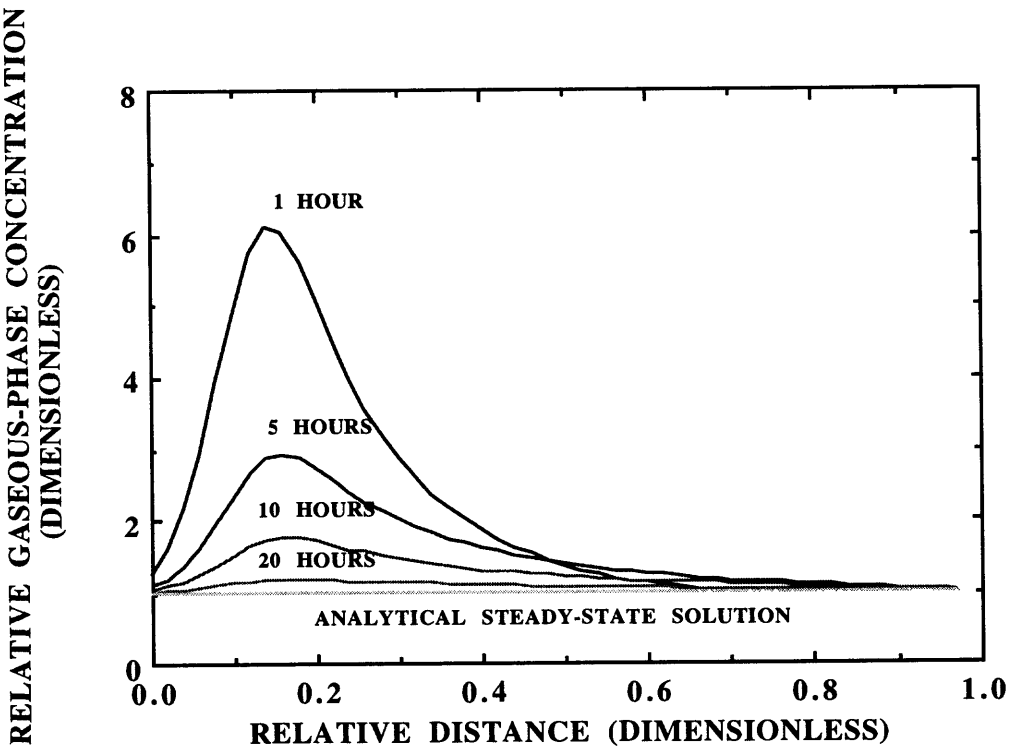

Figure 32. Plot of the transient approach to steady state for verification of the reaction-rate model.

REFERENCES CITED

Alberty, R. A., 1987, Physical Chemistry: New York, John Wiley and Sons, 934 p.

Baehr, A. L., 1987, Selective transport of hydrocarbons in the unsaturated zone due to aqueous and vapor phase partitioning: Water Resources Research, v. 23, p. 1926-1938.

Baehr, A. L., and Corapcioglu, M. Y., 1987, A compositional multiphase model for groundwater contamination by petroleum products, 2. Numerical solution: Water Resources Research, v. 23, p. 201-213.

Bird, R. B., Stewart, W. E., and Lightfoot, E. N., 1960, Transport Phenomena: New York, John Wiley and Sons, 780 p.

Borden, R. C., and Bedient, P. B., 1986, Transport of dissolved hydrocarbons influenced by oxygen-limited biodegradation, 1. Theoretical development: Water Resources Research, v. 22, p. 1983-1990.

Bruell, C. J., and Hoag, G. E., 1986, The diffusion of gasoline-range hydrocarbon vapors in porous media, experimental methodologies, *in* Proceedings of National Water Well Association/American Petroleum Institute Conference on Petroleum Hydrocarbons and Organic Chemical in Groundwater - Prevention, Detection and Restoration, Houston, Texas, November 12-14, 1986: Worthington, Ohio, National Water Well Association, p. 420-443.

Curtiss, C. F., and Hirschfelder, J. O., 1949, Transport properties of multicomponent gas mixtures: Journal of Chemical Physics, v. 17, p. 550-555.

Fischer, J. M., Baker, R. J., and Baehr, A. L., 1996, Determination of vapor-phase diffusion coefficients for unsaturated-zone sediments at Galloway Township, New Jersey, *in* Morganwalp, D.W., and Aronson, D.A., eds., U.S. Geological Survey Toxic Substances Hydrology Program--Proceedings of the Technical Meeting, Colorado Springs, Colorado, September 20-24, 1993: U.S. Geological Survey Water-Resources Investigations Report 94-4015, v. 1, p. 35-42.

Fuller, E. N., Schettler, P. D., and Griddings, J. C., 1966, A new method for prediction of binary gas-phase diffusion coefficients: Industrial Engineering Chemistry, v. 58, p. 19-27.

Hanks, R. J., and Ashcroft, G. L., 1980, Applied soil physics: Berlin, Springer-Verlag, 476 p.

Kreamer, D. K., Weeks, E. P., and Thompson, G.M., 1988, A field technique to measure the tortuosity and sorption-affected porosity for gaseous diffusion of materials in the unsaturated zone with experimental results from near Barnwell, South Carolina: Water Resources Research, v. 24, p. 331-341.

Lahvis, M. A., 1993, Estimating rates of microbial degradation of hydrocarbons at a gasoline-spill site based on vapor diffusion modeling in the unsaturated zone: Philadelphia, Pa., Drexel University, Department of Civil Engineering, unpublished Ph.D. dissertation, 204 p.

Lahvis, M. A., and Baehr, A. L., 1996, Estimation of rates of aerobic hydrocarbon biodegradation by simulation of gas transport in the unsaturated zone: Water Resources Research, v. 32, p. 2231-2249.

Landmeyer, J. E., Chapelle, F. H., and Bradley, P. M., 1996, Assessment of intrinsic bioremediation of gasoline contamination in the shallow aquifer, Laurel Bay Exchange, Marine Corps Air Station, Beaufort, South Carolina: U.S. Geological Survey Water Resources Investigations Report 96-4026, p. 50.

Massmann, J., and Farrier, D. F., 1992, Effects of atmospheric pressures on gas transport in the vadose zone: Water Resources Research, v. 28, p. 777-791.

Millington, R. J., 1959, Gas diffusion in porous media: Science, v. 130, p. 100-102.

Reibel, D. D., and Shair, F. H., 1982, A technique for the measurement of gaseous diffusion in porous media: Journal of Soil Science, v. 33, p. 165-174.

Reid, R. C., Prausnitz, J. M., and Sherwood, T. K., 1987, The properties of gases and liquids: New York, McGraw-Hill Book Company, 741 p.

Thorstenson, D. C., and Pollock, D. W., 1989, Gas transport in unsaturated zones: Multicomponent systems and the adequacy of Fick's Laws: Water Resources Research, v. 25, p. 477-507.

Tyn, M. T., and Calus, W. F., 1975, Diffusion in dilute binary liquid mixtures: Journal of Chemical Engineering Data, v. 21, p. 310-316.

Wiedemeier, T. H., Wilson, J. T., Kampbell, D. H., Miller, R. N., and Hansen, J. E., 1994, Technical protocol for implementing the intrinsic remediation with long-term monitoring option for natural attenuation of fuel-hydrocarbon contamination in ground water, *in* U.S. Environmental Protection Agency--Symposium on Intrinsic Bioremediation of Ground Water, Denver, Colorado, August 30-September 1, 1994: U.S. Environmental Protection Agency Report 540/R-94/515, p. 163-170.

Wilke, C. R., and Chang, P., 1955, Estimation of diffusion coefficients for gases and liquids: American Institute of Chemical Engineers Journal, v. 47, p. 264-275.

Appendix 1. Summary of model input for the numerical solutions for R-UNSAT computer model

Symbol	Definition	Model code designation	Unit(s)
	Indices		
i	radial-node index	IR	dimensionless
j	vertical-node index	IZ	dimensionless
k	constituent index	IK	dimensionless
l	sediment-layer index	IL	dimensionless
	Model domain parameters		
IDIM	model dimensionality	IDIM	dimensionless
R	length of model domain in r-direction	RF	cm
L	length of model domain in z-direction	ZSURF	cm
N_r	number of nodes in r-direction	NR	dimensionless
N_z	number of nodes in z-direction	NZ	dimensionless
CSA	cross-sectional area of model domain	CSA	cm^2
T	unsaturated-zone temperature	TEMP	°C
P	unsaturated-zone pressure	ATM	mm Hg
q_{wz}	vertical recharge rate	DARCY	cm/yr
	Constituent properties		
M	number of modeled constituents	NK	dimensionless
ICON	constituent-index designation	ICON	dimensionless
ω_k	molecular weight	WK(IK)	g/mol
ζ_k	atomic diffusion volume	DV(IK)	dimensionless
d_{ka}	gaseous-phase diffusivity	DKA(IR,IZ,IK)	cm^2/s
d_{kw}	aqueous-phase diffusivity	DKW(IK)	cm^2/s
v_k	specific volume	VK(IK)	cm^3/g
G_{klatm}	gaseous-phase concentration at (Ω_2), (Ω_3), or (Ω_5)	ATCONC(IK)	g/cm^3
H_k	Henry's Law constant	HAW(IK)	dimensionless
H_{kw}^{o}	aqueous-phase solubility	HWIK(IK)	g/cm^3
K_k	adsorption isotherm	HSW(IK)	dimensionless
r_k	stoichiometric coefficient relating mass of oxygen consumed to unit mass of hydrocarbon degraded	RK(IK)	dimensionless

Appendix 1. Summary of model input for the numerical solutions for R-UNSAT computer model--Continued

Symbol	Definition	Model code designation	Unit(s)
	Boundary and initial conditions		
J_{ko}	gas flux across lower vertical or inner radial boundary (Ω_1)	FLX(IR,IK)	g/cm²-s
G_{ko}	gaseous-phase concentration at lower vertical boundary (Ω_1)	Y0(IR, IZHI,IK)	g/cm³
χ_{ko}	initial mole fraction in immiscible plume (Ω_1)	XIK0(IK)	g/cm³
θ_i	immiscible plume volumetric content	THI0	dimensionless
r_2	radius of source	RIM	cm
z_1	vertical location of lower source boundary (Ω_1)	ZLOW	cm
z_2	vertical location of upper source boundary (Ω_1)	ZHI	cm
$r_{\Omega 3}$	radial location of boundary-condition variation along Ω_3	RASP	cm
$z_{\Omega 5}$	vertical location of boundary-condition variation along Ω_5	RASP(IR)	cm
λ_2	boundary-condition parameter: lower vertical boundary (Ω_2) ($0 < z < R$)	AZ3	dimensionless
λ_3	boundary-condition parameter: upper vertical boundary (Ω_3) ($0 < z < r_{\Omega 3}$)	AR1	dimensionless
λ_3	boundary-condition parameter: upper vertical boundary (Ω_3) ($r_{\Omega 3} < z < R$)	AR2	dimensionless
λ_5	boundary-condition parameter: outer radial boundary (Ω_5) ($0 < z < z_{\Omega 5}$)	AZ1	dimensionless
λ_5	boundary-condition parameter: outer radial boundary (Ω_5) ($z_{\Omega 5} < z < L$)	AZ2	dimensionless
	Physical properties of the unsaturated zone sediments		
ϕ	total porosity	POR(IZ)	dimensionless
θ_w	aqueous-phase porosity	THW(IZ)	dimensionless
τ_a	gaseous-phase tortuosity	TA(IZ)	dimensionless
δ_l	longitudinal dispersivity	AL(IL)	cm
δ_t	transverse dispersivity	ALT(IL)	cm
ρ_b	bulk density	BD(IZ)	g/cm³

Appendix 1. Summary of model input for the numerical solutions for R-UNSAT computer model--Continued

Symbol	Definition	Model code designation	Unit(s)
N_l	number of sediment layers (stratigraphic units)	NL	dimensionless
z_l	vertical location of top of sediment layer	ZLAY(IL)	cm
	Algorithm parameters		
Δt_1	initial time step	DT1	hr
Δt_2	final time step	DT2	hr
β	time-step multiplier	DTM	dimensionless
t_{trans}	transition time (time at which time-step adjustment is applied)	TRANS	hr
t_{end}	ending time	TEND	hr
$iter_{max}$	maximum number of iterations per time step	NITER	dimensionless
eps	convergence criterion (acceptable maximum relative error)	EPS	dimensionless
	Output parameters		
Δt_{prl}	printout increment for breakthrough data	YPR1	hr
t_{snap}	time for snapshot data	TSNAP	hr
N_{vw}	number of locations for output data	NW	dimensionless
r_{vw}	output-data location in r-direction	RVW(IW)	cm
z_{vw}	output-data location in z-direction	ZVW(IW)	cm

Appendix 2. Summary of model input for the analytical solutions for R-UNSAT computer model

Symbol	Definition	Model code designation	Unit(s)
	Boundary and initial conditions		
J_{ko}	constant gas flux at water table (z = 0)	FLUX	g/cm²-s
G_{ko}	constant gaseous-phase concentration at water table (z = 0)	UW	g/cm²-s
b′	thickness of confining unit	BP	cm
D_k'	effective-diffusion coefficient of confining unit	DP	cm²/s
G_U	gaseous-phase concentration above confining unit (z = L)	UP	g/cm³
$A_k(z)$	piecewise linear function of gaseous-phase concentration at time t = 0	XB0	
	Constituent properties		
d_{ka}	gaseous-phase diffusivity	DBIN	cm²/s
H_k	Henry's Law constant	HENRY	dimensionless
S_k	solid/water partition coefficient	SWPC	dimensionless
	Physical properties of the unsaturated zone sediments		
L	length of model domain	XL	cm
ϕ	total porosity	VOID	dimensionless
θ_a	gaseous-phase porosity	AIR	dimensionless
θ_w	aqueous-phase porosity	WAT	dimensionless
τ	gaseous-phase tortuosity	TOR	dimensionless
ρ_b	bulk density	BULK	g/cm³
	Output parameters		
t_{end}	maximum time for breakthrough data	TMAX	hr
Δt_b	time step for breakthrough data	DELT	hr
t_{snap}	time of snapshot	TSNAP	hr
L_{snap}	endpoint for snapshot data	XLL	cm
N_{snap}	number of snapshot data points	NIPTS	dimensionless
r_{vw}	output-data location in r-direction	ROUT	cm
z_{vw}	output-data location in z-direction	ZOUT	cm